

TRACE ELEMENTS IN HIGH CASCADE VOLCANIC ROCKS,
THREE SISTERS AREA, OREGON

A DISSERTATION
SUBMITTED TO THE DEPARTMENT OF GEOLOGY
AND THE COMMITTEE ON GRADUATE STUDIES
OF STANFORD UNIVERSITY
IN PARTIAL FULFILMENT OF THE REQUIREMENTS
FOR THE DEGREE OF
DOCTOR OF PHILOSOPHY

By

Gary Jacob Anttonen

GA
March 1972

I certify that I have read this thesis and that in my opinion it is fully adequate, in scope and quality, as a dissertation for the degree of Doctor of Philosophy.

William R. Dickinson
(Principal Adviser)

I certify that I have read this thesis and that in my opinion it is fully adequate, in scope and quality, as a dissertation for the degree of Doctor of Philosophy.

W. C. Lott

I certify that I have read this thesis and that in my opinion it is fully adequate, in scope and quality, as a dissertation for the degree of Doctor of Philosophy.

K. C. Deane

Approved for the University Committee
on Graduate Studies:

Lincoln E. Moses
Dean of Graduate Studies

ACKNOWLEDGMENTS

The author wishes to express his deepest gratitude for the assistance of Dr. E. M. Taylor at Oregon State University. The generosity he displayed in sharing his geologic maps of the Three Sisters area and the major element analyses he supplied, as well as his aid and direction in field sampling, helped make this research project possible.

Special thanks also go to Dr. W. R. Dickinson, thesis adviser for this work, and the late Dr. C. O. Hutton, both of whom supplied numerous helpful suggestions and critical comments during the course of the project. In addition, Dr. K. L. Williams and Dr. C. M. Taylor supplied the author with invaluable aid in learning the techniques of spectrochemical analysis. Final thanks go to Drs. W. R. Dickinson, K. L. Williams, W. C. Luth, and B. M. Page for their critical reading and evaluation of the thesis manuscript. Financial assistance was provided by the Geological Society of America, the Stanford Geology Department Shell Fund, and Sigma Xi. This aid helped defray the considerable expense of spectrochemical supplies and laboratory access.

ABSTRACT

The calc-alkaline volcanic suite from the Three Sisters area near Bend, Oregon consists of undeformed High Cascade rocks resting unconformably on the older Western Cascade calc-alkaline sequence. Most High Cascade rocks are younger than the last magnetic reversal 770,000 years ago, and the latest eruptions occurred less than 1400 years ago.

The rocks have been classified on the basis of their mineralogy and chemistry into the following five groups:

(1) Olivine basalt (<52% silica) contains phenocrysts of olivine and calcic plagioclase in a groundmass of intermediate to calcic plagioclase, pyroxene, iron oxides, and glass.

(2) Olivine andesite (52-58% silica), the most abundant rock type, has phenocrysts of calcic plagioclase, olivine, and occasionally hypersthene or calcic augite in a groundmass of intermediate plagioclase, pyroxene, iron oxides, and glass.

(3) & (4) Both pyroxene andesite (58-62% silica) and dacite (62-68% silica) have intermediate plagioclase, orthopyroxene, calcic augite, and iron oxide phenocrysts in a groundmass of intermediate to sodic plagioclase, pyroxenes, iron oxides, and glass; olivine is rarely present as phenocrysts or blebs in hypersthene phenocrysts.

(5) Rhyodacite (>71% silica) contains phenocrysts of sodic plagioclase, iron oxides, and ferrohypersthene in a groundmass of sodic plagioclase and abundant glass.

Three main types of volcanoes are present: (1) shield volcanoes constructed of thin flows of olivine basalt and olivine andesite, (2) composite cones predominantly built of pyroxene andesite and dacite with attendant eruptions of olivine basalt, olivine andesite, and rhyodacite, and (3) cinder cones constructed of olivine basalt and olivine andesite in most cases, but also of pyroxene andesite in some cases.

Ninety-three samples were analyzed for Ba, Sr, Mn, Ni, Cr, Co, V, Sc, Zr, Cu, and Zn using an emission spectrograph. Dr. E. M. Taylor supplied major element analyses for the group. The following trends are exhibited by the trace elements:

(a) Ba shows only moderate enrichment throughout most of the rock sequence, and Sr, only moderate depletion. Ba/Sr values are uniformly

low for olivine basalts, olivine andesites, pyroxene andesites, and dacites.

(b) Both V and Sc abundances are high throughout the olivine basalt-pyroxene andesite range of silica values. Neither shows sympathetic variation with a major element.

(c) Ni, Cr, and Co exhibit marked sympathetic variation with MgO. Olivine basalts and olivine andesites can be divided into two groups or series, one high and one low in MgO-Ni-Cr-Co content.

The mineralogic, petrographic, and chemical data do not appear to support hypotheses of mixing, contamination, or low pressure fractional crystallization to explain the origins of the erupted magmas or the variations among them. The analytical data are qualitatively consistent with a model involving partial fusion of abyssal tholeiite and eclogite transformed from tholeiite during subduction in an arc-trench system.

TABLE OF CONTENTS

	Page
ACKNOWLEDGMENTS	iii
ABSTRACT	iv
LIST OF TABLES	viii
LIST OF ILLUSTRATIONS	ix
INTRODUCTION	1
LOCATION AND GEOGRAPHY	2
GEOLOGIC SETTING	2
FIELDWORK AND SAMPLING	6
PETROGRAPHIC CLASSIFICATION	6
AGE RELATIONSHIPS OF THE LAVAS AND VOLCANOLOGY	7
Shield Volcanoes and Related Platform Rocks	9
Composite Cones and Related Forms	11
Cinder Cones	13
PETROGRAPHY	14
Techniques	14
Olivine Basalt (<52% Silica)	16
Olivine Andesite (52-58% Silica)	18
Pyroxene Andesite and Dacite (58-62% & 62-68% Silica)	23
Rhyodacite (>71% Silica)	26
ANALYTICAL PROCEDURES FOR TRACE AND MAJOR ELEMENT DETERMINATIONS	28
ANALYTICAL RESULTS	29
Major Element Chemistry	29
AMF and CNK Diagrams	32
Trace Element Geochemistry	34
Sr-Ba	34
V-Sc	37
Mn	40
Zr	40
Cu-Zn	42
Ni-Cr-Co	44
DISCUSSION: PETROGENESIS OF CALC-ALKALINE ROCKS	49
Mixing Hypotheses	51
Fractional Crystallization	52
Partial Melt Hypotheses	55
SUMMARY AND CONCLUSIONS	59

	Page
APPENDIX I: SPECTROCHEMICAL ANALYSIS	61
Sample Preparation	61
Semiquantitative Analysis	61
Quantitative Analysis	62
Preparation of Internal Standard	62
Preparation of External Standards	62
Analytical Procedures	64
Calculation of Intensity Ratios	64
Precision and Accuracy	68
APPENDIX II: MAJOR AND TRACE ELEMENT ANALYSES	71
BIBLIOGRAPHY	94

LIST OF TABLES

Table	Page
1. APPROXIMATE AGE RELATIONSHIPS OF VOLCANOES AND THEIR ASSOCIATED LAVAS IN THE THREE SISTERS AREA	10
2. SAMPLING OF PARTIAL MAJOR ELEMENT ANALYSES OF RECENT LAVA FLOWS FROM THE THREE SISTERS AREA	15
3. COMPOSITION OF THE MATRIX (FOR SPECTROCHEMICAL ANALYSIS)	63
4. COMPOSITION OF THE 1.0% EXTERNAL STANDARD	63
5. SPECTRAL LINES, DETECTION LIMITS, AND CONCENTRATION RANGES	65
6. EQUIPMENT AND MATERIAL FOR ANALYTICAL WORK	66
7. SUMMARY OF ANALYTICAL PROCEDURES	67
8. INTERNAL STANDARDS AND PRECISIONS	69
9. A COMPARISON OF TRACE ELEMENT CONCENTRATION VALUES OBTAINED FROM U. S. G. S. ROCK STANDARDS	70
10. PARTIAL CHEMICAL ANALYSES AND TRACE ELEMENT RESULTS FOR OLIVINE BASALTS AND OLIVINE ANDESITES	72-87
11. PARTIAL CHEMICAL ANALYSES AND TRACE ELEMENT RESULTS FOR PYROXENE ANDESITES, DACITES, AND RHYODACITES	88-93

LIST OF ILLUSTRATIONS

Figures	Page
1. Area and Sample Location Map	3
2. Histogram of Silica Values	8
3. Photomicrographs of (A) Diktytaxitic Basalt and (B) Olivine Andesite	17
4. Photomicrographs of (A) and (B) Olivine Andesites	21
5. A Plot of Per Cent Phenocrysts by Volume Versus Anorthite Content of Groundmass Plagioclase	22
6. Photomicrographs of (A) Pyroxene Andesite and (B) Dacite	25
7. Photomicrograph of Rhyodacite	27
8. Silica Variation Diagram for Al_2O_3 , FeO, MgO, and TiO_2 ...	30
9. Silica Variation Diagram for CaO, Na_2O , and K_2O	31
10. AMF-CNK Diagrams	33
11. Plots of Ba and Sr ppm Versus Weight % SiO_2	35
12. Plots of (A) Ba ppm Versus Potash and (B) Sr ppm Versus Lime	36
13. Plots of V ppm Versus Weight % SiO_2 and FeO	38
14. Plots of Sc ppm Versus Weight % SiO_2 , FeO, and MgO	39
15. Plots of Mn and Zr ppm Versus Weight % SiO_2	41
16. Plots of Cu and Zn ppm Versus Weight % SiO_2	43
17. Plots of Weight % MgO and ppm Ni Versus Weight % SiO_2	45
18. Plots of Cr and Co ppm and Ni/Co Ratios Versus Weight % SiO_2	46
19. Plots of Ni, Cr, and Co ppm Versus Weight % MgO	47
20. A Plot of Approximate Age of Samples for Series A and B Versus Number of Representative Analyses in Each Age Group	50

INTRODUCTION

The elongate volcanic belt forming the Cascade Range of British Columbia, Washington, Oregon, and northern California is dominated in central Oregon by the snow-capped peaks of the Three Sisters. These dissected cones and neighboring volcanoes constitute one of the most remarkable of the recently active calc-alkaline volcanic provinces in the United States. Callaghan (1933) divided the Cascade Range into two parallel belts: the older Western Cascades and the much younger High Cascades. Volcanoes of the Three Sisters area discussed in this report are exclusively High Cascade features.

Except for the early work by Callaghan and that of Williams (1932a, 1932b, 1933, 1935, 1942, 1944, 1957) and Thayer (1937, 1939), the imposing cones of the High Cascades were neglected by geologists until recently. The Three Sisters area in particular has received scant attention. The initial report by Hodge (1925) on these peaks advanced the rather fanciful theory that they rested inside the rim of a gigantic caldera reminiscent of Crater Lake. The supposed caldera marked the site of a colossal volcano, named Mount Multnomah, which was destroyed at the close of the Miocene or in the early Pliocene by catastrophic explosions. Howel Williams' excellent reconnaissance work in the area (1944) discarded Hodge's dramatic interpretation on a number of grounds. Since the work by Williams, no major geologic reports have been published on the Three Sisters or surrounding volcanic features. Dr. E. M. Taylor is currently conducting an extensive field program in the area. He is preparing detailed geologic maps of the extrusive units and has performed over 400 major element analyses of the volcanic rocks.

Trace element data and petrogenetic descriptions for the lava flows from the Three Sisters presented in this report throw new light on the petrogenesis of these rocks. Recent literature has emphasized the relationship between calc-alkaline suites and arc-trench systems (e.g., Isacks et al, 1968; Green and Ringwood, 1969; S. R. Taylor, 1969; Taylor et al, 1969; Dickinson, 1970, 1971). Trace element information sets limits on possible petrogenetic interpretations developed in these and related

papers. These data from the Three Sisters area suggest that this calc-alkaline suite of rocks was derived mainly from partial melting of eclogite produced at depth from inversion of oceanic tholeiite during Cenozoic subduction of oceanic lithosphere.

LOCATION AND GEOGRAPHY

The area discussed in this report lies along the crest of the High Cascades in Oregon from Santiam Pass on the north to Bachelor Butte on the south (see Fig. 1). Samples for analysis were collected as far east as the town of Bend on the south and as far east as Black Butte on the north. The western edge of sampling is nearly coincident with the boundary between the Western and High Cascades from Santiam Pass to McKenzie Pass. South of McKenzie Pass samples were collected along the western slopes of the Three Sisters themselves as far west as the Husband. The area is approximately 30 miles wide and 25 miles long, and covers portions of four counties: Linn, Lane, Jefferson, and Deschutes.

The crest of the Cascade Range in this region is dominated by the glacially eroded cones of the Three Sisters, each of which exceeds 10,000 feet in elevation. To the south and east, Broken Top and Bachelor Butte reach heights of 9,000 feet, and to the north, Mount Washington's central plug is nearly 8,000 feet high. Except for Bachelor Butte, U-shaped glacial canyons cut deeply into the flanks of all these peaks. Numerous cinder cones and eroded shield volcanoes dot the surrounding terrain, but few of these exceed 6,000 feet in elevation. The western slopes of the range drop swiftly from the crestral peaks into deep river canyons that cut through the older Western Cascade rocks, but the eastern flank falls more gently to merge with the high lava plateau of central Oregon.

GEOLOGIC SETTING

The Western Cascades have been described for much of their length in Oregon by Peck et al (1964). Earlier work includes that of Wells and Peck (1961) and Thayer (1936, 1937). This longitudinal belt consists of maturely dissected, folded, and faulted volcanic rocks ranging in age from Late Eocene to Pliocene. The topography bears no relationship to

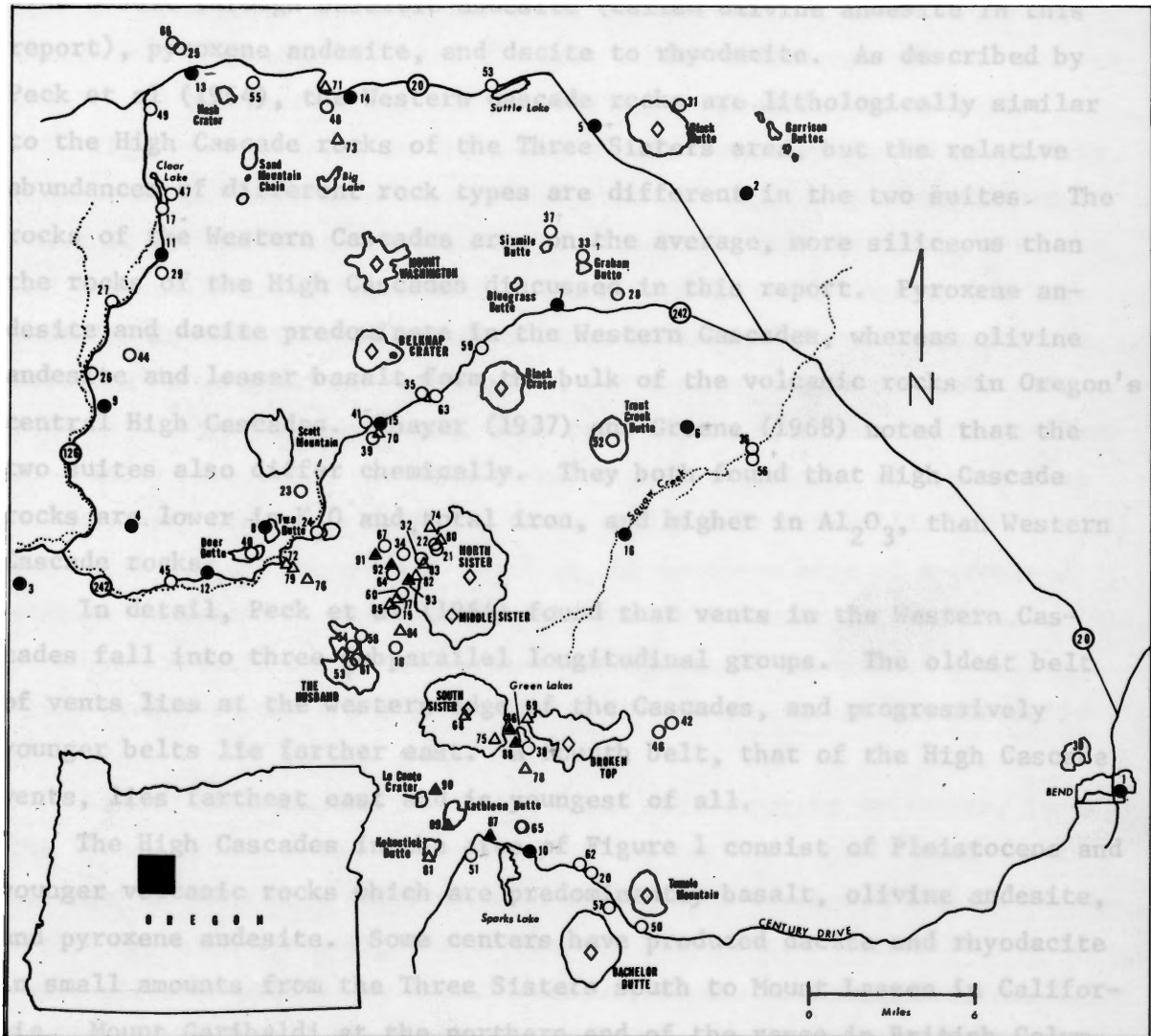


Figure 1. Sample location map for the Three Sisters area, Oregon. Sample numbers correspond to those in Appendix II. ● Olivine basalt; ○ Olivine andesite; △ Pyroxene andesite and dacite; and ▲ Rhyodacite.

original volcanic forms. The rocks attain a stratigraphic thickness of nearly 20,000 feet and consist of interbedded flows of tuff-breccia, lapilli-tuff, and other pyroclastic debris. Compositions range from olivine basalt through basaltic andesite (called olivine andesite in this report), pyroxene andesite, and dacite to rhyodacite. As described by Peck et al (1964), the Western Cascade rocks are lithologically similar to the High Cascade rocks of the Three Sisters area, but the relative abundances of different rock types are different in the two suites. The rocks of the Western Cascades are, on the average, more siliceous than the rocks of the High Cascades discussed in this report. Pyroxene andesite and dacite predominate in the Western Cascades, whereas olivine andesite and lesser basalt form the bulk of the volcanic rocks in Oregon's central High Cascades. Thayer (1937) and Greene (1968) noted that the two suites also differ chemically. They both found that High Cascade rocks are lower in K_2O and total iron, and higher in Al_2O_3 , than Western Cascade rocks.

In detail, Peck et al (1964) found that vents in the Western Cascades fall into three subparallel longitudinal groups. The oldest belt of vents lies at the western edge of the Cascades, and progressively younger belts lie farther east. A fourth belt, that of the High Cascade vents, lies farthest east and is youngest of all.

The High Cascades in the area of Figure 1 consist of Pleistocene and younger volcanic rocks which are predominantly basalt, olivine andesite, and pyroxene andesite. Some centers have produced dacite and rhyodacite in small amounts from the Three Sisters south to Mount Lassen in California. Mount Garibaldi at the northern end of the range in British Columbia also has produced highly siliceous rocks. The centers erupting varied lavas contrast with the large composite cones from the Middle Sister north to Garibaldi. These have erupted basalt and olivine andesite with a uniformly narrow range of silica content. McBirney (1968) has described the olivine andesite lava suites with limited compositional variation as the "coherent" type, and the contrasting suites displaying a large range of silica content as the "divergent" type. He noted that "divergent"

centers typically have an early history of andesitic and dacitic eruptions succeeded by a later period during which contrasting basalts and rhyodacites are erupted without associates of intermediate composition. In the "divergent" suite of the Three Sisters area, however, some rhyodacite was erupted early, and the most recent eruptions included not only basalt and rhyodacite, but olivine and pyroxene andesites as well.

High Cascade lavas in the Three Sisters area are almost completely undeformed and rest on a basement of eastward-dipping Western Cascade volcanic rocks. Tertiary strata which underlie the plateau to the east and presumably interfinger with Western Cascade rocks beneath the High Cascades include the Clarno, John Day, and Mascall Formations, and the Columbia River basalts. It is not known whether deeper basement rocks include the pre-Tertiary units that crop out in southwestern Oregon and apparently pass under the High Cascades in the vicinity of Crater Lake and Newberry Crater to reappear farther east near Prineville and Mitchell. The Three Sisters apparently stand at the southern edge of a proposed sinistral embayment in the pre-Tertiary sialic basement (see McBirney, 1968, p. 102). Significantly, not a single fragment of recognized pre-Tertiary rock has been found among the ejecta from cones in the Three Sisters area.

Linear arrangements of cinder cones and composite volcanoes, in both the Three Sisters area and the surrounding region, suggest that the locations of vents were controlled in detail by extensive normal faulting. Within the High Cascades, these presumed faults are obscured by the volcanic piles erupted along them. However, to the southeast numerous major faults strike toward the Three Sisters area. These include the Brothers Fault Zone, Walker Fault, and Green Mountain Fault. Newberry Crater southeast of the Three Sisters appears to stand at the juncture of these three faults (Higgins and Waters, 1967, 1968). To the north, the Hood River Fault displaces High Cascade rocks parallel to the trend of the range. East of the High Cascades, the faulting has produced typical basin-range topography which trends southeast into Nevada and northeastern California.

FIELDWORK AND SAMPLING

Fieldwork was completed during the summer of 1969 with the aid and direction of Dr. E. M. Taylor. Extensive use was made of his geologic maps and familiarity with the region during sample selection. Since many of the rocks are porphyritic, relatively large field samples, usually on the order of three to five pounds or more, were collected. Samples were selected to provide the most complete geochemical representation of the volcanic rocks in the area; samples for trace element analyses were chosen from flows that Dr. Taylor had analyzed for major elements. Several samples were collected from different points along the lengths of various flows to give some idea of variation in chemical composition within discrete batches of magma.

PETROGRAPHIC CLASSIFICATION

The petrographic classification used in this paper reflects both the chemical composition and modal mineralogy of the rocks and generally follows the scheme proposed by Williams et al (1954). Greene (1968) used a similar scheme in his description of volcanic rocks from Mt. Jefferson. For Mt. Hood lavas, Wise (1969) used plots of Differentiation Index and color index versus silica to separate rock types. The normative calculations required for this scheme were not suitable for this paper since all major element analyses available are only partial whole-rock analyses. Wise's use of the term "olivine andesite" is adopted here in a strictly descriptive sense in preference to "basaltic andesite". The latter has been defined in such a variety of ways that its present usage is confusing.

The following classification used here is based on mineralogy of phenocrysts and silica content:

Olivine Basalt.....<52 per cent silica; olivine phenocrysts>
calcic plagioclase phenocrysts.

Olivine Andesite....52-58 per cent silica; calcic plagioclase
phenocrysts>olivine phenocrysts; calcic
augite phenocrysts rare or absent; hyper-
sthene occasionally replaces olivine pheno-
crysts.

- Pyroxene Andesite...58-62 per cent silica; intermediate plagioclase phenocrysts>pyroxene phenocrysts; augite and hypersthene phenocrysts about equal in amount.
- Dacite.....62-68 per cent silica; intermediate to sodic plagioclase phenocrysts; hypersthene>augite phenocrysts.
- Rhyodacite.....>71 per cent silica; sodic, corroded plagioclase phenocrysts with ferrohypersthene microphenocrysts; augite phenocrysts absent.

The division between pyroxene andesite and dacite is arbitrary since the two are completely gradational in chemical and mineralogical properties. It has been set at 62% silica to accord with the usage of Wise (1969) and S. R. Taylor (1969). However, the divisions between olivine and pyroxene andesite and between dacite and rhyodacite are more distinct. Intermediate representatives are generally lacking or totally absent (Fig. 2). E. M. Taylor (personal communication) found a similar distribution in a plot of over 400 unpublished silica analyses from the area.

The basalts correspond to the high-alumina type described by Kuno (1960, 1968a, 1969a, 1969b). Alkali content is generally low, and the rock sequence as a whole lies on the boundary of the calcic and calc-alkaline series as defined by Peacock (1931) and discussed by McBirney (1969). Total alkalis exceed the weight percentage of CaO only above 61% silica (see Fig. 9).

AGE RELATIONSHIPS OF THE LAVAS AND VOLCANOLOGY

Recent work in the Three Sisters area has emphasized the apparent youth of all High Cascade rocks in the region. A paleomagnetic survey conducted by E. M. Taylor has revealed that only a few flows at the base of the High Cascade platform have reverse polarity. The entire series above this is normally polarized and must be younger than the last reversal 770,000 years ago. The most recent flows are probably less than 1400 years old (E. M. Taylor, 1965, p. 145). Despite these very youthful eruptions, there are virtually no active hot springs, fumaroles, solfataras, or any other signs of present volcanic activity in the area. The region can not be presumed dead, however, and eruptions may resume on

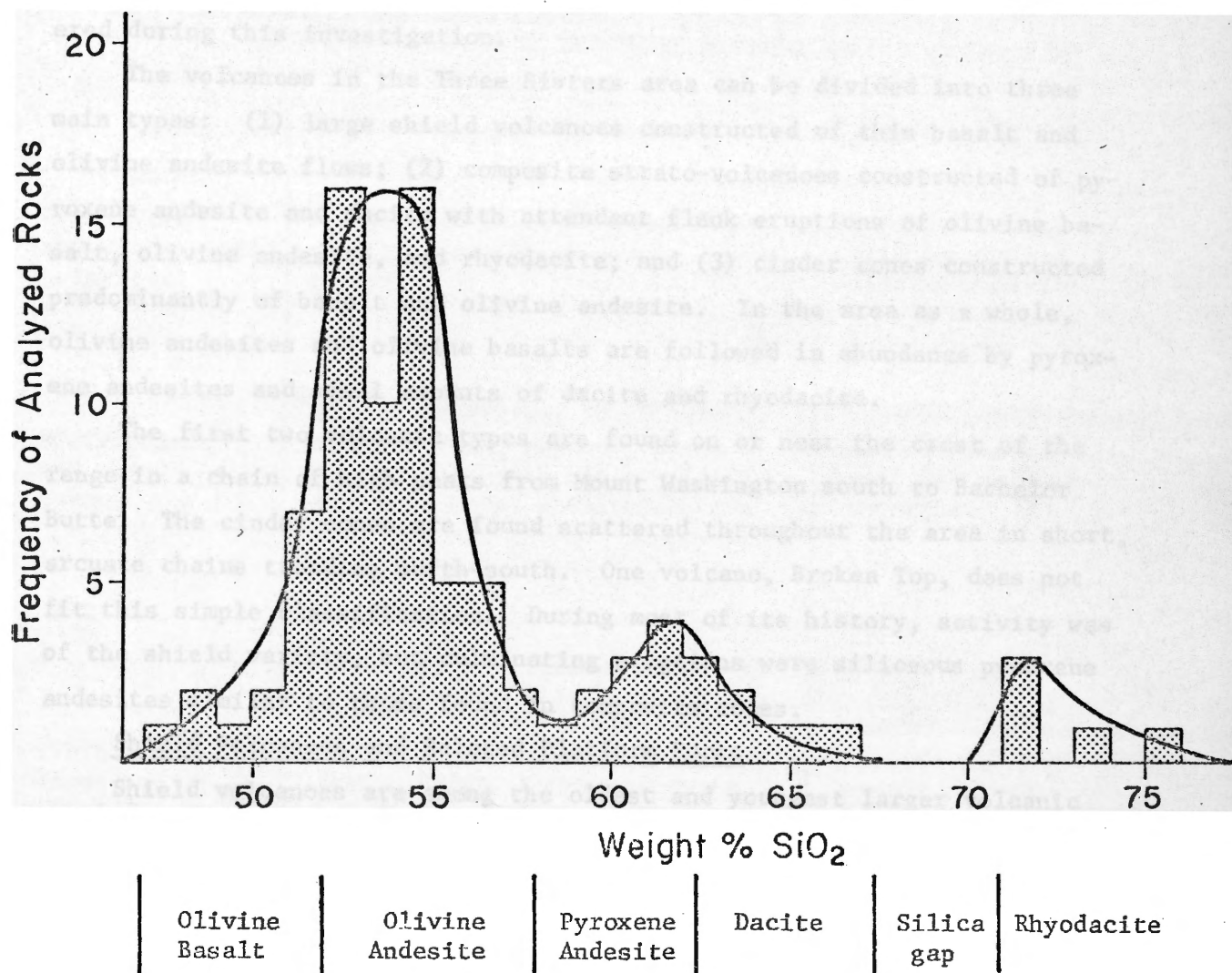


Figure 2. Histogram of Silica Values.

almost any scale in the future. Table 1 gives the approximate age relationships of eruptive centers for which analytical data have been gathered during this investigation.

The volcanoes in the Three Sisters area can be divided into three main types: (1) large shield volcanoes constructed of thin basalt and olivine andesite flows; (2) composite strato-volcanoes constructed of pyroxene andesite and dacite with attendant flank eruptions of olivine basalt, olivine andesite, and rhyodacite; and (3) cinder cones constructed predominantly of basalt and olivine andesite. In the area as a whole, olivine andesites and olivine basalts are followed in abundance by pyroxene andesites and small amounts of dacite and rhyodacite.

The first two volcanic types are found on or near the crest of the range in a chain of high peaks from Mount Washington south to Bachelor Butte. The cinder cones are found scattered throughout the area in short, arcuate chains trending north-south. One volcano, Broken Top, does not fit this simple classification. During most of its history, activity was of the shield variety, but culminating eruptions were siliceous pyroxene andesites similar to those found in composite cones.

Shield Volcanoes and Related Platform Rocks

Shield volcanoes are among the oldest and youngest larger volcanic structures in the area. The former include the North Sister, Mount Washington, Mount Scott, the Husband, and Broken Top (earlier history). Progressively younger shield volcanoes include Trout Creek Butte, Tumalo Mountain, and Belknap Crater, a very young structure. An early High Cascade platform was built by the coalescence of the oldest shield volcanoes and is composed of thin flows of diktytaxitic olivine basalt and olivine andesite. The oldest and least siliceous rocks, containing less than 50% silica, are found at the base of this platform.

Williams (1944) described the growth of the shield volcanoes with the North Sister as a model. Initial eruptions were of the quiet, effusive type which built an enormous, broad shield approximately 8000 feet high. This stage was capped by a steep summit cone, approximately 3000 feet high, built of pyroclastic material consisting of interbedded lapilli-

TABLE 1

APPROXIMATE AGE RELATIONSHIPS OF VOLCANOES AND THEIR
ASSOCIATED LAVAS IN THE THREE SISTERS AREA

Age	Volcanoes and Units	Rock Types
—Oldest		
Rocks have reverse magnetic polarity.	Flows with reverse magnetic polarity along Squaw Creek; Black Butte.	Mainly diktytaxitic basalt and olivine andesite.
—770,000 yrs. B. P.		
Early platform and shield lavas.	Diktytaxitic basalts from Tumalo Falls, near Trout Creek Butte, Santiam Pass, and near Black Butte; the North Sister, Little Brother, Mount Washington, the Husband, and the shield portion of Broken Top; Deer Butte.	All olivine basalt and olivine andesite.
Siliceous lavas and shield rocks of intermediate age.	Culminating siliceous eruptions of Broken Top (?); lavas of the Middle and South Sister; Two Butte; Garrison Butte; Scott Mt.; Graham Butte, Bluegrass Butte, and Sixmile Butte; Trout Creek Butte; siliceous flows of Kathleen Butte and Kokostick Butte; siliceous flows of Hayrick Butte and Hogg Rock; Hoodoo Butte; Tumalo Mountain.	Include olivine basalt, olivine andesite, pyroxene andesite, dacite, and rhyodacite.
Circa —10,000 yrs. B.P.		
Post-glacial shields and cinder cones. Earliest are forested.	Maxwell Butte; early Bachelor Butte and Belknap flows; Sims Butte; Sand Mountain group; Le Conte Crater; Nash Crater.	Include olivine basalt, olivine andesite, pyroxene andesite, dacite, and rhyodacite.
Recent shields, cinder cones, and siliceous flows. All are barren.	Later Bachelor Butte and Belknap flows; Cayuse Crater; Yapoah flows; Collier Cone; summit cone of South Sister; Newberry, Rock Mesa, and Devils Hill rhyodacites.	
—Youngest		

tuff, tuff-breccia, and scoria as well as vesicular basalt flows. This summit cone and the shield below it were cut by hundreds of dikes and sills during and after their growth. Late in the eruptive activity of the North Sister, a parasitic cone, the Little Brother, appeared on its western flank and duplicated the growth of its parent on a smaller scale.

The Husband and Mount Washington shield volcanoes (Brown, 1941) have very similar histories except for the presence of large central plugs. These shields and others in the area had their summit growth augmented by fissure eruptions on their flanks and by associated parasitic cones. Glaciation has bitten so deeply into the slopes of the older shields that their internal structures are almost completely exposed. All that remains of the summits of these older shields are radiating, knife-edge aretes separating deep, glacial cirques that lead into U-shaped canyons. Their original appearance prior to glaciation must have resembled that of Belknap Crater or Tumalo Mountain. The most siliceous lavas erupted by these volcanoes, as distinct from the composite cones, contain only 56-57% silica, except for the final eruptions of Broken Top, which are considerably more siliceous.

Composite Cones and Related Forms

The construction of the first large shields was followed by the development of centers that erupted more siliceous lavas. The two major volcanoes of this type are the Middle and South Sisters. The initial phases of activity for these two cones may have produced low broad shields (Williams, 1944), but the evidence for such forms has been obscured by later activity.

Both peaks consist chiefly of pale gray, platy pyroxene andesite and glassy, black dacite lavas interbedded with thin layers of scoria and pumice. Summit eruptions were accompanied by voluminous flank outpourings. Large, glassy dacite domes protruded from the slopes of both mountains. Somewhat less viscous andesites also erupted through fissures near the bases of the volcanoes. Rhyodacite flows with silica contents of 71% or more produced tabular obsidian sheets typified by obsidian cliffs on the western slopes of the Middle Sister. Just west of Green

Lakes at the eastern foot of the South Sister are some very old rhyodacitic flows which must have been among the initial eruptions of siliceous material from this volcano. The bulk of the foregoing activity was accomplished not long prior to and during the period of maximum glaciation.

Much later, the final eruptions near the summit of the Middle Sister, produced black, scoriaceous basalt flows. Similar rock occurs on the South Sister, whose summit is capped by two cones of dark scoria. The most recent cone still has a central crater lake and is quite youthful in appearance. The scoriaceous material on both peaks is more siliceous than its basaltic appearance would suggest. Analyses for silica of 57.5% (McBirney, 1968) and 59% (this report, Appendix II) show that these lavas can not properly be termed basalts, despite the presence of olivine, but rather fall near the boundary between olivine and pyroxene andesite.

Very recent fissure eruptions near the southern base of the South Sister have produced several large rhyodacitic domes and flows, notably the large flow that constructed Rock Mesa. In addition, a linear array of domical protrusions extends south parallel to the axis of the Cascade Range from Newberry (obsidian) to Devils Hill. The eruptions were undoubtedly very closely spaced in time. All of these lavas are extremely fresh in appearance and devoid of vegetation; surficial flow features are completely intact.

Other minor centers of siliceous eruptions include Hogg Rock and Hayrick Butte near Santiam Pass as well as several vents south of the South Sister at Kokostick and Kathleen Buttes. The latter two are probably closely associated with the history of the South Sister and may represent distant, flank-type eruptions. All of these flows are glaciated, siliceous, pyroxene andesites which closely resemble those found on the Middle and South Sisters.

Although the Middle and South Sister are imposing in stature relative to their surroundings, their siliceous andesites, dacites, and rhyodacites represent volumetrically a small fraction of the total material erupted along this segment of the High Cascades. The more basaltic flows from the surrounding shield volcanoes and cinder cones far outweigh them

in bulk.

Cinder Cones

Some of the numerous cinder cones merge with shield structures in cases where associated olivine basalt and olivine andesite flows form broad lava fields in and around the cones. Groups of cones commonly have distinct north-south alignments (E. M. Taylor, 1965) typified by the Sand Mountain group, Four-in-One alignment, and Yapoah-Collier cones. Other cones are erratically distributed about the area with no apparent relationship to other vents. These latter are typified by Le Conte Crater and Cayuse Cone to the south of the South Sister. The recently active cinder cones in all these groups have bleak slopes free of vegetation and are surrounded by fresh lava fields.

There are many examples of scoria cones that are much older. Black Butte to the east, despite its almost perfect symmetry, may be one of the oldest cones in the area (personal communication, E. M. Taylor). The Garrison Butte chain, Sixmile Butte, Graham Butte, and Hoodoo Butte are also older cinder cones with associated lava flows.

The cones are all similar in construction, and consist of small amounts of tuff-breccia and lapilli-tuff ejecta intermingled with the predominant scoria and cinders. Various sizes and shapes of bombs are also commonly present, together with accidental ejecta picked up by the eruptions as they passed through morainal debris and other ground cover. Voluminous lava flows often breached the walls of the cones and destroyed their otherwise perfect symmetry. These flows have scoriaceous, blocky, or ropy surfaces depending on their contents of silica and volatiles.

Cones and flows obviously related along lineaments have very similar lava types. The Sand Mountain group of vents built a large and complex lava field of thin, fluid, intertonguing flows with silica contents of 52 to 54%. The Yapoah-Collier vents and the vents in the Four-in-One alignment all produced significantly more siliceous lavas, 57-62% SiO₂, in distinctly lesser amounts. These more siliceous flows tend to be more blocky with high-standing margins, pressure-ridges, and lava-gutter drainage systems. Presumably, the near-surface plumbing produced a series of

cones closely related in time and composition in each of these instances.

Because of the physical similarity of all cinder cones in the area, regardless of the silica contents of their associated lavas, there has been a tendency by previous workers to emphasize the basaltic nature of this group at the expense of the more siliceous representatives. As a result, both Williams (1944) and later McBirney (1968), stressed the divergent character of the most recent eruptions. Very siliceous lavas were erupted south of the South Sister at Rock Mesa, Newberry, and Devils Hill during the same time interval that many of the younger cinder cones formed. However, Table 2 demonstrates the intermediate character of many recent flows and suggests that recent lavas of different composition were erupted in roughly the same proportions found among older flows in the area.

Both shield and cinder cone vulcanism have been continuous processes during the entire history of the High Cascades in this region. Older cinder cones are found only along the eastern edge of the area, but this is probably due to their total obliteration along the crest of the range by glacial advance. Undoubtedly their fragile structures were swept away by the ice. Black Butte and Garrison Butte are good examples of old cones that were beyond the reach of the glaciers.

PETROGRAPHY

Techniques

Ninety-seven thin sections were prepared for petrographic investigation. The universal stage was employed to determine compositions of feldspar, olivine, and pyroxene phenocrysts. Plagioclase microlites in the groundmass were also determined in some sections. Four polished sections were examined to determine compositions of groundmass opaque oxides in a representative sampling of olivine basalt, olivine andesite, pyroxene andesite, and dacite.

Olivine compositions were obtained by measuring the optic axial angle and correcting for refraction using Emmon's graph (1943, pl. 8). Forsterite was determined by comparing corrected values with those given on a graph prepared at Stanford by Dr. C. O. Hutton (personal communication).

TABLE 2
 SAMPLING
 OF PARTIAL MAJOR ELEMENT ANALYSES OF RECENT LAVA
 FLOWS FROM THE THREE SISTERS AREA
 (Total Iron Reported as FeO)

Sample *	10	29	67	68	80	87
SiO ₂	51.20	52.80	57.70	58.40	62.50	71.80
Al ₂ O ₃	16.00	17.30	18.00	17.20	18.00	15.30
FeO	9.00	8.60	7.00	7.20	6.50	2.90
MgO	8.50	7.20	5.00	3.50	2.30	0.70
CaO	9.40	8.20	7.20	6.40	4.70	2.10
Na ₂ O	**	**	3.15	4.43	3.40	**
K ₂ O	0.59	0.67	0.74	1.32	1.55	2.92
TiO ₂	1.06	1.30	0.74	1.29	0.63	0.32

* All analyses were performed by E. M. Taylor except for Na₂O, which were produced by the Oregon State Department of Geology and Mineral Industries.

** Na₂O analyses presently unavailable.

Location Key:

- 10 Flow from Cayuse Crater
- 29 Belknap Crater, western lava flow.
- 67 Collier Cone flow; sample collected near middle of series of related flows.
- 68 Cinder sample from summit cone of the South Sister.
- 80 Collier Cone; sample collected from flow near base of cone.
- 87 Devils Lake; recent extrusive dome of rhyodacite.

2V's are generally quite large for all the olivines measured (usually above 80°), and the corresponding large scatter for multiple determinations suggests that measurements are accurate to no more than $\pm 3^{\circ}$. This corresponds to $\pm 6\%$ Fo.

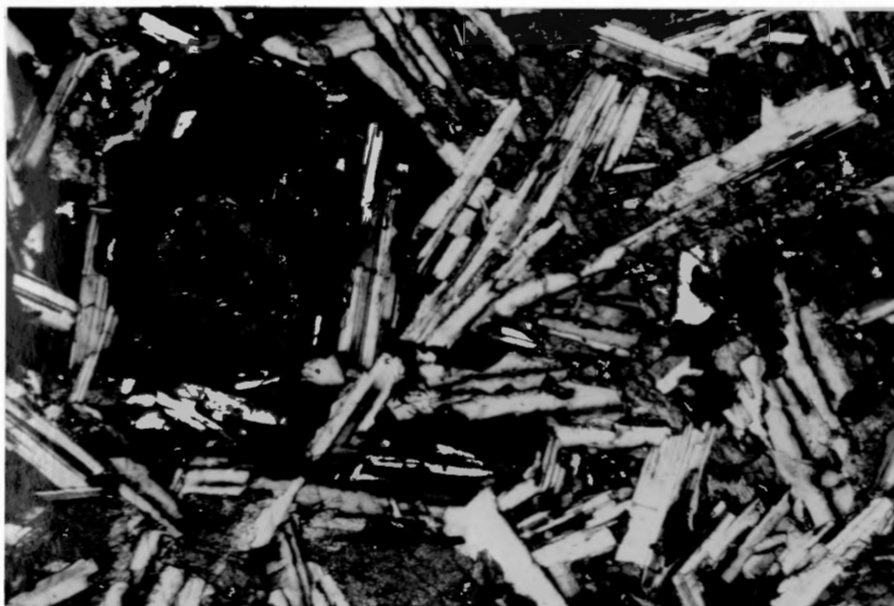
Plagioclase determinations were made using the a-normal method described by Rittmann (1929). This method is particularly good for rapidly and accurately obtaining compositions of zoned crystals. Extinction angles were compared to the high temperature curve on the graph by Tröger (1959, pl. 234, p. 111) to arrive at a composition for each crystal or multiple compositions for zones in zoned crystals. The measurements are accurate to less than $\pm 1^{\circ}$, which corresponds to about $\pm 2\%$ An.

Orthopyroxene compositions, accurate to $\pm 5\%$, were obtained by measuring optic axial angles and using the graph in Deer et al (1967, p. 28). Clinopyroxene determinations included both the measurement of 2V and the measurement of the beta refractive index by the oil immersion method. These values were plotted on the diagram of Hess (1949, p. 634) to give approximate compositions. The terminology for the pyroxenes is that of Poldervaart and Hess (1951). Clinopyroxenes in the rocks studied are exclusively augite.

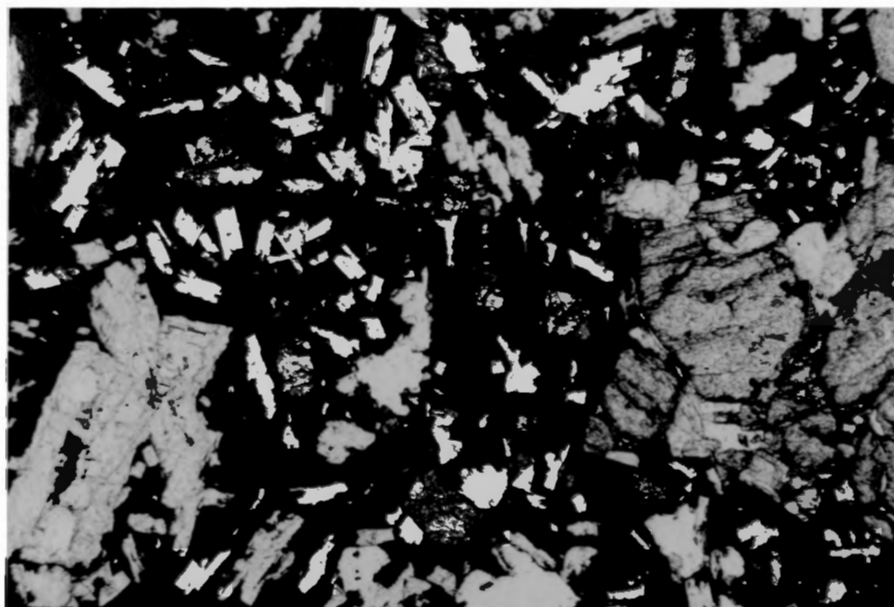
Olivine Basalt (<52% Silica)

Basalts occur as dense, pale to medium gray, nearly holocrystalline flows and as slaggy, scoriaceous, very dark gray to black, glassy flows. The former are predominant among the older shield and platform rocks while the latter are found among flows from recent cinder cones and shields like Belknap. Nowever, the subordinate variety in each case is not absent from either age group. In both types, olivine is the dominant phenocryst and constitutes from 3 to 10% of the rocks where present. Calcic plagioclase also occurs as phenocrysts but generally is distinctly subordinate to olivine. No completely aphanitic rocks were found; olivine is present in aphyric rocks as microphenocrysts. No oxide phenocrysts occur in any thin sections of basalt examined. Some specimens are quite vesicular, with 20-25% vesicles by volume, but most have only 5-15%.

The older, more coarsely crystalline flows have ophitic to subophitic, commonly diktytaxitic textures (Fig. 3a) with phenocrysts of olivine



A



B

Figure 3. Photomicrographs; X 60. (A) Diktytaxitic basalt from Look-out Point with ophitic calcic augite enclosing labradorite laths and iddingsitized olivine with a fresh core and rim (near extinction). Crossed nicols. (B) Olivine andesite from Belknap Crater with black glass enclosing phenocrysts and microphenocrysts of olivine and calcic labradorite. Plane-polarized light.

Fo₇₀₋₇₄ ($2V_{\gamma} = 83-85^{\circ}$). Calcic augite (Wo₄₁En₄₁Fs₁₈) encloses normally zoned plagioclase feldspars with bytownite cores (An₇₅₋₈₅) and labradorite rims (An₆₀ or greater). The olivines are commonly rimmed with opaques or altered to iddingsite. In some cases fresh cores of olivine have an outer zone of iddingsite overgrown by a rim of unaltered olivine of the same composition as the core. This phenomenon has been reported previously for the High Cascades by Greene (1968) at Mount Jefferson and by Sheppard (1962) in the Simcoe Mountains of Washington.

In many flows, the groundmass consists of a very fine-grained intergrowth of opaque minerals, clinopyroxene, and plagioclase microlites enclosing olivine and normally or oscillatorily zoned plagioclase phenocrysts. Olivine also occurs occasionally as a groundmass phase. The plagioclase microlites are commonly zoned with rims of intermediate to sodic andesine and with cores corresponding in composition to phenocryst rims. The predominant opaque oxide in the groundmass is magnetite with minor amounts of ilmenite also present. The textures in these rocks vary from intergranular to intersertal, with intergranular predominant; pilotaxitic textures are rare.

Glassy varieties of basalts have similar mineralogical characteristics. Olivine may be the only phenocryst present and commonly has a somewhat higher $2V_{\gamma}$, approximately $86-87^{\circ}$ and corresponding to Fo₇₇₋₈₀. Olivine in glassy rocks is generally fresh and unaltered. Plagioclase phenocrysts, where present, are typically complexly zoned with bytownite cores and intermediate to calcic labradorite rims. Groundmass plagioclase microlites are surrounded by black to brown glass rendered nearly opaque by oxide dust. Clinopyroxene needles are locally discernible in the glass. The textures are predominantly intersertal.

Pyroxene phenocrysts are completely lacking in the basalts. In most cases, groundmass clinopyroxene appears to be calcic augite. In the few instances where hypersthene (approximately En₆₉) occurs in the groundmass, olivine phenocrysts show signs of alteration to opaque oxides plus clay minerals or direct reaction to hypersthene.

Olivine Andesite (52-58% Silica)

The most abundant rock type in the area is low-silica, olivine-bearing andesite. Intergranular and intersertal textures grading to hyalophitic textures are common. Diktytaxitic and ophitic textures are rare. The lavas range from slabby, pale to medium gray, nearly holocrystalline flows to glassy, black vesicular varieties (Fig. 3b). These rocks generally contain more glass than the basalts, especially at the high-silica end of the range. Both olivine and plagioclase phenocrysts and microphenocrysts are typically present, and constitute from 3 to 50% of the rocks by volume. Most flows contain 10-15% phenocrysts. In rocks with less than 5% phenocrysts, olivine is typically more abundant than plagioclase, but plagioclase is dominant where more phenocrysts are present. In some instances, orthopyroxene takes the place of olivine. Augite and orthopyroxene are not common as phenocrysts in rocks with less than 57% silica. As with the basalts, magnetite is confined to the groundmass where it occurs either as tiny granules in holocrystalline lavas or as irresolvable, opaque dust in hypocrySTALLINE lavas. Minor amounts of ilmenite are also present in the groundmass of holocrystalline flows.

Olivine phenocrysts have $2V_Y = 80-87^\circ$ corresponding to compositions of Fe_{63-80} . Generally, olivines in the more recent glassy, black, scoriaceous lavas are relatively more magnesian (Fe_{75-78}) than those found in the holocrystalline older flows (Fe_{70-75}). Also, olivines from older flows more commonly show signs of iddingsitization or alteration to magnetite and other opaque minerals. Olivine alteration is especially marked where orthopyroxene is present as phenocrysts or in the groundmass. In these instances, olivine phenocrysts are either rimmed and embayed by granular hypersthene or by opaque minerals. Dark brown chrome spinel is a frequent inclusion in olivine phenocrysts of both basalt and olivine andesite. Olivine microphenocrysts (Fe_{63-70}) and groundmass olivine are relatively common as well. Groundmass olivine appears most frequently in flows that have clinopyroxene needles embedded in opaque, black glass but also occurs in holocrystalline rocks. Some groundmasses contain zoned olivines with very magnesian cores (Fe_{80} or higher) and ferrous rims (Fe_{65-75}). Olivine grains in rocks containing more than 56%

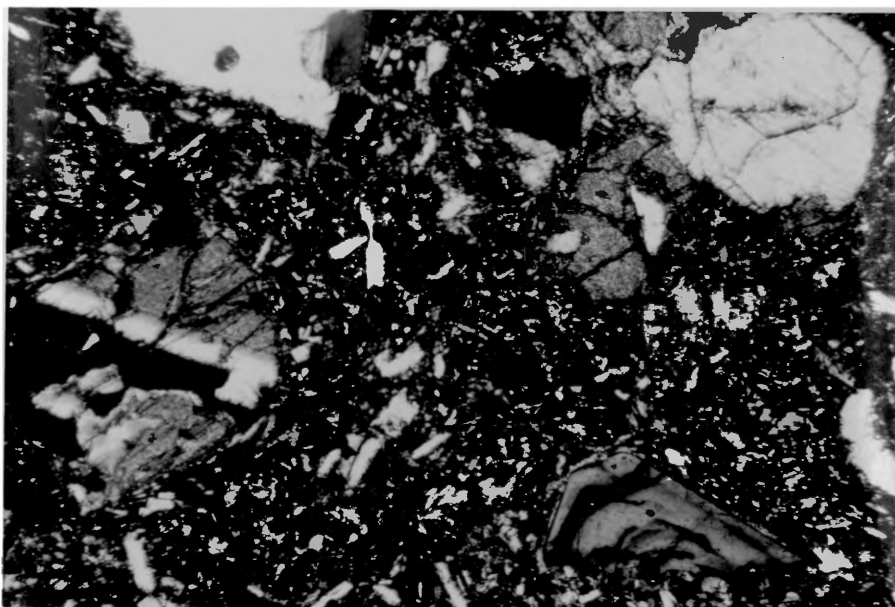
SiO_2 are invariably embayed, show replacement by hypersthene, or are altered in other ways.

Olivine andesites commonly contain 5-20% plagioclase phenocrysts by volume but locally contain 35% or more. The groundmass of holocrystalline flows is invariably 40% or more plagioclase microlites; glassy lavas usually have 20-30% plagioclase by volume in the groundmass. Most rocks display a complete range in size between microlites and phenocrysts, but rocks with only large plagioclase phenocrysts surrounded by tiny needles of plagioclase are also found. In some flows, plagioclase and other phenocrysts form clots producing glomero-porphyrritic textures (Fig. 4a). Normal, oscillatory, and reverse zoning is a prominent characteristic of the plagioclases. Phenocrysts invariably have cores with compositions ranging from calcic labradorite to calcic bytownite. Bytownite is by far the more common. Calcic andesine to intermediate labradorite form the outer zones. In low-silica rocks, the commonly euhedral bytownite cores are rimmed with a thin zone of labradorite. With increasing silica content, the outer zones become progressively wider as the cores are reduced in size. The most siliceous olivine andesites have irregular, embayed bytownite cores surrounded by wide, complexly zoned rims of andesine and labradorite. The inner zones and cores of the phenocrysts are often rimmed with granular opaque inclusions later covered by further crystal growth. Aligned or randomly oriented zircons and apatites are also often present within the cores or outer zones.

Although the more siliceous rocks tend to have more plagioclase phenocrysts, the phenocryst content does not increase in any regular way. Rocks with almost identical chemical analyses may contain from 5 to 45% plagioclase phenocrysts by volume. Without exception, the microphenocryst and groundmass plagioclase is more calcic (intermediate to calcic labradorite) in rocks with fewer phenocrysts (Fig. 5). Where plagioclase phenocrysts are abundant, groundmass microlites range from sodic andesine to sodic labradorite, depending on how prevalent and how calcic the larger plagioclase crystals are. Within any given rock, the outermost zones of the phenocrysts correspond in composition to the largest



A



B

Figure 4. Photomicrographs; X 60. (A) Glomero-porphyritic texture in olivine andesite from the Little Brother. Phenocrysts are olivine and labradorite in a groundmass of sodic labradorite, clinopyroxene, and oxides. Crossed nicols. (B) Olivine reacting to hypersthene in olivine andesite from the Middle Sister. Calcic augite and oscillatory zoned labradorite phenocrysts are also present in a groundmass of andesine microlites, granular oxides, clino- and orthopyroxene with minor glass. Crossed nicols.

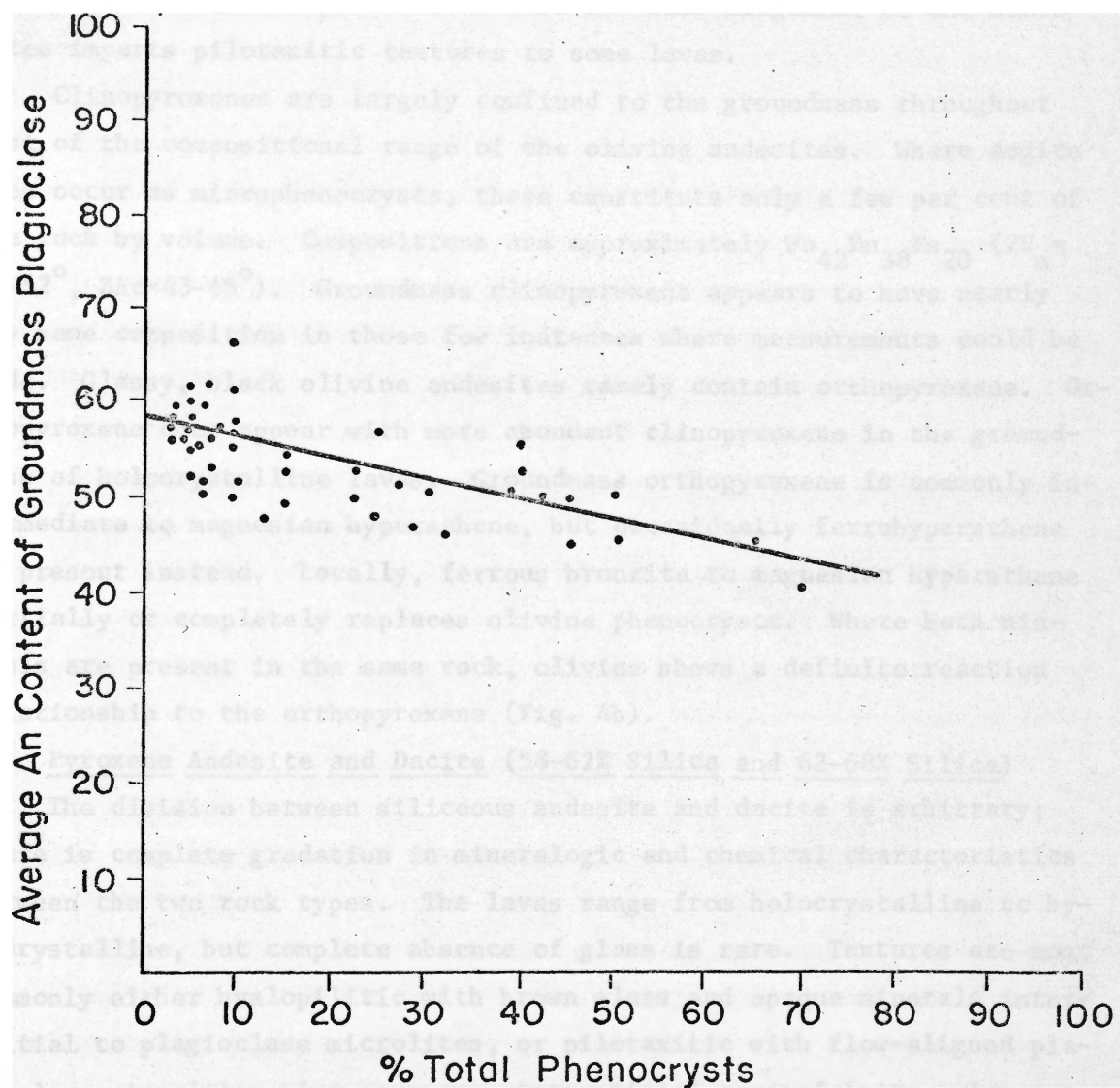


Figure 5. A plot of per cent phenocrysts by volume versus anorthite content of groundmass plagioclase for olivine basalts and olivine andesites from the Three Sisters area.

groundmass microlites present. Occasional flow alignment of the microlites imparts pilotaxitic textures to some lavas.

Clinopyroxenes are largely confined to the groundmass throughout most of the compositional range of the olivine andesites. Where augite does occur as microphenocrysts, these constitute only a few per cent of the rock by volume. Compositions are approximately $Wo_{42}En_{38}Fs_{20}$ ($2V_{\alpha} = 49-52^{\circ}$, $ZAc = 43-45^{\circ}$). Groundmass clinopyroxene appears to have nearly the same composition in those few instances where measurements could be made. Glassy, black olivine andesites rarely contain orthopyroxene. Orthopyroxene does appear with more abundant clinopyroxene in the groundmass of holocrystalline lavas. Groundmass orthopyroxene is commonly intermediate to magnesian hypersthene, but occasionally ferrohypersthene is present instead. Locally, ferrous bronzite to magnesian hypersthene partially or completely replaces olivine phenocrysts. Where both minerals are present in the same rock, olivine shows a definite reaction relationship to the orthopyroxene (Fig. 4b).

Pyroxene Andesite and Dacite (58-62% Silica and 62-68% Silica)

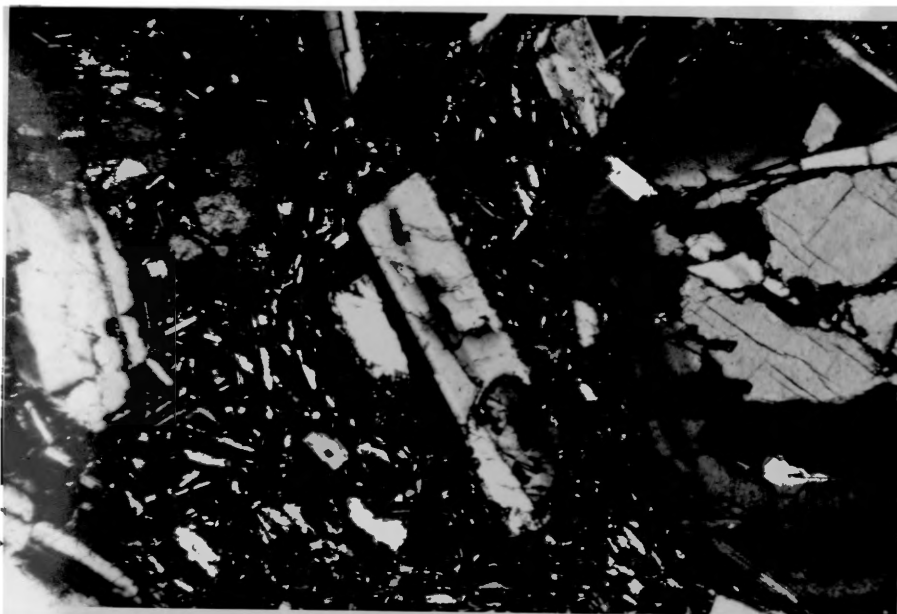
The division between siliceous andesite and dacite is arbitrary; there is complete gradation in mineralogic and chemical characteristics between the two rock types. The lavas range from holocrystalline to hypocrystalline, but complete absence of glass is rare. Textures are most commonly either hyalopilitic with brown glass and opaque minerals interstitial to plagioclase microlites, or pilotaxitic with flow-aligned plagioclase microlites plus pyroxene, interstitial cryptofelsite, glass, and iron oxides. In both cases, phenocrysts commonly constitute 5-20% of the rock by volume. Vitrophyric and aphyric (usually pilotaxitic) textures are less frequently encountered. The major phenocrysts are intermediate plagioclase, calcic augite, and hypersthene. Blocky, euhedral, magnetite microphenocrysts occur in the groundmass and as inclusions in larger plagioclase and pyroxene phenocrysts. Rarely, phenocrysts of olivine partly altered to hypersthene or opaque oxides plus quartz, but occasionally nearly euhedral, are present. Clustering of the various types of phenocrysts to produce glomero-porphyritic textures is common.

Vesicles are often lined with tiny opaque grains and cristobalite or tridymite. Groundmass opaque granules are predominantly magnetite; ilmenite is also present in minor amounts.

Plagioclase phenocrysts normally constitute 10-15% of the rocks by volume. As in olivine andesite, the phenocrysts exhibit normal, oscillatory, and, less frequently, reverse zoning. The cores, however, are usually calcic andesine to sodic labradorite. A few rocks, some with as much as 65% silica, have large phenocrysts with irregular, embayed, calcic labradorite and bytownite cores (Fig. 6a). These rocks usually have other phenocrysts, without calcic cores, of the same composition as the outer zones of the cored plagioclases. The outer zones range from sodic andesine to sodic labradorite in composition. There is typically a definite break in composition between the calcic, relatively unzoned cores and the complexly zoned outer portions. Brown glass blebs, opaque minerals, zircons, and apatite needles are frequently present as inclusions.

Groundmass plagioclase ranges from intermediate oligoclase to sodic labradorite. Sodic to calcic andesine is the most common microlitic composition. The largest groundmass microlites compare closely in composition with the outermost phenocryst zones. Aphyric rocks generally have aligned plagioclase needles ranging from calcic andesine to sodic labradorite. There is only a moderate increase of soda in plagioclase phenocrysts and microlites from the least to most siliceous rocks in the pyroxene andesite-dacite field.

Clinopyroxene is typically present both as a groundmass and phenocryst phase. Groundmass clinopyroxene grains interstitial to plagioclase microlites are far too small for determinations to be made optically. The phase locally constitutes up to 25% of the groundmass. Phenocrysts are invariably pale green, calcic augite with slightly smaller 2V's (48-49°) than those found in olivine andesites. Approximate compositions from R. I. and 2V measurements are $Wo_{40}En_{35}Fs_{25}$ to $Wo_{43}En_{42}Fs_{15}$. Augite phenocrysts become progressively less abundant as silica increases and usually amount to less than 5% of the total phenocrysts present in dacite. Zoning is relatively common; presumably the outer rim becomes



A



B

Figure 6. Photomicrographs; X 60. (A) Plagioclase phenocryst with bytownite core and oscillatory zoned labradorite rim in pyroxene andesite from Middle Sister. Uncored labradorite, augite, and olivine reacting to hypersthene also present in a groundmass of sodic labradorite laths, clinopyroxene, granular oxides, and glass. (B) Zoned sodic labradorite-calcic andesine phenocryst with magnetite inclusions in dacite from Middle Sister. Hypersthene phenocrysts with magnetite and olivine bleb-like inclusions in pilotaxitic groundmass of andesine laths, clinopyroxene, oxides, and glass. Both photographed with crossed nicols.

progressively enriched in ferrous iron.

Orthopyroxene occurs as a groundmass mineral as well as phenocrysts. The latter are ferrous to magnesian hypersthene (occasionally ferrous bronzite) in the andesitic range of silica values and ferrous hypersthene to magnesian ferrohypersthene toward the dacitic end. Very strongly zoned orthopyroxenes occasionally have eulite rims. Orthopyroxene is the dominant pyroxene in the dacites. Groundmass orthopyroxenes occurring as slender needles and ragged interstitial patches have approximately the same composition as the phenocrysts. In the few instances where 2V's could be measured, compositions of intermediate to magnesian hypersthene were obtained.

Olivine phenocrysts occur in a few of the flows. They are typically deeply embayed and partly altered to hypersthene or iron oxides plus quartz, and have compositions (Fo₇₀₋₈₀) similar to those found in olivine andesite (Fig. 6a). Although most crystals tend toward the more ferrous compositions, large phenocrysts in the Collier Cone lavas (57.5-62.0% SiO₂) are as magnesian (Fo₇₉₋₈₂) as any found in the least siliceous lavas. Olivine also occurs in even more siliceous rocks, containing up to 65% SiO₂, as irregular, highly birefringent blebs in ferrous hypersthene phenocrysts (Fig. 6b). Unconnected blebs within a single hypersthene crystal often exhibit simultaneous extinction when rotated on the microscope stage under crossed nicols.

Rhyodacite (>71% Silica)

The most siliceous rocks in the area are separated from the dacites by a "silica gap" in the continuum of rock compositions. Rocks containing 68-71% silica are not found. The rhyodacites form a small, distinctive group of lavas with very similar mineralogic and textural characteristics. Phenocrysts and microphenocrysts of plagioclase, orthopyroxene, and magnetite may constitute up to 20% of a sample by volume. Fresh flows have a dense, glassy, gray to black groundmass filled with needles of pyroxene (?) and streams of sodic plagioclase microlites (Fig. 7). Some flows are devoid of phenocrysts; others are streaked with frothy, pumiceous bands and layers. The groundmass of older flows has usually

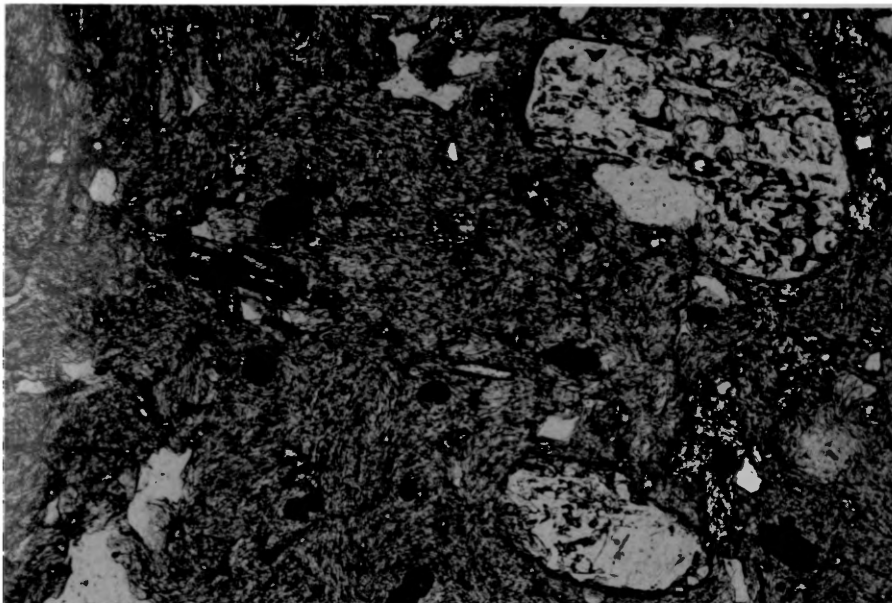


Figure 7. Photomicrograph; X 60. Rhyodacite from Devils Hill with corroded sodic andesine phenocrysts containing brown glass-bleb inclusions in a glassy matrix filled with needles of oligoclase. Microphenocrysts of magnetite and ferrohypersthene are also present. Plane-polarized light.

devitrified to a pinkish, banded cryptofelsite. Tridymite (?), cristobalite, opal, acicular apatite, and tiny prisms of oxyhornblende are minor accessories. Hornblende, biotite, and potassic feldspar are absent as crystalline phases.

Corroded phenocrysts of sodic to calcic andesine with oligoclase rims can constitute up to 15% of the rhyodacites by volume. Brown glass inclusions and weak normal, reverse, and oscillatory zoning are common in plagioclase phenocrysts. The orthopyroxene phenocrysts usually are less than 3-5% of the volume and range in composition from ferrous ferrohypersthene to intermediate hypersthene. Ferric varieties are the most prevalent. Groundmass plagioclase microlites have oligoclase compositions.

ANALYTICAL PROCEDURES FOR TRACE AND MAJOR ELEMENT DETERMINATIONS

Complete details of sample preparation and analytical techniques for trace element determination are given in Appendix I. Only a very brief summary is presented here.

Samples were reduced to -200 mesh with a jaw crusher and rotating disc pulverizer, each with aluminum oxide plates. Samples were split to appropriate weight fractions and ground to -350 mesh with an agate mortar and pestle.

The powdered sample was then mixed with an equal weight of -350 mesh, Spec-pure graphite, containing an internal standard, and burned in a Jarrell-Ash emission spectrograph. Line intensities obtained from photographic plates were compared with those from a series of artificial oxide standards.

All major elements but Na were determined for 85 samples by Dr. E. M. Taylor using an X-ray fluorescence technique at Oregon State University. Atomic absorption was employed in Na determinations; this work was performed by the Oregon State Department of Geology and Mineral Industries. Eighteen samples were analyzed for major elements by Dr. Norman Suhr of Pennsylvania State University, using emission spectrography. He reported an accuracy of $\pm 5\%$ relative error for each determination. Dr. Taylor's data on major elements is incomplete and subject to future revisions.

ANALYTICAL RESULTS

Major Element Chemistry

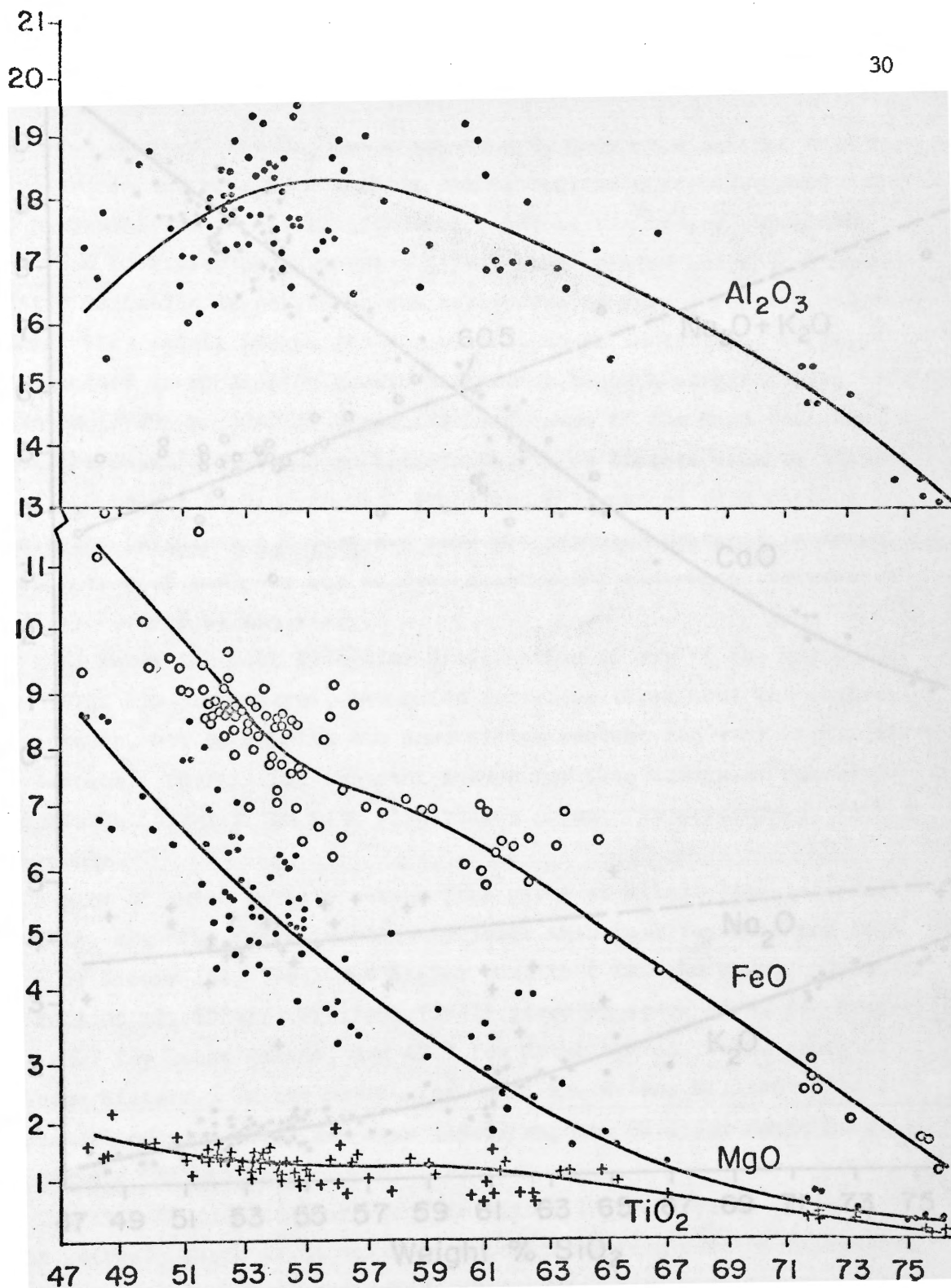
A complete list of partial silicate analyses for the Three Sisters area is presented in Appendix II, Tables 10 and 11. Unfortunately, Dr. Taylor could not forward complete determinations of sodium for all samples prior to this report. With this restriction in mind, silica variation diagrams and AMF-CNK diagrams have been constructed using the available data.

Alumina values show considerable scatter when plotted on a silica variation diagram (Fig. 8), especially at the low-silica end of the rock sequence. They appear to go through a maximum between 54 and 55 per cent silica. As far as can be ascertained from petrographic data, there is no relationship between Al_2O_3 weight per cent and the volume percentage of plagioclase phenocrysts present in a rock throughout the olivine andesite-olivine basalt field. High alumina values can be found in rocks containing from 5 to 35% or more plagioclase phenocrysts by volume. Alumina decreases in a regular way throughout the more silicic range of analyses, although there is still considerable scatter.

Both iron oxide and magnesia decrease with increasing silica content throughout the entire range of silica values, and both show considerable scatter when plotted against SiO_2 (Fig. 8). Ratios of FeO/MgO are always greater than 1.0 but are usually less than 2.0 for the olivine basalts, olivine andesites, and most of the pyroxene andesites. Dacites and rhyodacites have higher FeO/MgO values.

The trend of decreasing lime with increasing silica is almost linear and shows less scatter than most of the other major elements (Fig. 9). Lime content does not vary sympathetically with alumina content, suggesting that the two are not controlled by the behavior of the plagioclase phenocrysts. Since calcic augite is a very uncommon phenocryst phase in rocks with less than 58% SiO_2 , it also should not affect the CaO trend within the olivine basalt-olivine andesite range of silica values.

The alkalis show the expected increase with increasing silica content



Olivine Basalt	Olivine Andesite	Pyroxene Andesite	Dacite	Silica Gap	Rhyodacite
-------------------	---------------------	----------------------	--------	---------------	------------

Figure 8. Silica variation diagram for Al₂O₃, FeO, MgO, and TiO₂. Total iron reported as FeO. Plots based on analyses not recalculated to 100%.

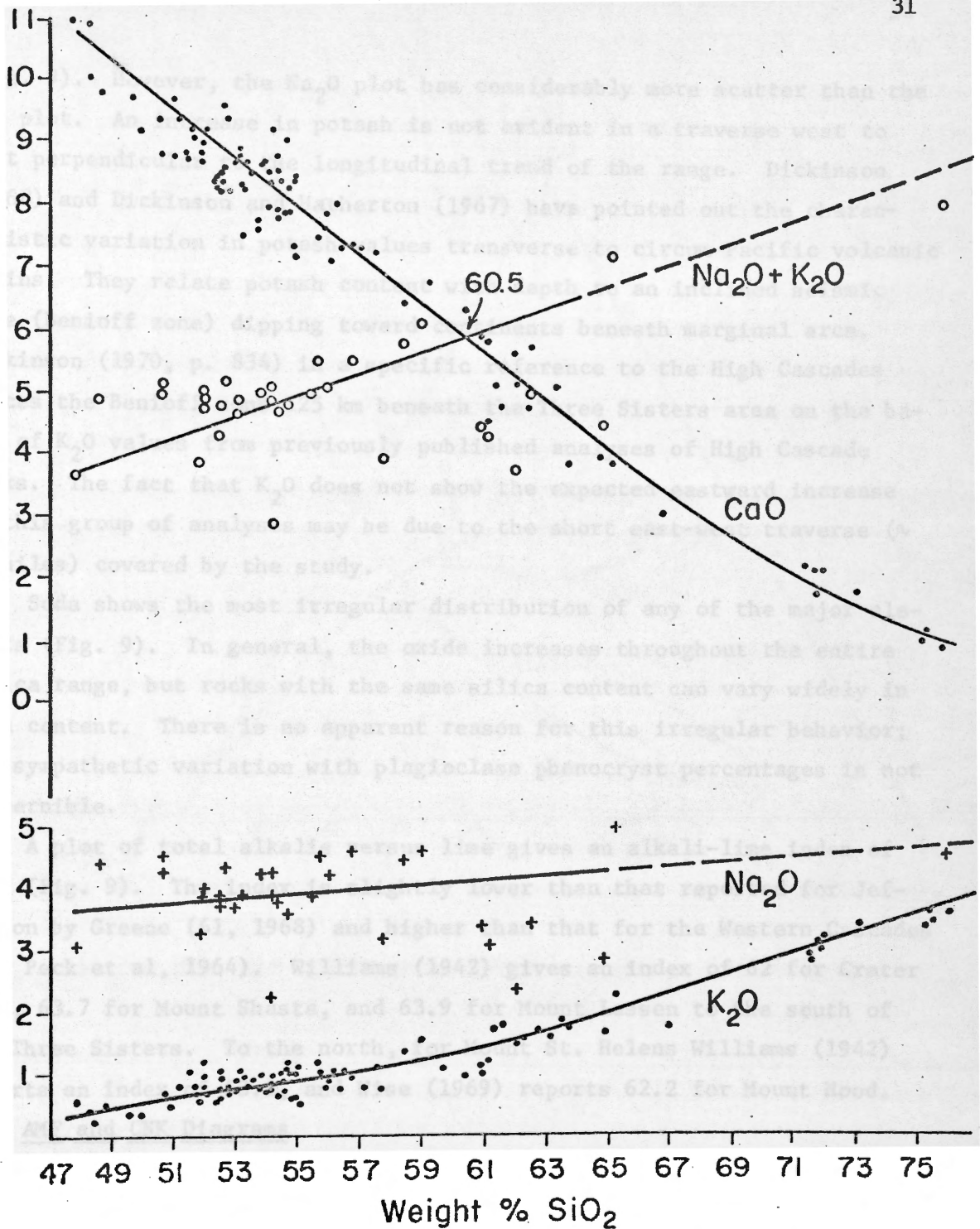


Figure 9. Silica variation diagram for CaO, Na₂O, and K₂O. Plots based on analyses in Appendix II; analyses not recalculated to 100%.

(Fig. 9). However, the Na_2O plot has considerably more scatter than the K_2O plot. An increase in potash is not evident in a traverse west to east perpendicular to the longitudinal trend of the range. Dickinson (1968) and Dickinson and Hatherton (1967) have pointed out the characteristic variation in potash values transverse to circum-Pacific volcanic chains. They relate potash content with depth to an inclined seismic zone (Benioff zone) dipping toward continents beneath marginal arcs. Dickinson (1970, p. 834) in a specific reference to the High Cascades places the Benioff zone 125 km beneath the Three Sisters area on the basis of K_2O values from previously published analyses of High Cascade rocks. The fact that K_2O does not show the expected eastward increase in this group of analyses may be due to the short east-west traverse (~ 25 miles) covered by the study.

Soda shows the most irregular distribution of any of the major elements (Fig. 9). In general, the oxide increases throughout the entire silica range, but rocks with the same silica content can vary widely in soda content. There is no apparent reason for this irregular behavior; any sympathetic variation with plagioclase phenocryst percentages is not discernible.

A plot of total alkalis versus lime gives an alkali-lime index of 60.5 (Fig. 9). The index is slightly lower than that reported for Jefferson by Greene (61, 1968) and higher than that for the Western Cascades (60, Peck et al, 1964). Williams (1942) gives an index of 62 for Crater Lake, 63.7 for Mount Shasta, and 63.9 for Mount Lassen to the south of the Three Sisters. To the north, for Mount St. Helens Williams (1942) reports an index of 63.2, and Wise (1969) reports 62.2 for Mount Hood.

AMF and CNK Diagrams

The AMF-CNK diagrams presented in Figure 10 are typical of calc-alkaline suites. There is no indication of strong iron enrichment typical of the Skaergaard or Hawaiian trends (Turner and Verhoogen, 1960, p. 234). Olivine basalts, olivine andesites, pyroxene andesites, and dacites plot as a cluster in the center of the AMF diagram. The two rhyodacite analyses for which Na_2O is available plot far toward the alkali corner.

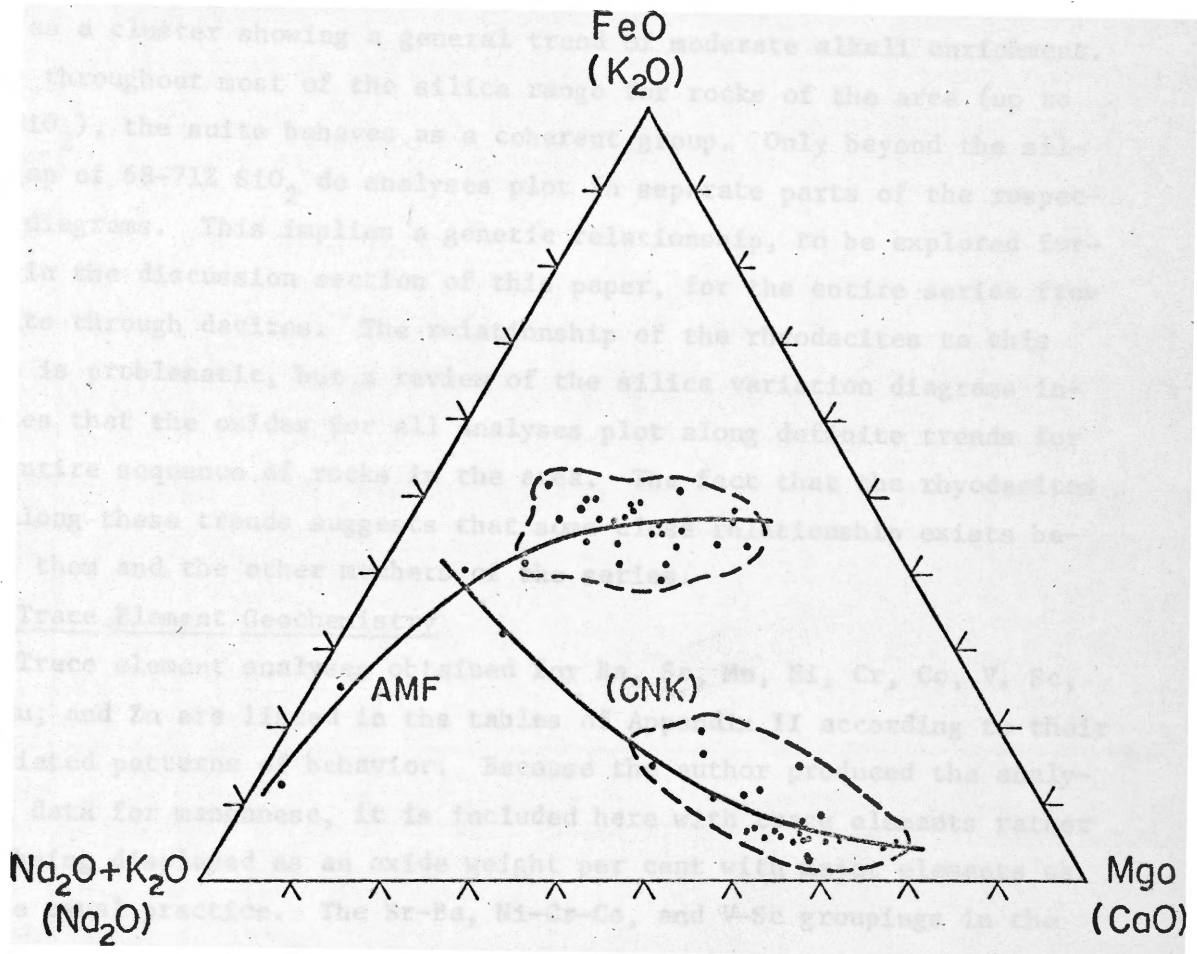


Figure 10. AMF-CNK diagrams. Total iron reported as FeO.

Likewise for the CNK diagram, all analyses but those of the rhyodacites plot as a cluster showing a general trend of moderate alkali enrichment. Thus, throughout most of the silica range for rocks of the area (up to 68% SiO_2), the suite behaves as a coherent group. Only beyond the silica gap of 68-71% SiO_2 do analyses plot in separate parts of the respective diagrams. This implies a genetic relationship, to be explored further in the discussion section of this paper, for the entire series from basalts through dacites. The relationship of the rhyodacites to this group is problematic, but a review of the silica variation diagrams indicates that the oxides for all analyses plot along definite trends for the entire sequence of rocks in the area. The fact that the rhyodacites lie along these trends suggests that some close relationship exists between them and the other members of the series.

Trace Element Geochemistry

Trace element analyses obtained for Ba, Sr, Mn, Ni, Cr, Co, V, Sc, Zr, Cu, and Zn are listed in the tables of Appendix II according to their associated patterns of behavior. Because the author produced the analytical data for manganese, it is included here with trace elements rather than being displayed as an oxide weight per cent with major elements as is the usual practice. The Sr-Ba, Ni-Cr-Co, and V-Sc groupings in the following discussion appear to have a petrogenetic basis; inferences made from trace element data will be discussed in the next section with specific reference to the validity of a fractional crystallization hypothesis as a model for the production of calc-alkaline rocks in the Three Sisters area. Ni, Cr, and Co trends in particular, appear to contain valuable petrogenetic information, and comments on these three elements come after discussions of the other trace elements.

(Sr-Ba)

The Sr-silica plot resembles the silica variation diagram for alumina (Fig. 11); both plots pass through maxima near 54% SiO_2 . However, there is no discernible sympathetic variation of the two elements when individual analyses from Appendix II are compared. Sr and CaO show only limited sympathetic variation in Figure 12; a plot of Na_2O against Sr.

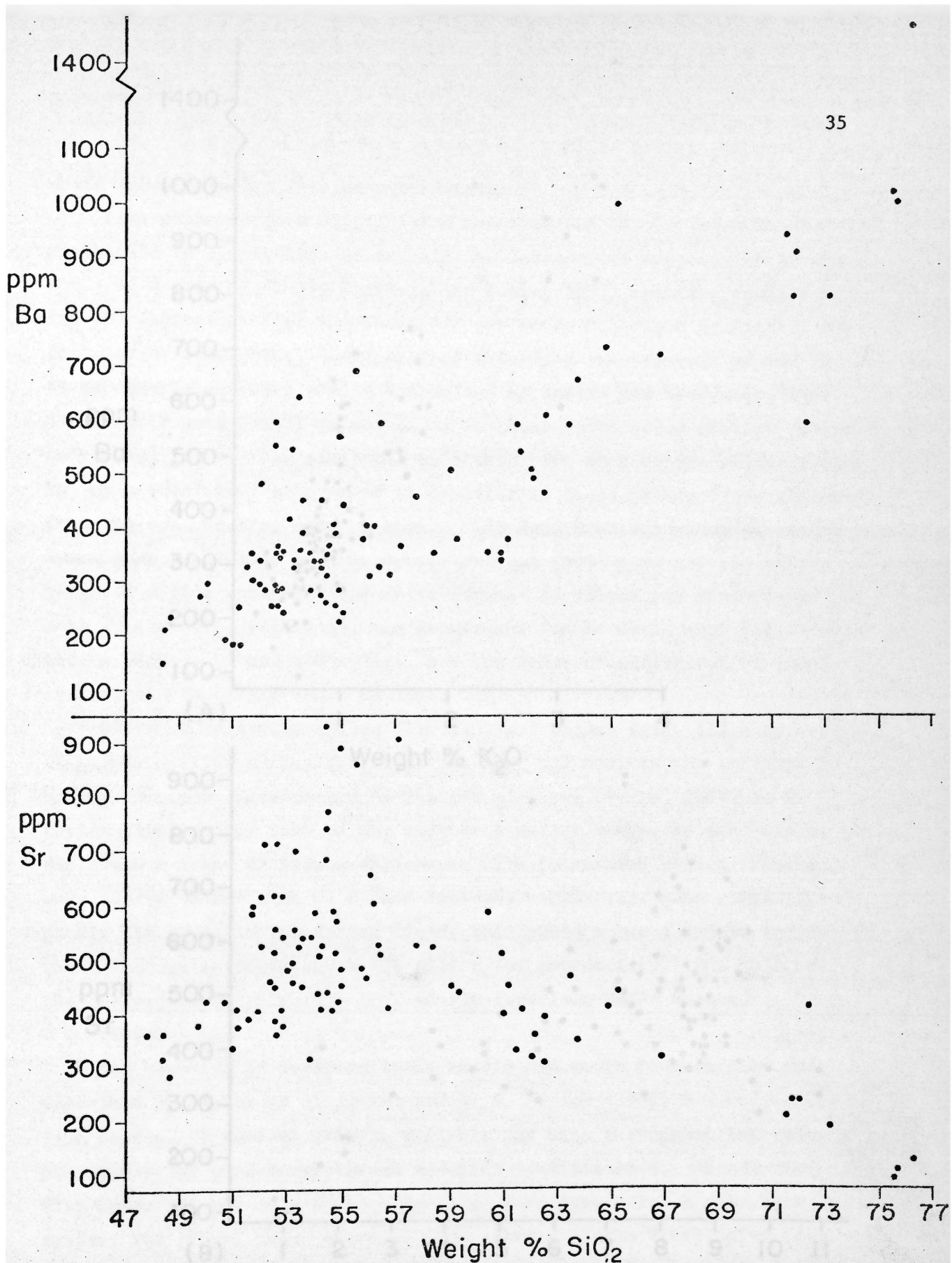


Figure 11. Plots of Ba and Sr ppm versus weight % SiO₂.

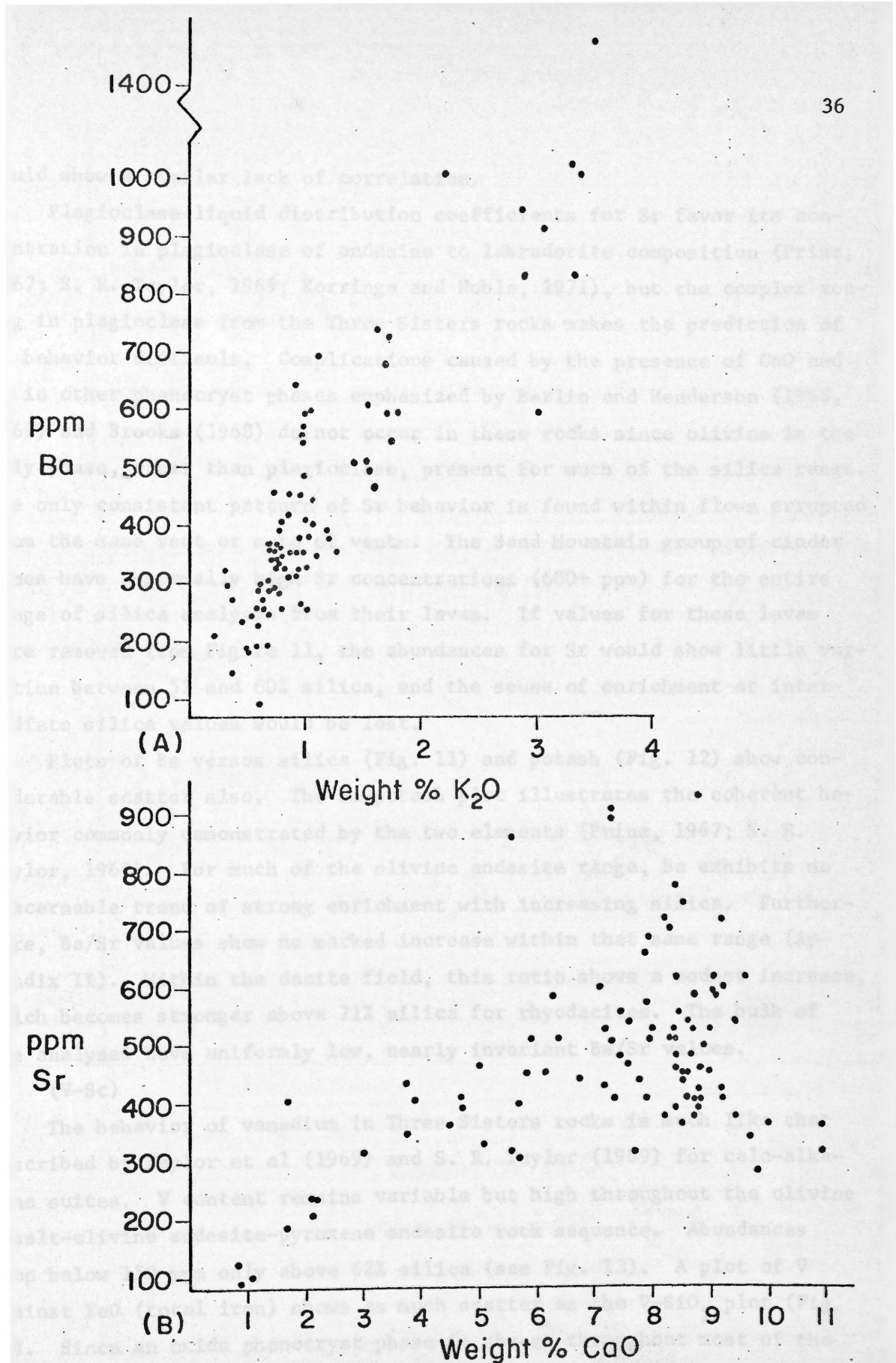


Figure 12. (A) Plot of Ba versus potash. (B) Plot of Sr versus lime.

would show a similar lack of correlation.

Plagioclase-liquid distribution coefficients for Sr favor its concentration in plagioclase of andesine to labradorite composition (Prinz, 1967; S. R. Taylor, 1969; Korrington and Noble, 1971), but the complex zoning in plagioclase from the Three Sisters rocks makes the prediction of Sr behavior difficult. Complications caused by the presence of CaO and Sr in other phenocryst phases emphasized by Berlin and Henderson (1968, 1969) and Brooks (1968) do not occur in these rocks since olivine is the only phase, other than plagioclase, present for much of the silica range. The only consistent pattern of Sr behavior is found within flows erupted from the same vent or sets of vents. The Sand Mountain group of cinder cones have abnormally high Sr concentrations (600+ ppm) for the entire range of silica analyses from their lavas. If values for these lavas were removed from Figure 11, the abundances for Sr would show little variation between 52 and 60% silica, and the sense of enrichment at intermediate silica values would be lost.

Plots of Ba versus silica (Fig. 11) and potash (Fig. 12) show considerable scatter also. The Ba-potash plot illustrates the coherent behavior commonly demonstrated by the two elements (Prinz, 1967; S. R. Taylor, 1969). For much of the olivine andesite range, Ba exhibits no discernable trend of strong enrichment with increasing silica. Furthermore, Ba/Sr values show no marked increase within that same range (Appendix II). Within the dacite field, this ratio shows a modest increase, which becomes stronger above 71% silica for rhyodacites. The bulk of the analyses have uniformly low, nearly invariant Ba/Sr values.

(V-Sc)

The behavior of vanadium in Three Sisters rocks is much like that described by Taylor et al (1969) and S. R. Taylor (1969) for calc-alkaline suites. V content remains variable but high throughout the olivine basalt-olivine andesite-pyroxene andesite rock sequence. Abundances drop below 150 ppm only above 62% silica (see Fig. 13). A plot of V against FeO (total iron) shows as much scatter as the V-SiO₂ plot (Fig. 13). Since an oxide phenocryst phase is absent throughout most of the

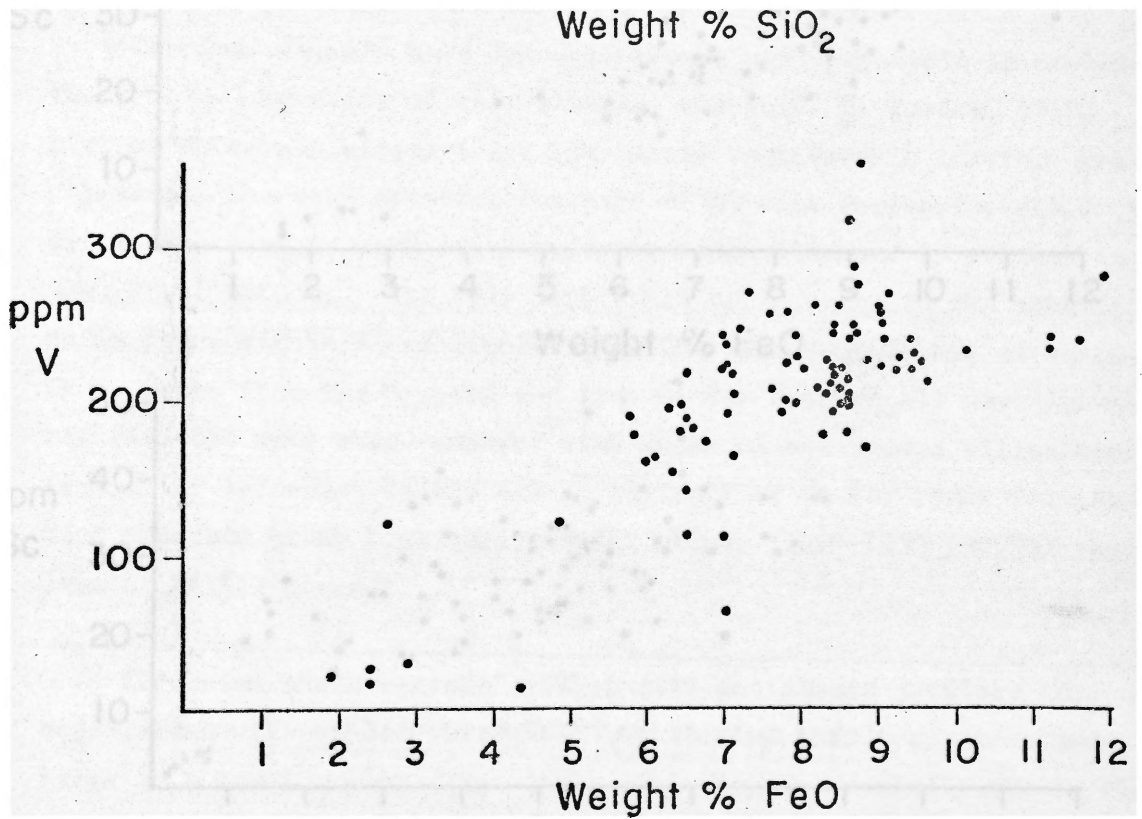
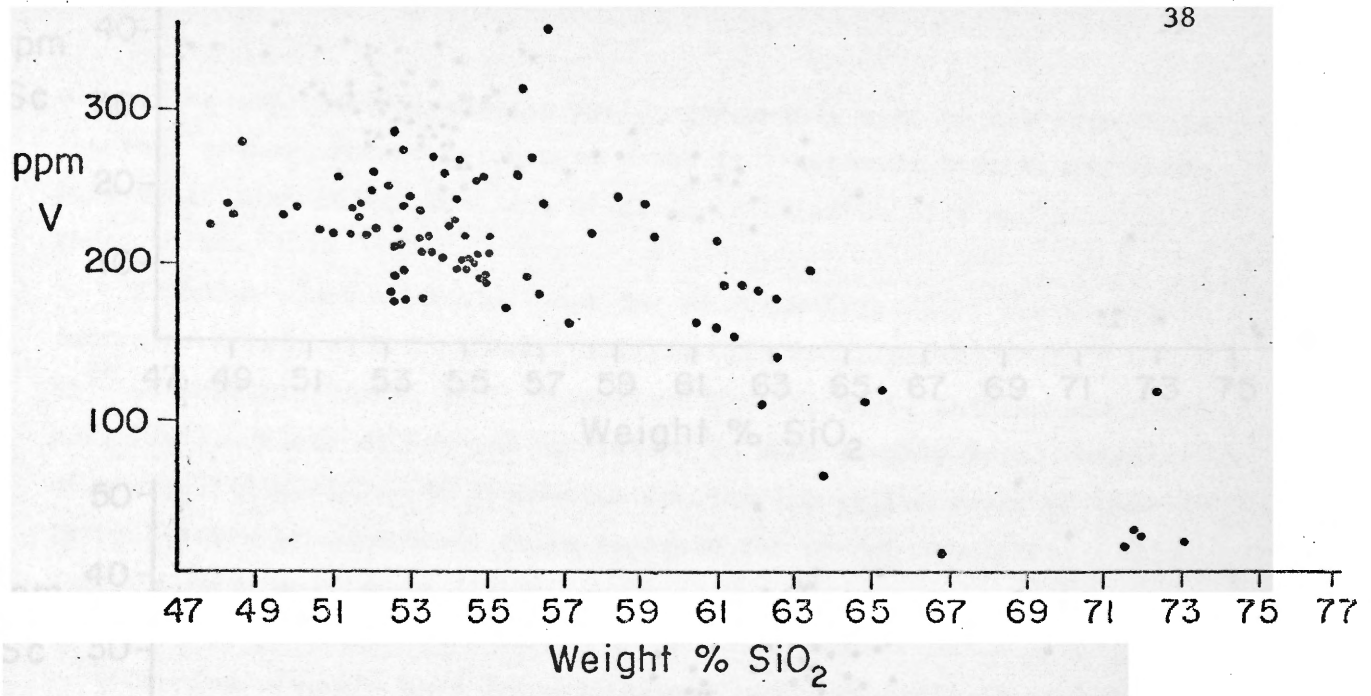


Figure 13. Plots of ppm V versus weight % SiO₂ and FeO.

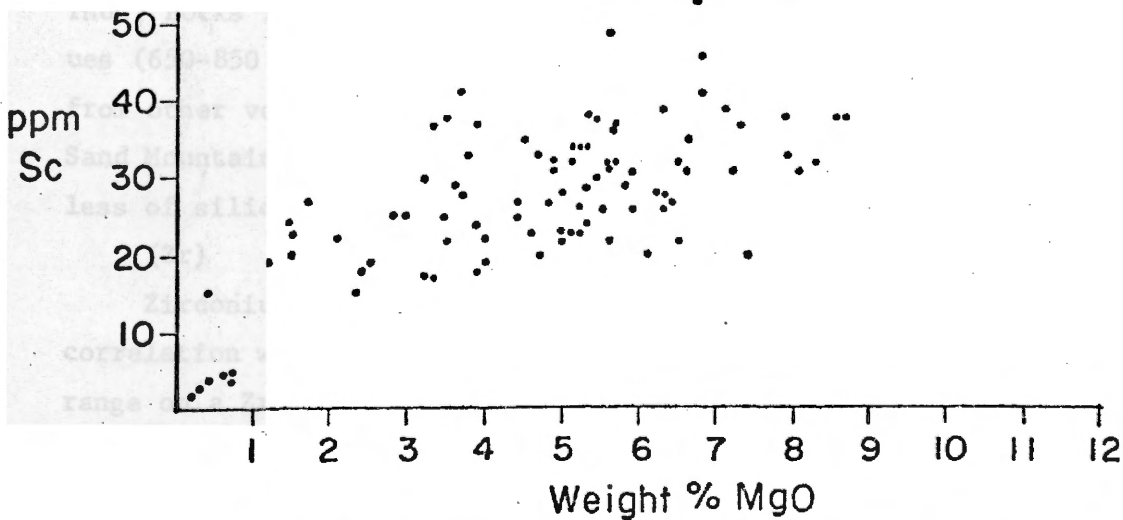
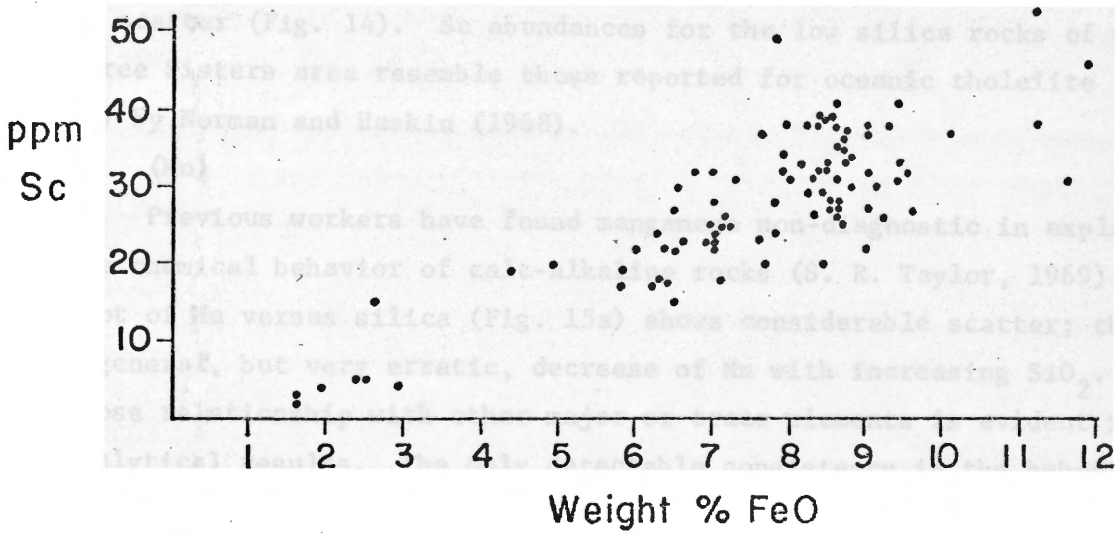
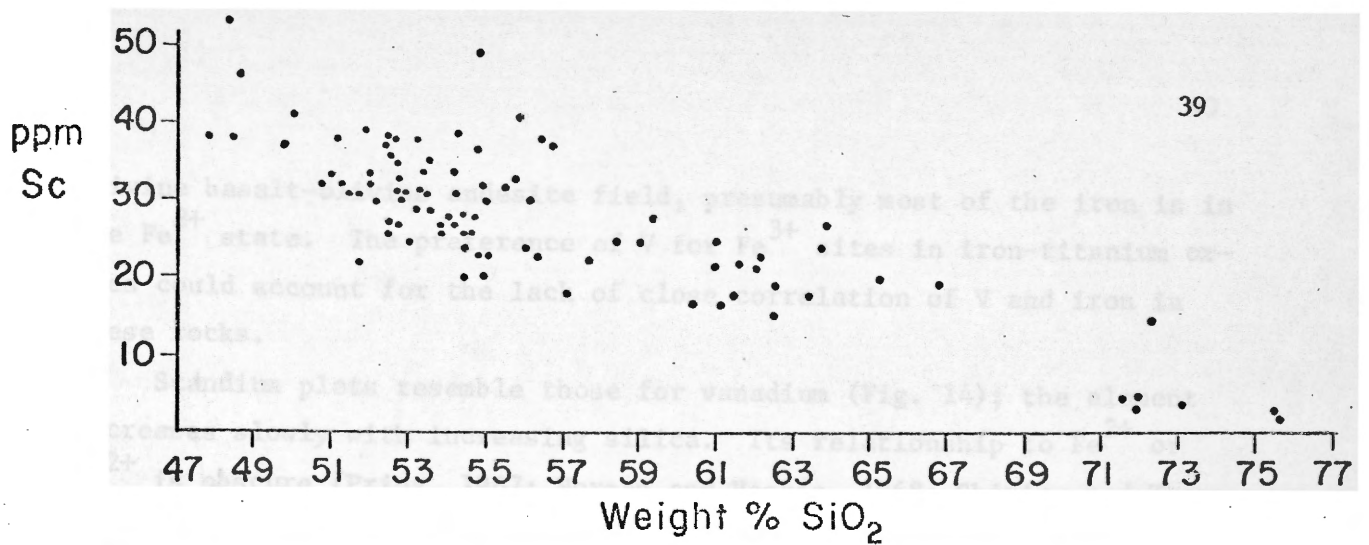


Figure 14. Plots of ppm Sc versus weight % SiO₂, FeO, and MgO.

olivine basalt-olivine andesite field, presumably most of the iron is in the Fe^{2+} state. The preference of V for Fe^{3+} sites in iron-titanium oxides could account for the lack of close correlation of V and iron in these rocks.

Scandium plots resemble those for vanadium (Fig. 14); the element decreases slowly with increasing silica. Its relationship to Fe^{2+} or Mg^{2+} is obscure (Prinz, 1967; Norman and Haskin, 1968; Shimizu and Kuroda, 1969). Plots of FeO and MgO versus Sc show roughly equal amounts of scatter (Fig. 14). Sc abundances for the low silica rocks of the Three Sisters area resemble those reported for oceanic tholeiite (38 ppm Sc) by Norman and Haskin (1968).

(Mn)

Previous workers have found manganese non-diagnostic in explaining the chemical behavior of calc-alkaline rocks (S. R. Taylor, 1969). A plot of Mn versus silica (Fig. 15a) shows considerable scatter; there is a general, but very erratic, decrease of Mn with increasing SiO_2 . No close relationship with other major or trace elements is evident in the analytical results. The only detectable consistency in the behavior of Mn is found within flows erupted from the same vent or set of vents. Thus, rocks from the Husband and from Little Brother all have low Mn values (650-850 ppm) when compared with rocks of equivalent silica content from other volcanoes in the area. Analyses of Mn for rocks from the Sand Mountain group have very similar values (1000-1150 ppm Mn) regardless of silica content.

(Zr)

Zirconium shows extreme irregularity and almost complete lack of correlation with silica throughout the olivine basalt-pyroxene andesite range on a Zr- SiO_2 plot (Fig. 15b). This may be partially due to the analytical data on the element. Zr determinations have the poorest precision values of any trace element examined in this report (Appendix I, Table 8). Furthermore, zircon crystals are present in every rock type, and as Prinz (1967) points out, sample preparation and homogenization is rendered especially difficult under these circumstances. Despite these

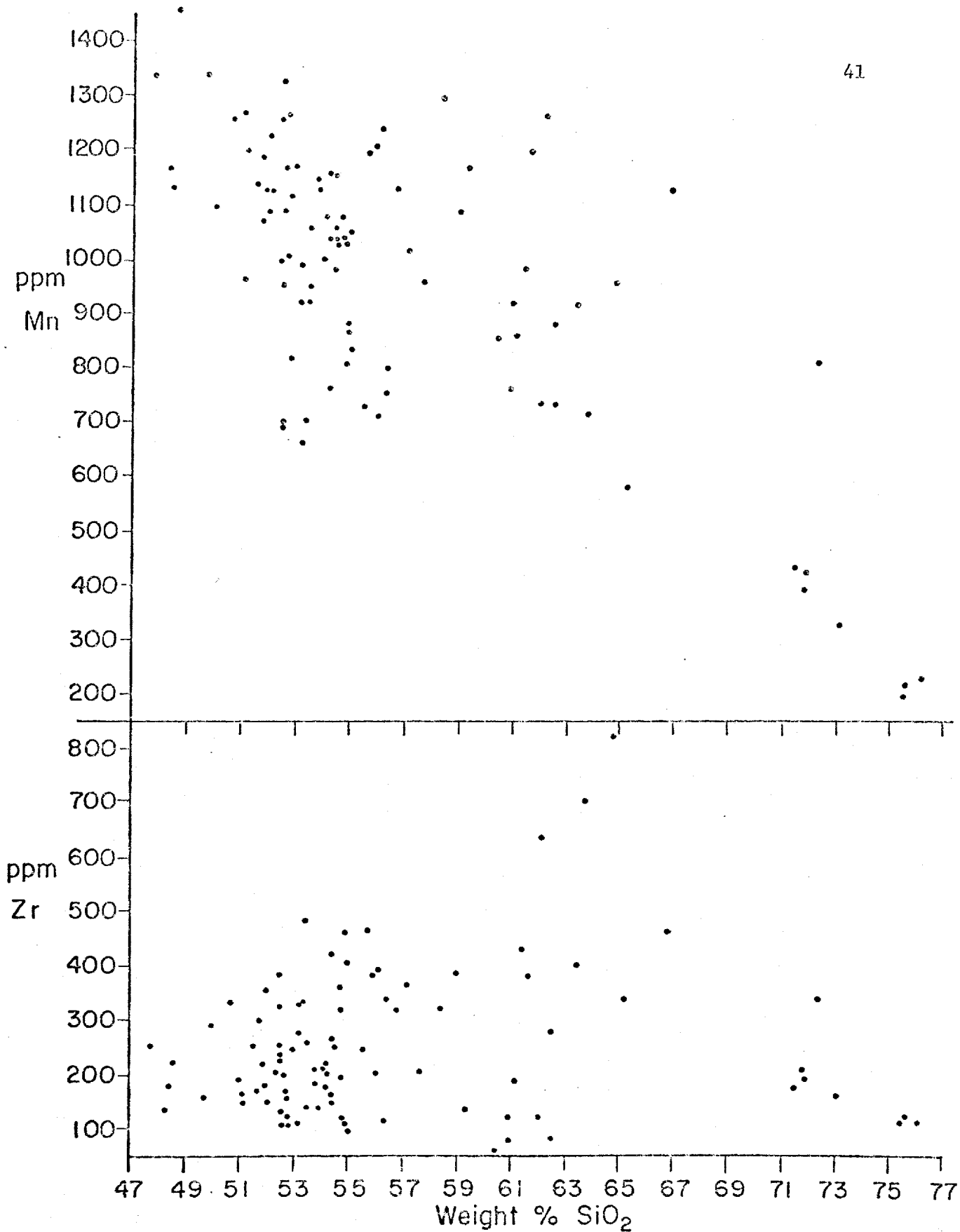


Figure 15. Plots of ppm Mn and ppm Zr versus weight % SiO₂.

considerations, the element must still vary greatly in concentration in rocks of similar silica content to show such scatter on Figure 15. Comparison of Zr concentrations in flows from the same vent or set of vents indicates that part of the scatter may represent variation of initial-abundance patterns between volcanoes, since related flows have similar Zr abundances.

Goldschmidt (1954), Chao and Fleischer (1960), S. R. Taylor (1969), and Borodin and Gladkikh (1967) among others have related increasing Zr abundances to increasing alkali contents in volcanic rocks. Thus, the Kuriles and Kamchatka have generally high Zr concentrations associated with relatively high potash (Markhinin and Sapozhnikova, 1962b) in volcanic rocks with more than 60% silica. No such correlation between total alkalis and Zr can be detected in rocks from the Three Sisters area. The Zr content is generally lower than the values reported for the Kuriles and Kamchatka, as is also the case for potash. The suggestion by Wager and Mitchell (1951), Cornwall and Rose (1957), and Wilkinson (1959) that Zr enters early and intermediate stage pyroxenes in basaltic rocks does not help explain the behavior of the element in this suite of rocks, since the phases are absent in rocks with less than 58% silica and could not control Zr distribution.

(Cu-Zn)

Both of these chalcophile elements, though commonly analyzed for, have received only minor consideration in discussions of trace elements from calc-alkaline rocks. Plots of Cu and Zn versus silica (Fig. 16) show that the two elements decrease slowly if at all through the olivine basalt-olivine andesite silica range. Pyroxene andesites, dacites, and rhyodacites have progressively decreasing abundances of both elements with increasing silica. Copper values are generally similar to those reported by Markhinin and Sapozhnikova (1962a) for the Kuriles and Kamchatka. Concentrations in olivine andesites correspond to S. R. Taylor's low-Si and low-K andesites (1969, p. 61), but values for olivine basalts from this area are high compared to the Cu concentration given for his high-alumina basalt. The fact that the two elements plot on definite

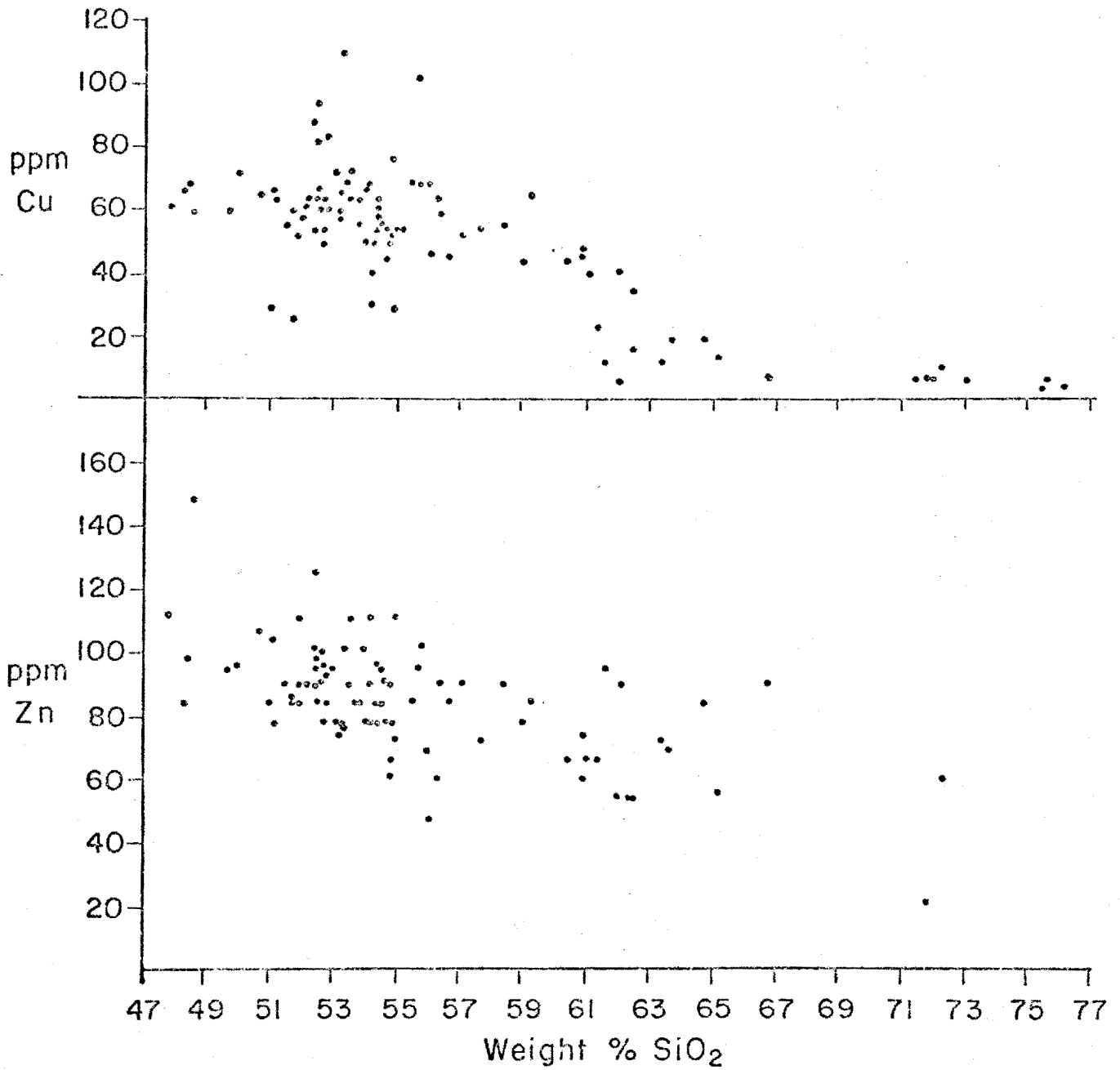


Figure 16. Plots of ppm Cu and ppm Zn versus weight % SiO₂.

trends for the entire suite of rocks from the Three Sisters area supports the premise that the entire range from basalts through rhyodacites are genetically related.

(Ni-Cr-Co)

The three elements, Ni, Cr, and Co, exhibit sympathetic variation with MgO throughout the range of silica values for rocks from the Three Sisters area. On the basis of the plots in Figures 17 to 19, olivine basalts and olivine andesites have been divided into two groups: a high MgO-Ni-Cr-Co series and a low MgO-Ni-Cr-Co series, hereafter referred to as Series A and Series B, respectively. Hedge (1971) and Turekian (1963) among others also note a correlation between MgO and Ni in high-alumina basalts and their related suites.

Data for the above four elements (MgO, Ni, Cr, and Co) plus data on silica for each series were processed by a stepwise linear discriminant analysis computer program* to test the validity of the division based on the graphical presentations. The program compared all five variables simultaneously for each series and presented both statistically and visually the degree to which the two data sets (series) exist as separate populations. The results completely substantiated the original division based on Figures 17 to 19; there was no overlap of the two populations (Series A and B) when canonical variables for the data sets were plotted by the program on a horizontal axis.

Plots of MgO, Ni, Cr, and Co versus silica (Figs. 17 and 18) show that all three elements have higher concentrations in Series A at any given silica value within the olivine basalt-olivine andesite range. Plots of Ni and Cr versus MgO (Fig. 19) demonstrate that the higher Ni and Cr abundances in Series A are not simply a function of the presence of a somewhat higher MgO content. For any given MgO content, Series A contains more Ni and Cr per oxide weight per cent of MgO. Thus, the simple subtraction of MgO via fractionation of olivine, a mechanism recommended by Hess (1970) to explain the sympathetic variation of Ni with Mg, would not bring high Cr-Ni contents onto the Series B curves, as long as

* Program BMD-07M from Biomedical Computer Programs, U. of Cal. Press.

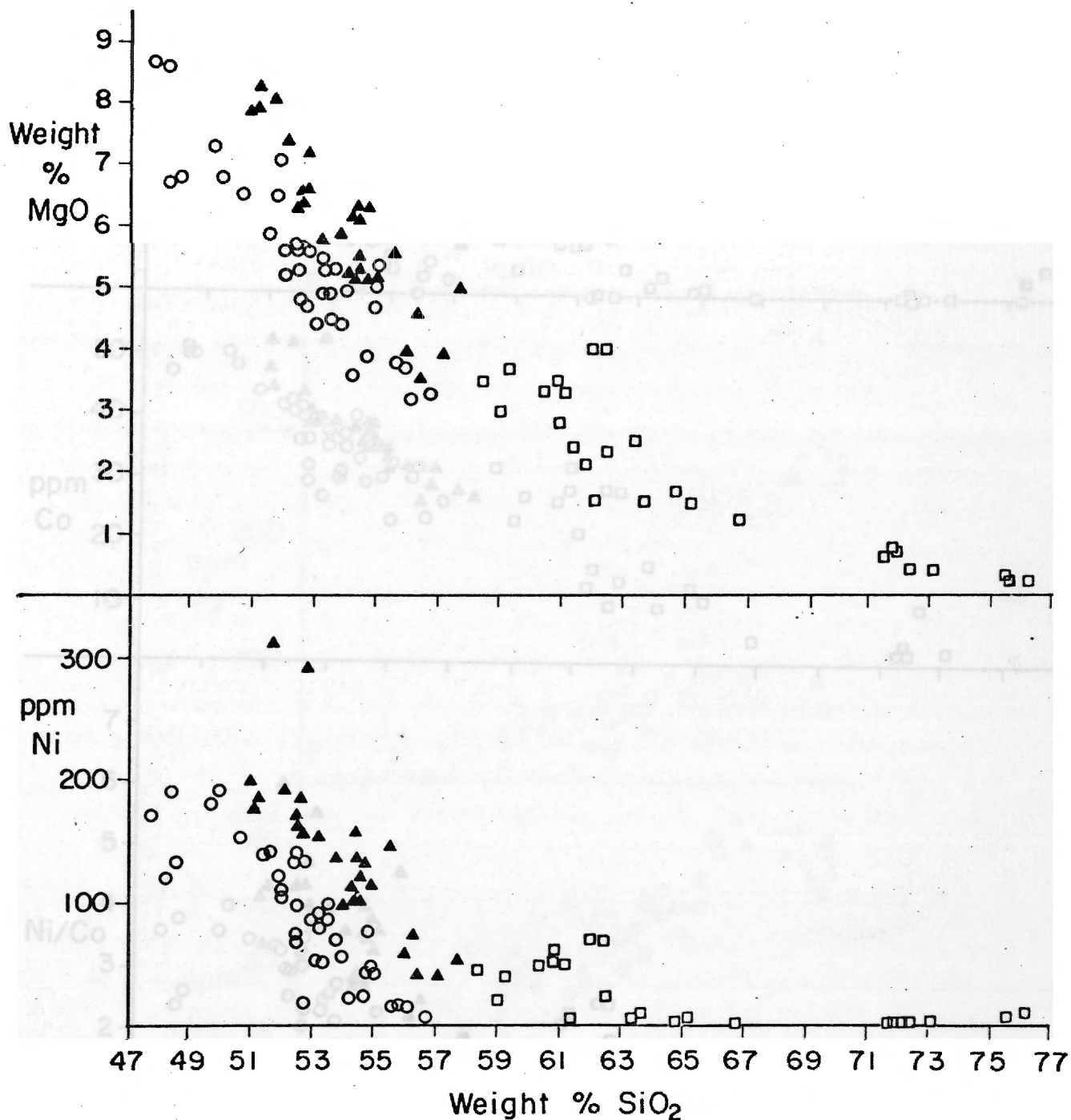


Figure 17. Plots of weight % MgO and ppm Ni versus weight % SiO₂;
 ▲ Series A high MgO-Ni-Cr-Co; ○ Series B low MgO-Ni-Cr-Co; □ undif-
 ferentiated pyroxene andesites, dacites, and rhyodacites.

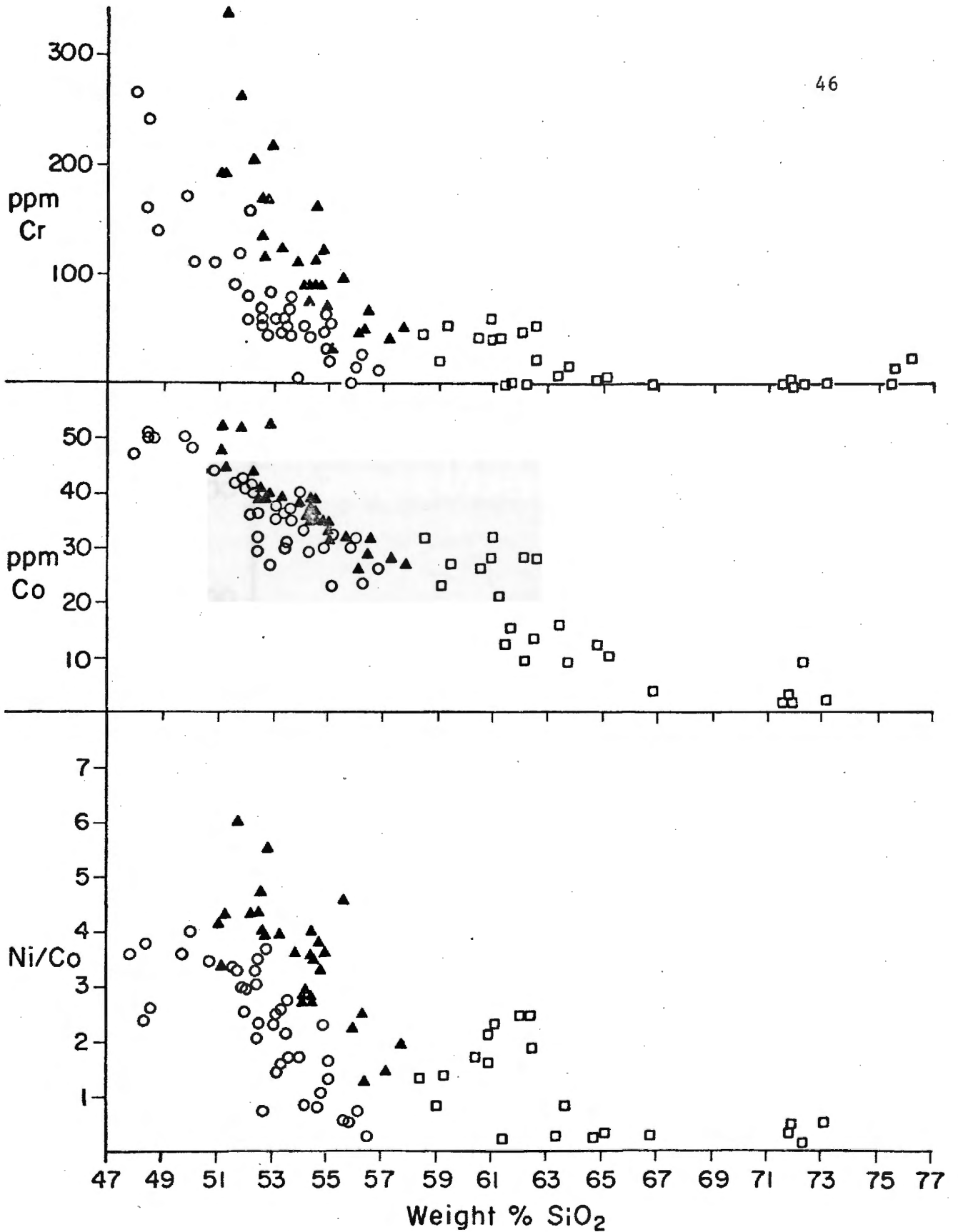


Figure 18. Plots of ppm Cr, ppm Co, and the Ni/Co ratio versus weight % SiO₂. ▲ Series A; ○ Series B; □ pyroxene andesite, dacite, and rhyodacite.

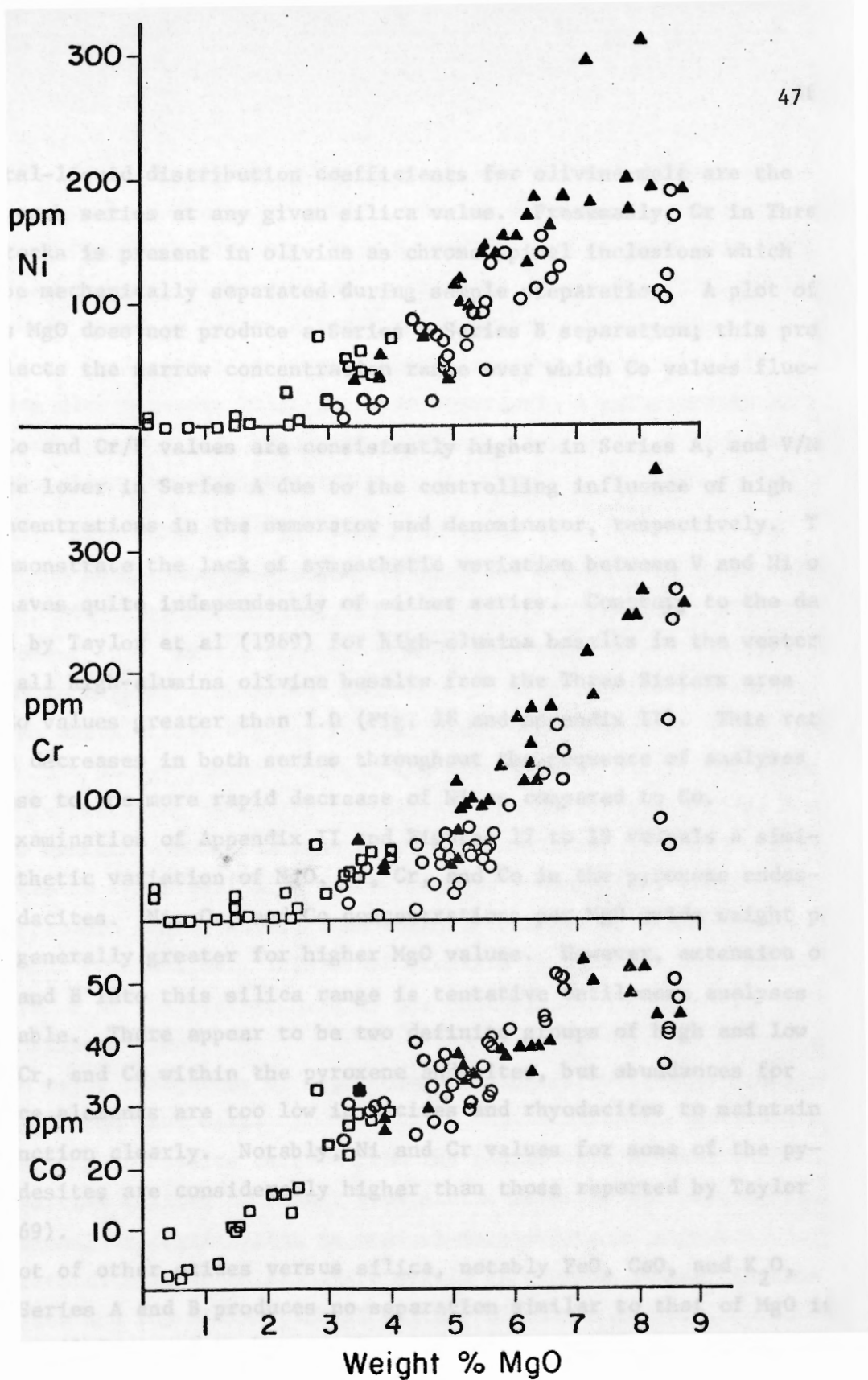


Figure 19. Plots of ppm Ni, ppm Cr, and ppm Co versus weight % MgO.
 ▲ Series A; ○ Series B; □ pyroxene andesite, dacite, and rhyodacite.

the crystal-liquid distribution coefficients for olivine-melt are the same for each series at any given silica value. Presumably, Cr in Three Sisters rocks is present in olivine as chrome spinel inclusions which can not be mechanically separated during sample preparation. A plot of Co versus MgO does not produce a Series A-Series B separation; this probably reflects the narrow concentration range over which Co values fluctuate.

Ni/Co and Cr/V values are consistently higher in Series A, and V/Ni values are lower in Series A due to the controlling influence of high Ni-Cr concentrations in the numerator and denominator, respectively. The ratios demonstrate the lack of sympathetic variation between V and Ni or Cr; V behaves quite independently of either series. Contrary to the data published by Taylor et al (1969) for high-alumina basalts in the western Pacific, all high-alumina olivine basalts from the Three Sisters area have Ni/Co values greater than 1.0 (Fig. 18 and Appendix II). This ratio gradually decreases in both series throughout the sequence of analyses in response to the more rapid decrease of Ni as compared to Co.

An examination of Appendix II and Figures 17 to 19 reveals a similar sympathetic variation of MgO, Ni, Cr, and Co in the pyroxene andesites and dacites. Ni, Cr, and Co concentrations per MgO oxide weight per cent are generally greater for higher MgO values. However, extension of Series A and B into this silica range is tentative until more analyses are available. There appear to be two definite groups of high and low MgO, Ni, Cr, and Co within the pyroxene andesites, but abundances for these trace elements are too low in dacites and rhyodacites to maintain the distinction clearly. Notably, Ni and Cr values for some of the pyroxene andesites are considerably higher than those reported by Taylor et al (1969).

A plot of other oxides versus silica, notably FeO, CaO, and K₂O, based on Series A and B produces no separation similar to that of MgO in Figure 17. Al₂O₃ seems to be somewhat lower in rocks of similar silica content in series A. However, numerous exceptions are common. Though data for Na₂O are incomplete, in every instance where two analyses for

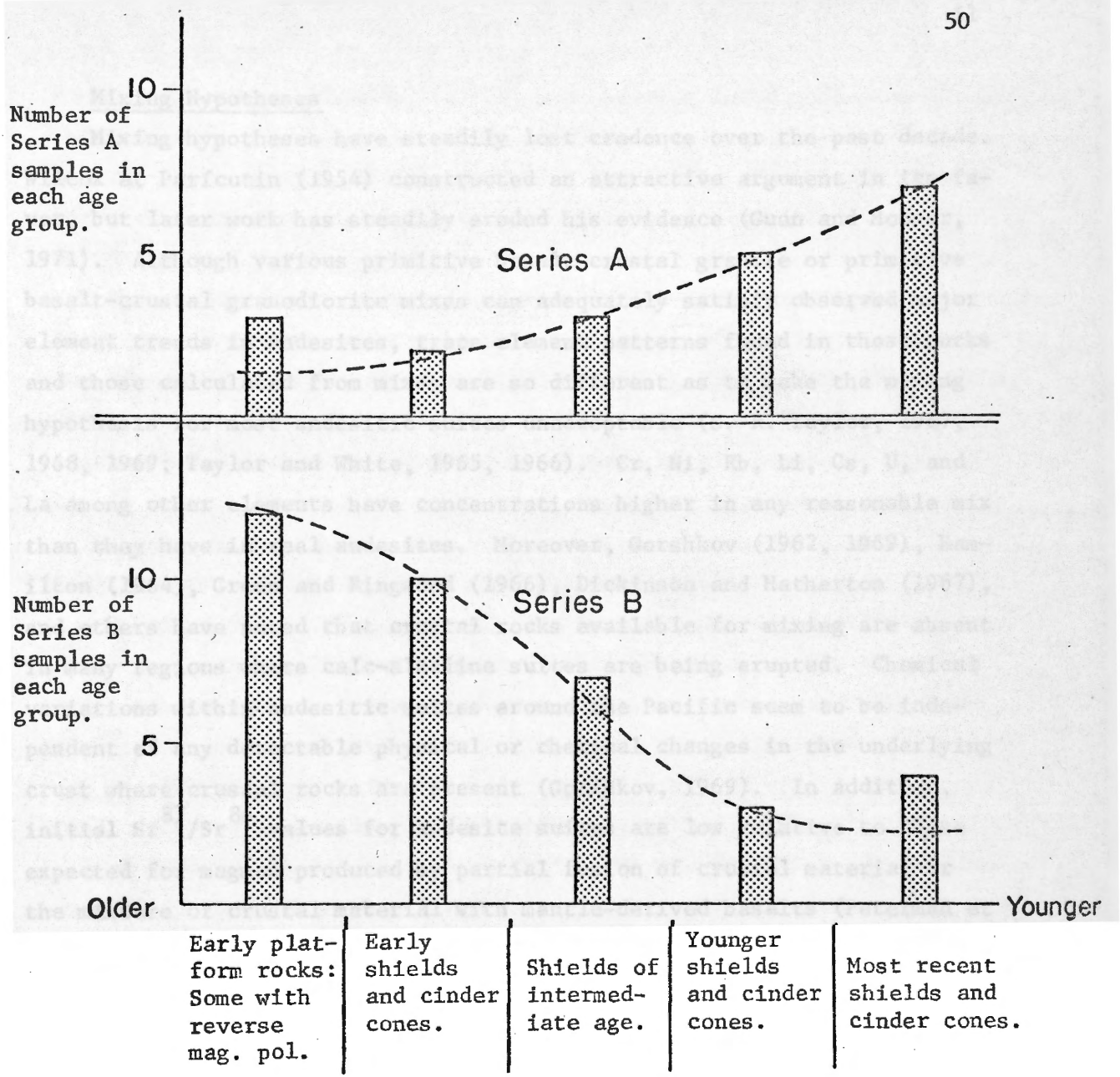
soda can be compared between Series A and B for rocks of similar silica, Na_2O appears to be definitely higher in Series B rocks (Appendix II, Table 10). Of the trace elements, only Ba and Zr seem to show correlations with the two series. Plots similar to those in Figures 11, 12, and 15 for Ba and Zr based on Series A and B reveal that both elements are typically higher in Series B rocks than Series A rocks for similar silica values (see also Appendix II). There is apparently a relationship of Series A and B with time. Figure 20 indicates that Series B rocks are, in general, older than Series A rocks.

DISCUSSION: PETROGENESIS OF CALC-ALKALINE ROCKS

With the advent and progressive development of plate tectonic theory (see Hess, 1962; Vine and Mathews, 1963; Vine, 1966; Isacks et al, 1968; and Dickinson, 1970, 1971), discussion about the genesis of calc-alkaline suites has increasingly centered upon the extrusion of andesites and related lavas above active dipping seismic zones related to arc-trench systems. Oceanic plates produced at mid-ocean rises with their thin veneer of sediments overlying tholeiitic basalts are subducted along these Benioff zones beneath either continents or oceanic plates. Partial melting at depth due to frictional dissipation of heat (Oxburgh and Turcotte, 1970) may produce magmas which, upon reaching the surface, constitute calc-alkaline rock suites. This brief scenario is accepted as a basis for discussion of the petrogenesis of the calc-alkaline rock suite in the Three Sisters area.

Three major categories of hypotheses for the derivation of andesites have emerged from past work:

- (1) Mixing of basalts derived from the mantle with crustal material.
- (2) Partial melting of basalt from mantle material and ensuing fractional crystallization to produce more siliceous magmas.
- (3) Partial melting of primitive mantle to produce abyssal tholeiites and subsequent partial melting of this material to produce calc-alkaline volcanic rocks; i. e. the two-stage model of Green and Ringwood (1968) discussed in terms of trace elements by S. R. Taylor (1969) and Taylor et al (1969).



Approximate Age Relationships

Figure 20. A plot of approximate age of samples for Series A and B versus number of representative analyses in each age group.

Mixing Hypotheses

Mixing hypotheses have steadily lost credence over the past decade. Wilcox at Parícutin (1954) constructed an attractive argument in its favor, but later work has steadily eroded his evidence (Gunn and Mooser, 1971). Although various primitive basalt-crustal granite or primitive basalt-crustal granodiorite mixes can adequately satisfy observed major element trends in andesites, trace element patterns found in these rocks and those calculated from mixes are so different as to make the mixing hypothesis for most andesitic suites unacceptable (S. R. Taylor, 1967, 1968, 1969; Taylor and White, 1965, 1966). Cr, Ni, Rb, Li, Cs, U, and La among other elements have concentrations higher in any reasonable mix than they have in real andesites. Moreover, Gorshkov (1962, 1969), Hamilton (1964), Green and Ringwood (1966), Dickinson and Hatherton (1967), and others have noted that crustal rocks available for mixing are absent in many regions where calc-alkaline suites are being erupted. Chemical variations within andesitic suites around the Pacific seem to be independent of any detectable physical or chemical changes in the underlying crust where crustal rocks are present (Gorshkov, 1969). In addition, initial $\text{Sr}^{87}/\text{Sr}^{86}$ values for andesite suites are low relative to those expected for magmas produced by partial fusion of crustal material or the mixture of crustal material with mantle-derived basalts (Peterman et al, 1967; Pushkar, 1968). Instead, results for Sr isotopic ratios usually compare favorably with those reported for oceanic island tholeiites (Powell and Delong, 1966; Hedge, 1966). These low values for Sr isotope ratios strongly favor mantle derivation of calc-alkaline rocks.

The last two arguments against mixing hypotheses apply directly to the Three Sisters area. As previously noted, the area may be underlain by only Western Cascade rocks with little or no pre-Tertiary crustal material present. Although complete fusion of Western Cascade rocks near their base could produce High Cascade lavas of appropriate compositions, the process is self-limiting; the genesis of Western Cascade andesites and dacites would still require explanation. In addition, inclusions of pre-Tertiary rocks are completely absent in this section of

the High Cascades. Finally, the $\text{Sr}^{87}/\text{Sr}^{86}$ ratios for High Cascade rocks (Peterman et al, 1970; Hedge et al, 1970) uniformly coincide with those for oceanic tholeiites and are generally too low to allow for a crustal origin or contamination of these rocks by crustal material.

Fractional Crystallization

The production of andesitic magmas by high-level fractional crystallization of basalts generated by partial melting of mantle material has been advocated by a number of authors, including Kuno (1966, 1967, 1968b, 1969a), Osborn (1969a, 1969b), Best (1969), and Greene (1968). Recent literature has linked the production of these basalt magmas to dipping seismic zones. Much of the discussion supporting fractional crystallization centers on previous work with synthetic systems by Osborn (1959, 1962), Roeder and Osborn (1966), and Presnall (1966).

Osborn (1959, 1962) contended that basaltic differentiation follows one of two paths, silica or iron enrichment depending on the oxygen fugacity of the system. Iron enrichment occurs at low partial pressures of oxygen with concentration of FeO in the residual liquid as early forming, low-FeO phases are fractionally crystallized. A silica enrichment trend occurs at higher oxygen fugacities with the attendant removal of iron in an oxide phase (magnetite) during fractionation. Roeder and Osborn (1966) found that these general trends are not affected by the addition of CaO to the original $\text{MgO-FeO-Fe}_2\text{O}_3\text{-SiO}_2$ system, and Osborn (1969a) indicated that the further addition of Al_2O_3 also does not change the crystallization paths. Presnall (1966) concluded that only during the later stages of fractionation was the influence of oxygen fugacity and external buffering important. Osborn called for a system which "inhaled" H_2O from the surrounding country rocks and "exhaled" H_2 in order to provide the required amounts of O_2 to achieve silica enrichment via the crystallization and removal of magnetite.

However, at Medicine Lake, Mount Shasta, and Mount Lassen Smith and Carmichael (1968) note that a beta oxide phase is not an early crystallizing phase. The same is true for rocks from the Three Sisters area and from Mount Jefferson (Greene, 1968). To argue that the oxides are

fractionated at depth would require their complete removal but, at the same time, the attendant incomplete removal of early crystallizing olivine and calcic plagioclase (Osborn, 1969b). In view of the large number of High Cascade rocks that have been examined, this seems unlikely, even though the density differences between magnetite and plagioclase or olivine would favor selective removal of magnetite. The importance attached to the absence of an oxide phase can not be minimized; such a phase is essential in naturally occurring calc-alkaline suites if the experimental work of Osborn, Roeder, and Presnall is to be advanced as an explanation of the observed trends.

Other fractionation schemes are limited by the presence of only two phenocryst phases, olivine and calcic plagioclase, in most rocks with less than 60% silica from the Three Sisters area. Calculations based on the subtraction of oxide weight per cents representing the removal of olivine and calcic plagioclase phenocrysts of the appropriate composition can not reconcile recalculated oxide weight per cents of the "residual melts" to those found in real rocks at higher silica values; K_2O , TiO_2 , and Na_2O are too high, and CaO is usually too low. FeO/MgO ratios can be maintained between 1.0 and 2.0 in such schemes by adjusting weight per cent FeO in the olivine to nearly equal MgO , which is true for olivines of Fe_{80-85} (Deer et al, 1962, p. 10-13). However, strong TiO_2 enrichment should occur since olivine contains only small amounts of Ti . Even though Ti will enter pyroxene under high temperature, reducing conditions (Al'mukhamedov, 1967), this can not explain the lack of Ti enrichment in these rocks since pyroxenes are an uncommon phenocryst phase in olivine andesites. A treatment of the data using the graphical scheme employed by Wilcox (1954, p. 331) at Parícutín also indicates that the observed major element trends can not be produced by the fractionation of available phenocrysts.

The following arguments based on the trace element data from the Three Sisters area also do not support crystal fractionation using either Osborn's or any other reasonable scheme:

- (1) If plagioclase-liquid distribution coefficients for Ba of 0.16

(An_{90}) and 0.30 (An_{50-60}) are used (Korringa and Noble, 1971), a strong Ba enrichment at intermediate to high silica values should be expected, since other phenocryst phases that might be fractionated along with calcic-plagioclase contain even less Ba. Such Ba enrichment does not occur throughout most of the silica range.

(2) If the plagioclase-liquid distribution coefficients for Sr of Korringa and Noble (1971) of 3.8 (An_{60}) and 5.4 (An_{45}) are used, an average value for outer zones in plagioclase from Three Sisters olivine basalts and andesites would be 4.5 to 5.0. Fractionation of plagioclase using this value should produce pyroxene andesites and dacites with less than 100 ppm Sr. Berlin and Henderson (1968, 1969) and Brooks (1968) have also emphasized the preference of Sr over Ca for plagioclase in the absence of interfering pyroxenes, as is the case in Three Sisters rocks. Early crystallization and removal of calcic plagioclase should produce a marked depletion of Sr in the residual melt. Pyroxene andesites and dacites do not exhibit strong Sr depletion.

(3) High Ba/Sr values indicate fractionation and the removal of intermediate plagioclase containing abundant Sr and of associated mafics, all of which are Ba-poor (S. R. Taylor, 1969; Ewart et al 1968). However, Ba/Sr values for Three Sisters rocks show no increase throughout the entire olivine basalt-dacite range.

(4) Strong V depletion would be expected if the element were removed in an oxide phase according to Osborn's model during fractionation (Duncan and Taylor, 1968; Taylor et al, 1969). In the presence of fractional crystallization of olivine and plagioclase without an oxide phase, as is the case in rocks from the Three Sisters area, a V enrichment trend would be expected until removal of the element was accomplished by a fractionating oxide phase in pyroxene andesites. However, the element shows no variation other than a gradual depletion across most of the silica range; it exhibits stronger depletion in rocks with more than 62% SiO_2 . Likewise, Sc should be enriched if olivine and plagioclase, in the absence of pyroxenes, were being fractionally crystallized. As with V, Sc shows no such early enrichment.

(5) The depletion of Ni, Cr (as spinel inclusions in olivine), and Co could be ascribed to the fractionation of olivine, but the sympathetic variation of MgO with the three elements in pyroxene andesites and dacites continues despite the absence of olivine as a common phase. Ni and Co should demonstrate a somewhat independent behavior relative to Cr if these silicic rocks are products of fractional crystallization in the absence of olivine.

Peculiarities of the distribution of volcanoes and their associated flows also do not favor fractionation. Vents which have erupted siliceous lavas are highly localized; the two main centers are the Middle and South Sisters. Their rocks constitute a secondary maximum on a histogram of silica values (Fig. 2). If fractionation were a general phenomenon, representatives with 56-59% SiO₂ content should be more common than rocks with higher silica contents. Furthermore, there is complete absence of rocks with 68-71% SiO₂.

Crystal fractionation very likely does occur on a smaller scale. The phenocrysts present in Three Sisters rocks may be a response to near-surface adjustments of rising undifferentiated liquids. Minor fractionation within rocks from the same volcano could explain the scatter exhibited by many elements on the various plots. However, the overall trends exhibited by the entire suite from the Three Sisters area appear to preclude crystal fractionation as a fundamental factor in their production.

Partial Melt Hypotheses

The experimental work by Green and Ringwood (1968) indicates that the essential characteristics of major element trends for calc-alkaline suites can be reproduced by partial melting of a quartz eclogite similar in composition to high-alumina tholeiite under 27-36 kb pressure (corresponding to depths of 100-150 km). If melting occurs under dry conditions, olivine andesite and pyroxene andesite melts are formed. Under progressively wetter conditions, dacite and rhyodacite magmas appear. The experimentally determined pressures agree remarkably well with the inferred depth of 125 km to the zone of magma production estimated by Dickinson on the basis of potash contents plotted against depths to Benioff.

zones for circum-Pacific volcanic chains. Green and Ringwood (1968) observed an early alumina enrichment in the generation of low-silica andesites due to the separation of pyroxenes from the melt to form part of the crystal residua during experimental work. This early alumina enrichment is similar to the silica variation diagram of Al_2O_3 for rocks from the Three Sisters area.

The high-alumina basalts from the area most likely represent part of the continuum of partial melts derived from a tholeiitic parent. There is no break between them and the olivine andesites either petrographically or chemically. Despite previous articles by Taylor et al (1969) and S. R. Taylor (1969) which purport to show the relatively low abundances of Ni, Cr, and Co in high-alumina basalts, it is doubtful that such deficiencies in these elements are universal in high-alumina basalts around the Pacific. Hedge (1971) points out that Taylor et al (1969) based many of their conclusions on the derivation of calc-alkaline rocks and their relationship to eclogites on only 14 samples. The overall trace element patterns for basalts from the Three Sisters area compare favorably with tholeiite abundances for these elements (see Prinz, 1967, p. 278-280). An examination of rocks divided into Series A and B earlier in this report and a comparison with data on pyroxene andesite and dacite from the Three Sisters area reveals that there are both high and low MgO, Ni, Cr, and Co representatives in the sequence. The curves for these elements show, in fact, that high Ni/Co values (>2.0) are common in olivine basalts and olivine andesites and are also present in many pyroxene andesites (see Appendix II). Likewise, V/Ni ratios are lower than Taylor et al (1969) reported for these rock types. Thus, their arguments against partial melting of eclogites and the resulting enrichment of the melts in Ni due to early fusion of pyroxenes do not appear to apply to at least some of the rocks from the Three Sisters area.

On the basis of crystal-liquid distribution coefficients, Gast suggested that partial melting of an eclogite would produce magmas with significantly more Ni and presumably more Cr than partial melting of an abyssal tholeiite in which Ni and chrome spinel inclusions have a strong

preference for refractory olivine in the crystal residua. Series A and B may reflect partial melting of rocks of essentially the same composition: olivine-bearing tholeiite and eclogite transformed from the tholeiite as the basalts are subducted along a dipping seismic zone. The transformation of basalt to eclogite may be spread over a large depth-range due to the effect of relatively low temperatures in the basaltic crust at the initiation of subduction (Oxburgh and Turcotte, 1970; Ringwood, 1969, p. 13). The presence or absence of water could also affect the process. A partial melt of either rock type should have similar major element distributions but persistent differences in minor elements (and MgO). Presumably it would require more extensive fusion of tholeiite than eclogite at any given degree of partial melting to produce melts of equivalent silica content; melts derived from eclogite would always be higher in MgO, Ni, Cr, and Co at given silica contents in this model. Because pyroxene andesites and dacites represent less extensive partial melting under wetter conditions, the distinction of derivation from eclogite or unaltered basalt may be less marked but still noticeable in rocks of 62% or more silica. It is worth noting that Figure 20 shows Series A rocks are, in general, younger than Series B rocks. This relationship with age may reflect the increased rate of conversion of basalt to eclogite as the initially depressed temperature gradients along the Benioff zone are adjusted upwards with time. Thus, the differences between high and low Ni and Cr contents in rocks from the Three Sisters area and in circum-Pacific andesites may be a response to the uneven transformation of basalt to eclogite and the respective melts derived from each of the two during subduction.

Crystal-liquid partition coefficients under conditions of progressive partial melting of basalts and eclogites in the presence of water are not well known for most of the other trace elements. K group elements should be concentrated in initial, siliceous melts and would be steadily diluted in the liquid fraction during increased partial melting. Sr in the clinopyroxenes of eclogite and feldspars and pyroxenes of tholeiite (Gast, 1968, Table 1) would increase in the melt as these phases were incorporated

in preference to garnet or olivine. As the Sr-poor, refractory phases are incorporated during extensive partial melting, dilution of Sr abundances in the liquid should occur. This may account for the slight tendency of Sr to show a maximum at intermediate silica values. Similar speculative arguments can be advanced to explain the behavior of other trace elements.

Green and Ringwood (1968, 1969) and Green (in press) note that high pressure (27-36 kb, corresponding to depths of 100-150 km) crystal fractionation of andesitic partial melts requiring the removal of garnet and pyroxene can also produce more siliceous rocks which follow the calc-alkaline trend. They characterize progressive partial melting and deep-seated fractionation as being complementary processes which produce essentially similar results. However, Green (in press) requires contamination of the peridotite wedge above the Benioff zone by water-rich andesitic magmas generated along the Benioff zone and subsequent partial melting of the peridotite and mixing with the andesitic magmas to produce island arc tholeiites and low-silica andesite found in calc-alkaline suites. Nothing in the major or trace element trends of Three Sisters rocks suggests such a two-stage, separate process for the generation of the low-silica members of the rock suite. It appears that all lavas erupted at the surface are the products of a single set of mechanisms operating at or near the level of the Benioff zone involving progressive partial melting of oceanic crustal rocks or partial melting of these rocks followed by deep-seated crystal fractionation. Cr, Ni, V, and Co abundances preclude extensive participation of mantle material. Presumably trace element trends of Ni, Cr, and Co for magmas derived from partial melts of eclogite versus olivine tholeiite are not obscured if subsequent garnet-pyroxene fractionation occurs at mantle depths, assuming the previous discussion concerning the origins of Series A and B is correct.

One final problem to be considered, that of the "silica gap" and origin of rhyodacites, has been noted and discussed for other calc-alkaline suites. In New Zealand, Ewart et al (1968) ascribed the occurrence

of rhyolitic rocks in the area to the partial fusion of a eugeosynclinal sedimentary sequence derived from the destruction of a previous calc-alkaline eruptive complex. The trace element abundances and trends in the rhyolites would be expected to reflect their source rocks. A similar genesis could apply to rhyodacites in the Three Sisters area; the Western Cascades would take the place of the sedimentary sequence. However, as Green and Ringwood (1968, p. 154) point out, partial melting of tholeiitic material at low pressures (0-18 kb) leads to K_2O enrichment relative to Na_2O in the resulting siliceous magmas. The K_2O/Na_2O ratio is greater than unity. Limited partial melting in the presence of water at depths equivalent to the proposed derivation of the rest of the suite (100-150 km or 27-36 kb) leads to the production of rhyodacitic magmas with K_2O/Na_2O ratios less than unity, which is the case for dacites and rhyodacites for which Na_2O analyses are available from the Three Sisters area. This agreement with experimental data coupled with the tendency of major and trace elements to plot on trends defined by the rest of the suite, suggests that rhyodacites are closely related in origin to less siliceous lavas in the area; a derivation from mantle levels is preferred for this reason. However, the silica gap separating rhyodacite from the rest of the suite remains unexplained.

SUMMARY AND CONCLUSIONS

1. Eruptions in the Three Sisters area resulted in three main types of volcanic structures: (1) shield volcanoes composed of thin flows of uniform olivine basalt and olivine andesite, (2) composite cones built of pyroxene andesite and dacite with minor amounts of olivine basalt, olivine andesite, and rhyodacite, and (3) cinder cones composed of olivine basalt and olivine andesite. Some cinder cones are partly or entirely constructed of pyroxene andesite flows.

2. The majority of the lavas in the area were erupted after the last magnetic reversal. Initial eruptions appear to have been exclusively olivine basalt and olivine andesite, but lavas of pyroxene andesite to rhyodacite compositions began to be erupted long prior to the period of maximum glacial advance. Frequency of appearance of specific rock types

has apparently not changed since the advent of siliceous eruptions.

3. Phenocrysts include olivine and calcic plagioclase in olivine basalt and olivine andesite; pyroxene, intermediate plagioclase, and magnetite in pyroxene andesite and dacite; and sodic plagioclase, ferrohypersthene, and magnetite in rhyodacite. Groundmass phases include plagioclase, pyroxene, iron oxides, and glass in most rocks.

4. Ba exhibits only moderate enrichment throughout most of the rock sequence, and Sr, only moderate depletion. The Ba/Sr ratio is low for most of the sequence. Both V and Sc abundances are high throughout the olivine basalt-pyroxene andesite range of silica values, and neither shows sympathetic variation with a major element. Mn, Zr, Cu, and Zn are generally non-diagnostic in their behavior.

5. Ni, Cr, and Co abundances vary sympathetically with MgO. Olivine basalts and olivine andesites from the Three Sisters area are divided into two series, one high and one low in MgO-Ni-Cr-Co content.

6. Crystal fractionation at crustal depths is dismissed as the major mechanism for the production of the calc-alkaline suite found in this area on the basis of petrographic and chemical data, and mixing hypotheses requiring mixes of mantle-derived basalts and crustal material or crustal anatexis also fail to explain the chemistry of the volcanic rocks in this area.

7. Evaluation of petrographic and chemical data appears to support an origin of partial melting of subducted oceanic tholeiite or eclogite transformed from tholeiite. The entire suite from basalts through rhyodacites is believed to represent partial melts that have undergone only minor crystal fractionation and change in bulk composition during ascent to the surface. This model for the petrogenesis of rocks from the Three Sisters area essentially conforms to the "two-stage" mechanism for andesite genesis proposed by Green and Ringwood and by S. R. Taylor.

APPENDIX I
SPECTROCHEMICAL ANALYSIS

SAMPLE PREPARATION

Two to three kilograms of sample were reduced to inch-square pieces with a hardened steel hammer and then fed through a jaw crusher with aluminum oxide plates. The material was quartered using a splitter and reduced to -200 mesh with a rotating disc pulverizer, also fitted with aluminum oxide plates. This fraction was homogenized by shaking for ten minutes in a glass jar mounted in a Spex mechanical mixer. A five-gram sample was obtained from the homogenized portion by further splits using the cone method. For quantitative analysis, this sample was hand ground to -350 mesh with an agate mortar and pestle. Each piece of equipment was cleaned carefully between samples, and a quartz blank was run through the grinding procedure, mixed with graphite containing the internal standard, and arced with the unknowns to check for contamination.

SEMIQUANTITATIVE ANALYSIS

The procedure for semiquantitative spectrochemical analysis used at Stanford has been described elsewhere by Darling (1968) and Zantop (1969, p. 143). Briefly, a standard mix supplied by Spex Industries* containing 1.28% of each of 49 elements by weight was diluted with graphite to produce standards containing 1.0%, 0.1%, 0.01%, and 0.001% of each element. 100 mg of unknown, ground to -200 mesh, were mixed with an equal weight of -200 mesh graphite. Likewise, 500 mg of matrix comparable in composition to the unknown were prepared with Spec-pure reagents and mixed with an equal weight of each of the standards. To check the purity of the artificial matrix, 100 mg were also mixed with Spec-pure graphite. The sample, standards, and blank were all arced and the spectra recorded on photographic plates.

Concentrations of the trace elements in the unknown were determined by reading the plates with a densitometer, converting transmission values to intensities, and comparing the intensity value of the unknown with a

*Spex Industries, Inc., 3880 Park Avenue, Metuchen, New Jersey.

graph of intensity values versus concentration obtained from the standards. Tables 6 and 7 give instrument settings and arcing conditions used for semiquantitative work.

QUANTITATIVE ANALYSIS

Preparation of Internal Standard

The following compounds were mixed with 40 grams of -350 mesh spectrographic graphite: 20.46 mg In_2O_3 , 11.37 mg Lu_2O_3 , 11.42 mg CdO , and 28.06 mg $[(\text{NH}_3)_4\text{Pd}](\text{NO}_3)_2$. Initial amounts of the four oxides were combined with an equal weight of graphite and mixed for 10 minutes in a Wig-L-Bug mixer. This mixture was then doubled by adding more graphite and mixed by shaking. The process was repeated a third time, but after removal from the Wig-L-Bug, the material was ground under Spec-pure acetone for 15 minutes with an agate mortar and pestle to assure homogenization of the oxides with the fine-grained graphite. After drying the material for four hours at 110°C , the final batch of graphite internal standard was produced by progressively doubling each previous mixture with graphite dilutions until 40 grams of internal standard mix were obtained. Progressively longer mixing times were used between successively larger dilutions. The final batch was rolled for 24 hours in a glass bottle on a pair of motor-driven rollers. The procedures have been described in detail by Darling (1968, p. 100).

Preparation of External Standards

Nine external standards were prepared in an artificial matrix constructed of Spec-pure reagents, using component oxides approximating the composition of andesite. Tables 3 and 4 give the compositions of the matrix and the 1.0% external standard. Each standard was produced by progressive dilution of the initial 1.0% standard (containing 1.0% by weight of each trace element being sought) with matrix. This procedure yielded 0.3%, 0.1%, 0.03%, 0.01%, 0.003%, 0.001%, 0.0003%, and 0.0001% external standards. Homogenization of the matrix and of each standard was achieved by grinding the separate mixtures in Spec-pure acetone for 20 minutes with an agate mortar and pestle, drying for four hours at 110°C , and shaking in a Spex mechanical mixer for one hour. The final

TABLE 3
COMPOSITION OF THE MATRIX

Component	Weight in Grams	Oxide	Oxide Weight %
SiO ₂	8.363	SiO ₂	56.8
Al ₂ O ₃	2.427	Al ₂ O ₃	16.2
MgO	0.494	MgO	3.3
Fe ₂ O ₃	0.945	FeO	5.6
Na ₂ CO ₃	0.961	Na ₂ O	4.1
CaCO ₃	1.811	CaO	7.4
Total	15.001		

TABLE 4
COMPOSITION OF THE 1.0% EXTERNAL STANDARD*

Component	Weight in Grams
BaCO ₃	0.0216
Co ₃ O ₄	0.0206
Cr ₂ O ₃	0.0220
CuO	0.0188
MnO	0.0194
NiO	0.0192
Sc ₂ O ₃	0.0231
SrCO ₃	0.0253
TiO ₂	0.0252
V ₂ O ₅	0.0268
ZnO	0.0187
ZrO ₂	0.0204
MATRIX	1.2389

* Each trace element is 1.0% of the total by weight.

products were mixed with an equal weight of graphite internal standard by similar grinding in acetone, drying, and shaking in the mechanical mixer. An unused portion of the initial matrix was also mixed with the internal standard for use as a blank to check for contamination.

Analytical Procedure

Between 125 and 150 mg of unknown were placed with an identical weight of graphite internal standard in a plastic vial and shaken in a Wig-L-Bug mixer for three minutes. The mixture was then loaded into type 4001 cup electrodes produced by Spex Industries, Inc. Counter electrodes were tipped graphite rods, type 4039, from the same company.

The samples and standards were burned to completion at 10 amps in a closed Stallwood jet with an argon-oxygen atmosphere. Burning to completion is advisable (C. M. Taylor, personal communication), even though the ratio, $\frac{\text{Line Intensity}}{\text{Background Intensity}}$, on the photographic plates is considerably decreased. The latter problem is partly remedied by placing a 60 mesh brass screen in the optical path. Zantop (1969) has demonstrated that this device significantly increases the (L/B) ratio for all types of burning conditions. Burning to completion considerably improved results for involatile elements without greatly affecting the reproducibility of the results for volatile elements.

All burns were made with a rotating step sector included in the optical path. Further details for camera settings, development of photographic plates, and materials employed are given in Tables 6 and 7. Darling (1968, p. 103) has described the photometric methods used for reading photographic plates. The spectral lines given in Table 5 were selected on the basis of their relative intensities and freedom from interference, using data from the M. I. T. Wavelength Tables (Harrison, ed., 1963) and Tables of Spectral Line Intensities (Meggers et al, 1961).

Calculation of Intensity Ratios

A %T-%T (T=transmission) curve was constructed for the emulsion batch of Kodak SA-3 plates used for all spectrographic work. A Seidel curve, a plot of $(\frac{105}{\%T} - 1)$ against intensity, was constructed using %T for adjacent steps taken from the %T-%T curve and the intensity ratio,

TABLE 5

SPECTRAL LINES, DETECTION LIMITS, AND CONCENTRATION RANGES

Element	Spectral lines (A)	Detection limits (ppm)	Observed Con. ranges (ppm)
Ba	4130.66	50	90-1480
Co	3453.50	1	1-50
Cr	4254.35 2843.25	1 33	1-300
Cu	3273.96	1	1-120
Mn	2933.06	100	200-1300
Ni	3515.05	1	1-200
Sc	4023.56	3	<3-40
Sr	3464.57	50	90-900
Ti	2956.13	100	500-10,000
V	3183.98	3	<3-350
Zn	3345.02	50	65-120
Zr	3391.98	50	70-900

TABLE 6
EQUIPMENT AND MATERIAL FOR ANALYTICAL WORK

Spectrograph	Model 70-000 Jarrell-Ash Mark IV
Microphotometer	Model 21-000 Jarrell-Ash, non-recording
Filter	60 mesh brass screen
Arcing Chamber	Closed Stallwood jet
Step Sector	Quantitative analysis; 5 steps; step factor 1.585
	Semiquantitative analysis; 2 steps; 5% and 50% transmission
Positive Electrode	SPEX Industries, Inc., type 4039
Negative Electrode	SPEX Industries, Inc., type 4001
Graphite	Ultra Carbon U-200 (screened to -350 mesh)
Photographic Plates	Kodak SA-3
Developer	Kodak D-19
Stop Bath	Kodak stop bath
Fixer	Kodak Rapid Fixer

TABLE 7
SUMMARY OF ANALYTICAL PROCEDURES

Electrode Gap	4 millimeters
Slit Width	15 microns
Slit Height	Quantitative analysis: 7 millimeters Semiquantitative analysis: 2 1/2 mm
Current	10 amps
Pre-burn	None
Burn Time	Completion
Burns per sample and standards	2
Atmosphere	8 liters/minute: Argon-6 liters/ min. Oxygen-2 liters/min.
Spectral Range	2300 \AA -4600 \AA
Grating Angle	610
Camera Transport	Quantitative analysis: 7 mm; camera settings 83-13; 11 burns/plate Semiquantitative analysis: 3 mm; camera settings 80-20; 20 burns/plate
Developing	69 $^{\circ}$ F for 3 3/4 minutes
Stopping	20 seconds
Fixing	5 minutes
Rinsing	With Kodak Photoflc solution and distilled water
Drying	3 hours

1.5850, for the step sector employed. The Seidel curve is used to convert microphotometer %T readings to intensity values (Ahrens and Taylor, 1961).

A computer program written by Half Zantop at Stanford University was used to convert %T microphotometer readings of lines and adjacent background to $\frac{\text{Intensity of Analysis Element Line}}{\text{Intensity of Internal Standard Line}}$. The Seidel function is used in the program to convert all transmission values to intensity values for two consecutive steps for an analysis line and three steps for its associated internal standard line. Background intensities read on either side of a line are averaged and subtracted from the intensity of the line peak. The intensities are then converted to the equivalent intensities for the third step using the 1.585 intensity factor of the step sector, and the above ratio is calculated for each step read on an analysis line in a single burn, for the average of the two steps read for each burn, and for the average of the four steps read in two burns for each sample. A listing of the program is given by Zantop (1969). Intensity ratios thus obtained from external standards were used to plot working curves (intensity ratio versus concentration) in the standard manner.

Precision and Accuracy

The precision of the method was checked by burning three unknowns six times each. The three had 53.2%, 62.0%, and 76.2% silica by weight corresponding to olivine andesite, pyroxene andesite, and rhyodacite respectively. The six burns for each were recorded on the same plate. The internal standard selection for each element was based on the best results obtained for precision calculations of all three internal standard lines for each element in each of the six burns for the three rock types. The statistical results on precision are presented in Table 8.

No real information is available on the accuracy of the results. No independent analyses were made by other methods or by other laboratories. However, Table 9 presents the data obtained from the processing of U. S. G. S. rock standards. It compares concentrations reported by Flanagan (1967, 1969) with those obtained by plotting rock-standard

intensity ratios on working curves used for trace element analyses in this report.

TABLE 8
INTERNAL STANDARDS AND PRECISIONS
(RELATIVE VARIATIONS AT 2/3 CONFIDENCE LEVEL)

Element	Internal Standard*	% Relative Variation **		
		Olivine Andesite	Pyroxene Andesite	Rhyodacite
Ba	In	4.2	5.0	8.3
Co	Lu	9.2	11.3	----
Cr	In	6.7	8.5	12.4
Cu	In	8.2	7.1	12.8
Mn	Cd	10.7	6.3	11.8
Ni	Lu	12.5	12.9	11.3
Sc	Lu	7.8	6.1	----
Sr	In	7.0	8.5	15.3
Ti	Lu	8.9	6.5	7.5
V	Lu	7.9	6.4	----
Zn	Cd	8.1	14.3	----
Zr	Lu	22.3	32.8	30.4

* Internal Standard Spectral Lines (\AA)

Cd-3261.06

In-3039.36

Lu-3376.50

** Calculated from six repetitive burns of three unknowns.

TABLE 9

A COMPARISON OF TRACE ELEMENT CONCENTRATION VALUES
OBTAINED FROM U. S. G. S. ROCK STANDARDS

Element	G-2		GSP-1		AGV-1		BCR-1		PCC-1	
	This* Report	USGS** Value	This Report	USGS Value	This Report	USGS Value	This Report	USGS Value	This Report	USGS Value
Ba	1900***	1860	1410	1320	1180	1240	645	690	---	6.9
Co	4.3	4.9	6.7	7.5	18.0	15.5	45.5	35.5	112	112
Cr	7.0	9.0	9.5	13.2	8.2	12.9	8.2	16.3	3300	3090
Cu	12.0	10.7	33.5	35.2	54.0	63.7	19.3	22.4	18.5	10.4
Mn	246	265	290	326	835	728	1520	1350	990	889
Ni	1	6.4	6.6	10.7	18.0	17.8	10.3	15.0	2000	2430
Sc	4.9	3.9	7.6	9.2	15.0	13.3	37.0	36.5	7.1	8.7
Sr	495	463	252	247	630	657	330	345	---	.3
Ti	2720	3180	3200	4140	5250	6480	10,300	13,380	---	200
V	41.0	37.0	56.0	52.0	121	121	403	384	32.0	31.2
Zn	68.0	74.9	72	143	83	112	137	132	68	53
Zr	182	316	425	544	382	227	330	185	16	---

* Concentrations obtained from plotting intensity ratios for elements in U. S. G. S. rock standards on working curves used in analytical work for this report.

** Average compositions for elements in U. S. G. S. rock standards reported by Flanagan (1969).

*** All values expressed as ppm.

APPENDIX II
MAJOR AND TRACE ELEMENT ANALYSES

TABLES 10 AND 11

Table 10 contains major and trace element data for olivine basalts and olivine andesites. Table 11 contains major and trace element data for pyroxene andesites, dacites, and rhyodacites.

TABLE 10

PARTIAL CHEMICAL ANALYSES AND TRACE ELEMENT RESULTS
 FOR OLIVINE BASALTS AND OLIVINE ANDESITES: TOTAL IRON REPORTED AS FEO
 (MAJOR ELEMENTS GIVEN AS OXIDE WEIGHT PERCENTAGES--TRACE ELEMENTS GIVEN IN PPM)

SAMPLE SERIES**	1* B	2 B	3 B	4 B	5 B	6 B	7 B	8 A	9 A
SiO2	47.80	48.30	48.40	48.60	49.70	50.00	50.70	51.00	51.10
Al2O3	17.20	16.70	17.80	15.40	18.60	18.80	17.50	16.60	17.10
FEO	9.29	11.20	11.20	11.90	10.10	9.40	9.50	9.40	9.00
MGO	8.65	6.70	8.60	6.80	7.30	6.80	6.50	7.90	7.90
CAO	10.92	10.90	10.00	9.80	8.70	9.20	8.80	9.70	8.80
NA2O	3.06	***	***	4.40	***	***	4.25	***	***
K2O	0.55	0.37	0.21	0.45	0.36	0.34	0.67	0.50	0.78
TiO2	1.59	1.41	1.42	2.10	1.58	1.65	1.72	1.34	1.42
FEO/MGO	1.07	1.67	1.30	1.75	1.38	1.38	1.46	1.19	1.14
BA	90	147	210	235	272	299	192	183	257
SR	360	314	360	283	375	420	420	339	405
MN	1340	1170	1130	1460	1340	1095	1260	962	1270
NI	169	120	189	130	179	190	152	198	172
CR	265	158	241	135	170	112	112	193	193
CO	47	51	50	50	50	48	44	48	52
SC	38	53	38	46	37	41	32	33	38
V	226	240	234	280	236	240	224	221	256
ZR	248	130	174	212	156	285	329	188	160
CU	61	66	68	59	60	72	65	29	66
ZN	112	84	98	148	95	96	107	84	104
BA/SR	0.25	0.47	0.58	0.83	0.73	0.71	0.46	0.54	0.63
NI/CO	3.60	2.35	3.78	2.60	3.58	3.96	3.45	4.13	3.31
CR/V	1.17	0.66	1.03	0.48	0.72	0.47	0.50	0.87	0.75
V/NI	1.34	2.00	1.24	2.15	1.32	1.26	1.47	1.12	1.49

* ANALYSES PERFORMED BY N. R. SUHR. ALL
 OTHERS PERFORMED BY E. M. TAYLOR (NA ANALYSES
 PROVIDED BY OREG. DEPT. GEOL. MIN. IND.).

** HIGH (A) AND LOW (B)
 MGO-NI-CR-CO SERIES.

*** NA ANALYSES NOT AVAILABLE.

SAMPLE:

1. Diktytaxitic olivine basalt from east side of Bend, Oregon. Collected on Sixth Street 1/2 block north of high school.
2. Olivine basalt from Garrison Butte chain of cinder cones.
3. Lookout Point diktytaxitic, High Cascade platform olivine basalt.
4. Columnar olivine basalt from above Scott Creek. Basal High Cascade unit.
5. Diktytaxitic olivine basalt from east side of High Cascade platform. Collected in highway cut southwest of Black Butte.
6. Diktytaxitic olivine basalt from High Cascade platform southwest of Trout Creek Butte.
7. Olivine basalt from terminus of east flow, Belknap Crater.
8. Olivine basalt collected from near the summit of Two Butte.
9. Olivine basalt from Scott Mountain. Collected at Ollalie Road turnoff near base of cliffs.

TABLE 10 (CONT.)

PARTIAL CHEMICAL ANALYSES AND TRACE ELEMENT RESULTS
 FOR OLIVINE BASALTS AND OLIVINE ANDESITES: TOTAL IRON REPORTED AS FEO
 (MAJOR ELEMENTS GIVEN AS OXIDE WEIGHT PERCENTAGES--TRACE ELEMENTS GIVEN IN PPM)

SAMPLE SERIES**	10 A	11 B	12 B	13 A	14 B	15* B	16* B	17 A	18 B
SIO2	51.20	51.50	51.70	51.70	51.90	52.00	52.00	52.10	52.40
AL2O3	16.00	17.10	17.70	16.20	18.00	17.60	17.90	16.30	18.50
FEO	9.00	11.60	9.00	9.40	8.50	8.44	8.46	8.80	9.00
MGO	8.30	5.90	6.50	8.10	7.10	5.58	5.20	7.40	5.70
CAO	9.40	8.80	9.20	9.10	8.70	9.02	8.97	9.20	8.40
NA2O	***	***	***	***	3.22	3.83	3.94	***	***
K2O	0.59	1.02	0.69	0.80	0.60	0.97	0.78	0.70	0.57
TIO2	1.06	1.33	1.32	1.50	1.41	1.37	1.32	1.60	1.37
FEO/MGO	1.14	1.97	1.38	1.16	1.20	1.51	1.63	1.19	1.58
BA	192	328	306	353	299	485	340	286	257
SR	374	390	599	585	405	615	525	715	457
MN	1200	1140	1190	1070	1130	1230	1090	1130	1000
NI	185	139	141	312	122	107	103	139	133
CR	363	90	118	265	158	79	58	205	68
CO	44	42	43	52	41	36	41	44	41
SC	32	31	22	31	39	32	33	30	37
V	221	239	240	231	221	249	261	225	253
ZR	144	249	295	167	212	350	175	140	200
CU	64	55	25	60	52	58	64	62	88
ZN	78	90	86	84	84	90	111	90	90
BA/SR	0.51	0.84	0.51	0.60	0.74	0.79	0.65	0.40	0.56
NI/CO	4.20	3.31	3.28	6.00	2.98	2.97	2.51	4.30	3.24
CR/V	1.64	0.38	0.49	1.15	0.71	0.32	0.22	0.91	0.27
V/NI	1.19	1.72	1.70	0.74	1.81	2.33	2.53	1.19	1.90

* ANALYSES PERFORMED BY N. R. SUHR. ALL
 OTHERS PERFORMED BY E. M. TAYLOR (NA ANALYSES
 PROVIDED BY OREG. DEPT. GEOL. MIN. IND.).

** HIGH (A) AND LOW (B)
 MGO-NI-CR-CO SERIES.

*** NA ANALYSES NOT AVAILABLE.

SAMPLE:

10. Olivine basalt from Cayuse Crater. Collected along Century Drive.
11. Pseudodiktytaxitic olivine basalt from road cut near Beaver Marsh. Basal High Cascade unit.
12. Olivine basalt from high cliffs near Payne Creek.
13. Olivine basalt from Sawyer's Cave, an early Nash Crater flow.
14. Pseudodiktytaxitic olivine basalt from junction of Highway 20 and road to Hoodoo ski area.
15. Olivine basalt collected near Craig Monument on McKenzie Pass.
16. Pre-North Sister olivine basalt from road cut between Snow and Squaw Creeks.
17. Olivine basalt from the south group of Sand Mountain cones.
18. Olivine basalt from the west base of the Middle Sister. Collected along the Skyline Trail.

TABLE 10 (CONT.)

PARTIAL CHEMICAL ANALYSES AND TRACE ELEMENT RESULTS
 FOR OLIVINE BASALTS AND OLIVINE ANDESITES: TOTAL IRON REPORTED AS FEO
 (MAJOR ELEMENTS GIVEN AS OXIDE WEIGHT PERCENTAGES--TRACE ELEMENTS GIVEN IN PPM)

SAMPLE SERIES**	19* B	20 B	21* B	22 B	23 A	24 A	25 A	26 B	27 A
S102	52.50	52.50	52.50	52.50	52.50	52.60	52.60	52.70	52.70
AL2O3	18.10	17.90	17.20	18.50	17.70	18.00	18.10	18.30	17.80
FEO	8.68	9.60	8.22	8.60	9.20	8.60	8.60	8.70	8.30
MGO	5.66	5.10	5.63	5.30	6.30	6.60	6.40	4.70	6.60
CAO	8.98	8.30	8.48	8.40	8.40	8.50	8.20	9.60	8.60
NA2O	3.63	***	3.82	***	***	***	***	4.33	***
K2O	0.62	0.71	0.96	1.00	0.70	0.77	0.75	0.79	0.68
TiO2	1.30	1.45	1.33	1.45	1.31	1.35	1.31	1.38	1.22
FEO/MGO	1.53	1.88	1.64	1.62	1.46	1.30	1.54	1.85	1.26
BA	257	353	555	598	292	286	368	347	286
SR	450	510	555	615	389	361	715	615	405
MN	955	1330	700	697	1260	1170	1090	1290	1010
NI	150	73	96	66	169	160	185	19	157
CR	58	54	58	58	169	169	112	45	135
CO	40	36	32	29	39	40	39	27	40
SC	36	27	38	38	26	35	27	33	31
V	289	213	178	180	219	213	195	275	225
ZR	226	230	321	380	249	127	102	151	151
CU	82	54	94	66	64	64	60	49	54
ZN	84	125	98	95	101	90	101	96	78
BA/SR	0.57	0.69	1.00	0.97	0.75	0.79	0.51	0.56	0.71
NI/CO	3.50	2.03	3.00	2.28	4.33	4.00	4.74	0.70	3.92
CR/V	0.20	0.25	0.33	0.32	0.77	0.79	0.57	0.16	0.60
V/NI	2.06	2.92	1.85	2.73	1.30	1.33	1.05	14.47	1.43

* ANALYSES PERFORMED BY N. R. SUHR. ALL
 OTHERS PERFORMED BY E. M. TAYLOR (NA ANALYSES
 PROVIDED BY OREG. DEPT. GEOL. MIN. IND.).

** HIGH (A) AND LOW (B)
 MGO-NI-CR-CO SERIES.

*** NA ANALYSES NOT AVAILABLE.

SAMPLE:

19. Olivine basalt from west base of the Middle Sister.
20. Olivine basalt from north base of Bachelor Butte.
21. Olivine basalt from dike on north shoulder of Little Brother.
22. Olivine basalt from outcrop north of Little Brother.
23. Olivine basalt from quarry near Scott Lake.
24. Olivine andesite from Sims Butte flow.
25. Olivine andesite from Little Nash Crater flow.
26. Olivine andesite (welded tuff?) from highway cut south of Tamolitch Falls.
27. Diktytaxitic olivine andesite from highway cut near Tamolitch Falls overlook.

TABLE 10 (CONT.)

PARTIAL CHEMICAL ANALYSES AND TRACE ELEMENT RESULTS
 FOR OLIVINE BASALTS AND OLIVINE ANDESITES: TOTAL IRON REPORTED AS FEO
 (MAJOR ELEMENTS GIVEN AS OXIDE WEIGHT PERCENTAGES--TRACE ELEMENTS GIVEN IN PPM)

SAMPLE SERIES**	28 B	29 A	30* B	21 B	32* B	33 A	34 B	35 B	36 B
SI02	52.80	52.80	53.00	53.20	53.20	53.20	53.30	53.40	53.50
AL2O3	19.00	17.30	17.90	20.80	17.30	18.70	17.80	19.40	18.40
FEO	7.90	8.60	8.69	7.00	8.34	8.40	8.80	8.00	8.70
MGO	5.60	7.20	4.40	4.90	5.48	5.80	5.30	4.90	4.50
CAO	9.40	8.20	8.67	8.90	7.45	8.80	8.30	8.70	8.50
NA2O	***	***	3.66	***	3.86	***	***	***	***
K2O	0.71	0.67	0.87	0.30	0.98	0.74	0.91	0.80	0.76
TiO2	1.14	1.30	1.28	1.04	1.34	1.12	1.47	1.31	1.46
FEO/MGO	1.41	1.19	1.97	1.43	1.52	1.45	1.66	1.63	1.93
BA	353	244	420	328	548	340	645	360	393
SR	540	374	480	497	555	459	700	525	450
MN	817	1120	1170	922	660	991	705	925	1060
NI	131	290	86	51	89	155	77	49	79
CR	83	217	58	58	47	124	50	68	43
CO	35	53	38	37	36	39	30	31	37
SC	32	31	25	32	38	29	34	31	35
V	198	240	245	235	210	217	170	220	271
ZR	118	102	241	105	325	273	329	478	136
CU	84	60	72	60	58	66	110	69	64
ZN	93	84	95	78	74	78	101	77	111
BA/SR	0.65	0.65	0.88	0.66	0.99	0.74	0.92	0.69	0.87
NI/CO	3.74	5.47	2.26	1.38	2.47	3.97	2.57	1.58	2.14
CR/V	0.42	0.90	0.24	0.25	0.22	0.57	0.29	0.31	0.16
V/NI	1.51	0.83	2.85	4.61	2.36	1.40	2.21	4.49	3.43

* ANALYSES PERFORMED BY N. R. SUHR. ALL
 OTHERS PERFORMED BY E. M. TAYLOR (NA ANALYSES
 PROVIDED BY OREG. DEPT. GEOL. MIN. IND.).

** HIGH (A) AND LOW (B)
 MGO-NI-CR-CO SERIES.
 *** NA ANALYSES NOT AVAILABLE.

SAMPLE:

28. Margin of olivine andesite flow from Bluegrass Butte.
29. Olivine andesite from west lobe of a Belknap Crater flow.
30. Olivine andesite from Aubry Butte, Bend, Oregon. Collected near the radio tower.
31. Olivine andesite from north side of Black Butte.
32. Olivine andesite from Little Brother.
33. Graham Butte olivine andesite from road cut, highly vesicular.
34. Olivine andesite from Madness Ridge near Skyline Trail. From lower western flank of Little Brother.
35. Belknap Crater olivine andesite collected on McKenzie Pass.
36. Very old olivine andesite with reverse mag. pol. from outcrop along Squaw Creek.

TABLE 10 (CONT.)

PARTIAL CHEMICAL ANALYSES AND TRACE ELEMENT RESULTS
 FOR OLIVINE BASALTS AND OLIVINE ANDESITES: TOTAL IRON REPORTED AS FEO
 (MAJOR ELEMENTS GIVEN AS OXIDE WEIGHT PERCENTAGES--TRACE ELEMENTS GIVEN IN PPM)

SAMPLE SERIES**	37 B	38 B	39 A	40 B	41 A	42* B	43 A	44* A	45 A
S102	53.50	53.80	53.80	54.00	54.10	54.20	54.20	54.20	54.40
AL2O3	19.30	18.50	17.70	18.60	18.40	18.60	17.60	17.30	17.20
FEO	8.20	9.00	8.60	7.80	7.90	7.31	8.40	8.51	8.40
MGO	5.30	4.40	5.90	5.00	5.20	3.59	6.30	5.14	6.10
CAO	8.60	7.60	7.70	8.70	8.50	8.38	9.20	7.91	7.80
NA2O	***	4.24	***	***	***	4.21	2.20	3.88	***
K2O	0.85	0.71	0.95	0.71	0.75	0.83	0.64	0.95	0.99
TiO2	1.18	1.50	1.34	1.15	1.23	1.03	1.24	1.25	1.25
FEO/MGO	1.55	2.05	1.46	1.56	1.52	2.04	1.33	1.66	1.38
BA	453	286	353	340	340	328	271	453	265
SR	540	540	314	585	436	525	405	509	437
MN	950	1130	1150	1000	1080	1040	783	1160	1160
NI	96	68	137	56	96	22	114	95	156
CR	74	5	112	52	90	42	90	74	163
CO	35	40	38	33	36	29	39	34	39
SC	29	27	26	28	34	31	39	27	20
V	209	260	205	225	227	270	244	199	221
ZR	253	178	203	134	207	199	215	171	156
CU	72	63	56	50	68	30	40	50	61
ZN	90	84	84	101	78	90	78	111	96
BA/SR	0.84	0.53	1.12	0.58	0.78	0.62	0.67	0.89	0.61
NI/CO	2.74	1.70	3.61	1.70	2.67	0.76	2.92	2.79	4.00
CR/V	0.35	0.02	0.55	0.23	0.40	0.16	0.37	0.37	0.74
V/NI	2.18	3.82	1.50	4.02	2.36	12.27	2.14	2.09	1.42

* ANALYSES PERFORMED BY N. R. SUHR. ALL
 OTHERS PERFORMED BY E. M. TAYLOR (NA ANALYSES
 PROVIDED BY OREG. DEPT. GEOL. MIN. IND.).

** HIGH (A) AND LOW (B)
 MGO-NI-CR-CO SERIES.
 *** NA ANALYSES NOT AVAILABLE.

SAMPLE:

37. Olivine andesite collected at Skylight Cave. Sixmile Butte flow.
38. Olivine andesite from Broken Top. Collected from knob at south end of Green Lakes.
39. Olivine andesite underlying flow from Four-in-One. Collected from near terminus of Four-in-One flow.
40. Olivine andesite collected from Deer Butte.
41. Olivine andesite, West Lava Camp flow from Belknap Crater.
42. Olivine andesite half way down the northern slope of Tam McArthur Ridge, Broken Top.
43. Olivine andesite flow on southeast ridge of the Husband.
44. Olivine andesite from Bunchgrass Ridge.
45. Olivine andesite from Sims Butte flow. Collected from highway cut.

TABLE 10 (CONT.)

PARTIAL CHEMICAL ANALYSES AND TRACE ELEMENT RESULTS
 FOR OLIVINE BASALTS AND OLIVINE ANDESITES: TOTAL IRON REPORTED AS FEO
 (MAJOR ELEMENTS GIVEN AS OXIDE WEIGHT PERCENTAGES--TRACE ELEMENTS GIVEN IN PPM)

SAMPLE SERIES**	46* A	47 A	48 A	49 A	50* B	51 A	52 B	53 A	54 A
SI02	54.40	54.40	54.40	54.50	54.70	54.70	54.80	54.80	54.90
AL2O3	18.20	16.90	18.70	18.20	17.70	16.60	17.60	19.40	17.60
FEO	7.11	8.60	7.80	8.30	7.61	8.50	7.80	7.00	8.40
MGO	5.51	6.20	5.30	5.20	3.90	6.30	5.60	5.10	5.10
CAO	8.51	8.80	7.90	8.40	9.03	7.90	8.30	7.90	7.20
NA2O	3.77	***	***	***	3.53	***	***	***	***
K2O	0.86	0.86	0.67	0.69	1.18	1.05	1.02	0.59	0.98
TIO2	0.92	1.32	1.05	1.32	1.01	1.34	1.07	0.87	1.08
FEO/MGO	1.29	1.39	1.47	1.60	1.95	1.35	1.39	1.37	1.65
BA	312	353	353	368	394	406	257	228	573
SR	742	930	685	773	586	405	510	570	420
MN	1060	981	1040	1030	1080	1040	1035	803	880
NI	135	102	97	120	23	132	40	115	113
CR	90	112	90	90	42	123	65	30	68
CO	38	37	35	34	30	35	39	35	31
SC	26	28	24	26	37	28	49	23	32
V	204	204	200	204	255	206	258	192	194
ZR	265	419	153	249	353	319	192	111	460
CU	58	54	64	56	45	54	53	50	77
ZN	84	84	78	95	90	78	90	60	78
BA/SR	0.42	0.38	0.52	0.48	0.67	1.00	0.50	0.40	1.36
NI/CO	3.55	2.76	2.77	3.53	0.77	3.77	1.03	3.29	3.65
CR/V	0.44	0.55	0.45	0.44	0.16	0.60	0.25	0.16	0.35
V/NI	1.51	2.00	2.06	1.70	11.09	1.56	6.45	1.67	1.72

* ANALYSES PERFORMED BY N. R. SUHR. ALL
 OTHERS PERFORMED BY E. M. TAYLOR (NA ANALYSES
 PROVIDED BY OREG. DEPT. GEOL. MIN. IND.).

** HIGH (A) AND LOW (B)
 MGO-NI-CR-CO SERIES.

*** NA ANALYSES NOT AVAILABLE.

SAMPLE:

46. Olivine andesite from Tam McArthur Ridge near eastern end.
47. Olivine andesite, Clear Lake flow from Sand Mountain.
48. Hoodoo Bowl lava, olivine andesite from southeast corner of mesa above ski area.
49. Fish Lake flow from Nash Crater, olivine andesite.
50. Olivine andesite from Tumalo Mountain highway cut just east of Bachelor Butte ski area turnoff.
51. Le Conte Crater olivine andesite flow. Collected along Century Drive
52. Olivine andesite from Trout Creek Butte lookout.
53. Very old olivine andesite from highway cut (Highway 20) opposite west end of Suttle Lake. Has reverse mag. pol.
54. Olivine andesite from margin of north plug of the Husband.

TABLE 10 (CONT.)

PARTIAL CHEMICAL ANALYSES AND TRACE ELEMENT RESULTS
FOR OLIVINE BASALTS AND OLIVINE ANDESITES: TOTAL IRON REPORTED AS FEO
(MAJOR ELEMENTS GIVEN AS OXIDE WEIGHT PERCENTAGES--TRACE ELEMENTS GIVEN IN PPM)

SAMPLE SERIES**	55 B	56 B	57 B	58* A	59* B	60 B	61* A	62 B	63 A
SiO ₂	54.90	55.00	55.00	55.50	55.70	55.90	56.00	56.10	56.30
Al ₂ O ₃	19.60	19.10	17.60	17.20	17.30	17.50	18.70	17.40	19.00
FEO	7.70	6.50	7.60	6.75	8.16	8.60	6.26	9.10	6.60
MGO	4.70	5.40	5.00	5.58	3.78	3.70	3.94	3.20	4.60
CAO	7.30	8.40	8.50	5.55	7.45	7.60	7.88	7.10	8.00
NA ₂ O	***	***	***	3.84	4.49	***	4.18	***	***
K ₂ O	0.58	0.55	1.06	1.12	0.97	0.79	0.84	1.00	0.74
TiO ₂	1.08	1.02	1.08	0.93	1.28	1.84	0.89	1.52	0.74
FEO/MGO	1.64	1.20	1.52	1.21	2.16	2.32	1.59	2.84	1.43
BA	286	244	446	695	380	406	312	406	328
SR	890	480	450	860	480	465	658	600	525
MN	870	1050	835	730	1200	1210	710	1240	755
NI	75	44	42	145	15	15	57	14	72
CR	30	58	20	96	2	16	43	27	47
CO	33	33	26	32	30	32	26	24	29
SC	20	30	23	32	33	41	24	30	23
V	191	217	209	174	260	316	195	269	183
ZR	105	93	400	242	460	383	197	390	108
CU	29	54	54	69	69	102	69	46	64
ZN	66	111	72	84	95	102	72	84	60
BA/SR	0.32	0.51	0.99	0.81	0.79	0.87	0.47	0.68	0.62
NI/CO	2.27	1.33	1.62	4.53	0.50	0.47	2.19	0.58	2.48
CR/V	0.16	0.27	0.10	0.55	0.01	0.05	0.22	0.10	0.26
V/NI	2.55	4.93	4.98	1.20	17.33	21.07	3.42	19.21	2.54

* ANALYSES PERFORMED BY N. R. SUHR. ALL
OTHERS PERFORMED BY E. M. TAYLOR (NA ANALYSES
PROVIDED BY OREG. DEPT. GEOL. MIN. IND.).

** HIGH (A) AND LOW (B)
MGO-NI-CR-CO SERIES.

*** NA ANALYSES NOT AVAILABLE.

SAMPLE:

55. Olivine andesite from High Cascade platform, Potatoe Hill on Jack Pine Road.
56. Very old olivine andesite collected above Squaw Creek. Has reverse magnetic polarity.
57. Olivine andesite from Bachelor Butte. Collected on road to ski area.
58. Olivine andesite from dike at south end of Eileen Lake.
59. Olivine andesite from Windy Point on McKenzie Pass highway.
60. Olivine andesite from west base of Middle Sister along Skyline Trail.
61. Olivine andesite from south plug of the Husband.
62. Olivine andesite from Todd Lake volcano.
63. Olivine andesite, Yapoah flow, collected just east of Dee Wright Observatory.

TABLE 10 (CONT.)

PARTIAL CHEMICAL ANALYSES AND TRACE ELEMENT RESULTS
 FOR OLIVINE BASALTS AND OLIVINE ANDESITES: TOTAL IRON REPORTED AS FEO
 (MAJOR ELEMENTS GIVEN AS OXIDE WEIGHT PERCENTAGES--TRACE ELEMENTS GIVEN IN PPM)

SAMPLE SERIES**	64 A	65* B	66 A	67 A
SiO2	56.40	56.70	57.10	57.70
Al2O3	18.50	16.50	19.10	18.00
FEO	7.90	8.73	7.10	7.00
MGO	3.50	3.33	3.90	5.00
CAO	7.30	7.33	7.30	7.20
NA2O	***	4.62	***	3.15
K2O	1.02	0.92	0.72	0.74
TiO2	1.30	1.40	1.07	0.74
FEO/MGO	2.26	2.62	1.82	1.40
BA	598	312	368	458
SR	507	405	910	525
MN	800	1130	1020	960
NI	39	6	40	52
CR	64	12	44	42
CO	32	30	28	27
SC	38	37	18	22
V	243	355	164	223
ZR	337	315	360	197
CU	59	45	52	54
ZN	90	84	90	72
BA/SR	1.18	0.77	0.40	0.87
NI/CO	1.22	0.20	1.43	1.93
CR/V	0.26	0.03	0.27	0.19
V/NI	6.23	59.17	4.10	4.29

* ANALYSES PERFORMED BY N. R. SUHR. ALL
 OTHERS PERFORMED BY E. M. TAYLOR (NA ANALYSES
 PROVIDED BY OREG. DEPT. GEOL. MIN. IND.).

** HIGH (A) AND LOW (B)
 MGO-NI-CR-CO SERIES.

*** NA ANALYSES NOT AVAILABLE.

SAMPLE:

64. Olivine andesite from Montague Memorial, Skyline Trail on the west side of the Middle Sister.
65. Olivine andesite from Broken Top. Collected at Fall Creek Falls.
66. Olivine andesite from Maxwell Butte. Collected west of Little Nash Crater.
67. Collier Cone olivine andesite collected near center of flow where Frog Camp Trail crosses lava field.

TABLE 11

PARTIAL CHEMICAL ANALYSES AND TRACE ELEMENT RESULTS
 FOR PYROXENE ANDESITES, DACITES, AND RHYODACITES: TOTAL IRON GIVEN AS FEO
 (MAJOR ELEMENTS GIVEN AS OXIDE WEIGHT PERCENTAGES--TRACE ELEMENTS GIVEN IN PPM)

SAMPLE	68	69*	70	71	72	73	74	75	76
S102	58.40	59.00	59.30	60.40	60.90	60.90	61.10	61.40	61.60
AL2O3	17.20	16.60	17.30	19.30	17.70	19.00	18.40	17.00	16.90
FEO	7.20	6.98	7.00	6.10	7.10	6.00	5.80	6.30	6.50
MGO	3.50	2.98	3.70	3.30	2.80	3.50	3.30	2.40	2.10
CAO	6.40	6.18	6.75	6.30	5.70	5.90	5.80	5.10	4.70
NA2O	4.43	4.53	**	**	3.30	**	3.03	4.78	**
K2O	1.32	1.53	1.01	0.90	1.10	0.99	1.20	1.72	1.75
TiO2	1.29	1.22	1.01	0.68	0.92	0.64	0.72	1.10	1.27
FEO/MGO	2.06	2.34	1.89	1.85	2.54	1.71	1.76	2.63	3.10
BA	353	508	380	353	347	353	380	598	548
SR	510	450	437	585	397	509	450	330	405
MN	1500	1090	1170	859	922	762	863	990	1200
NI	41	18	37	46	70	60	48	2	--
CR	45	19	52	36	58	33	34	2	3
CO	32	23	27	26	32	28	21	12	15
SC	25	25	28	17	25	22	17	18	22
V	246	241	224	164	217	162	188	154	189
ZR	315	380	133	54	76	120	185	427	378
CU	56	44	65	44	48	46	40	23	12
ZN	90	78	84	66	74	60	66	66	95
BA/SR	0.69	1.13	0.87	0.60	0.87	0.69	0.84	1.81	1.35
NI/CO	1.28	0.78	1.37	1.77	2.19	2.14	2.29	0.17	----
CR/V	0.18	0.08	0.23	0.22	0.27	0.20	0.18	0.01	0.02
V/NI	6.00	13.39	6.05	3.57	3.10	2.70	3.92	77.00	----

* ANALYSES PERFORMED BY N. R. SUHR. ALL OTHERS PERFORMED BY E. M. TAYLOR (NA ANALYSES PROVIDED BY OREG. DEPT. GEOL. MIN. IND.).

** NA ANALYSES NOT AVAILABLE.

SAMPLE:

68. Summit cinder cone of the South Sister; cindery pyroxene andesite.
69. Pyroxene andesite from north end of Green Lakes; Broken Top lava.
70. Pyroxene andesite, terminus of flow from Four-in-One cinder cone chain.
71. Pyroxene andesite from Hogg Rock, Highway 20, Santiam Pass.
72. Pyroxene andesite from terminus of Collier Cone west flow.
73. Hayrick Butte pyroxene andesite collected south of Hoodoo Bowl ski area.
74. Pyroxene andesite from Collier Cone. Collected just west of the cone.
75. South Sister pyroxene andesite collected on trail to summit from Green Lakes at about the 8,000 ft. elevation.
76. Pyroxene andesite collected at the south end of Linton Lake.

TABLE 11 (CONT.)

PARTIAL CHEMICAL ANALYSES AND TRACE ELEMENT RESULTS
 FOR PYROXENE ANDESITES, DACITES, AND RHYODACITES: TOTAL IRON GIVEN AS FEO
 (MAJOR ELEMENTS GIVEN AS OXIDE WEIGHT PERCENTAGES--TRACE ELEMENTS GIVEN IN PPM)

SAMPLE	77	78	79	80	81	82	83	84*	85
SiO ₂	62.00	62.10	62.50	62.50	63.40	63.70	64.80	65.20	66.80
Al ₂ O ₃	17.00	16.90	17.00	18.00	16.90	16.60	17.20	15.40	17.50
FEO	6.40	7.00	5.80	6.50	6.40	7.00	6.50	4.88	4.35
MGO	4.00	1.50	4.00	2.30	2.50	1.50	1.70	1.49	1.20
CAO	5.60	4.50	5.70	4.70	5.00	3.80	3.90	3.82	3.00
NA ₂ O	2.30	**	**	3.40	**	**	2.80	4.90	**
K ₂ O	1.43	1.55	1.60	1.55	1.80	1.70	1.63	2.22	1.72
TiO ₂	0.73	1.49	0.73	0.63	1.07	1.08	1.10	0.91	0.74
FEO/MGO	1.60	4.67	1.45	2.83	2.56	4.67	3.82	3.28	3.63
BA	510	497	467	610	598	680	740	1010	728
SR	314	360	306	390	465	345	405	437	314
MN	737	1270	737	880	917	715	960	580	1130
NI	68	--	68	24	4	7	2	3	1
CR	47	1	52	20	7	15	3	7	3
CO	28	9	28	13	16	9	12	10	4
SC	22	23	19	15	18	24	27	20	19
V	180	111	178	142	197	64	113	122	14
ZR	117	635	78	273	399	700	825	339	463
CU	41	5	35	26	12	19	19	14	7
ZN	54	90	54	54	72	69	84	56	90
BA/SR	1.62	1.38	1.53	1.56	1.29	1.97	1.83	2.31	2.32
NI/CO	2.43	----	2.43	1.85	0.25	0.78	0.17	0.30	0.25
CR/V	0.26	0.01	0.29	0.14	0.04	0.23	0.03	0.06	0.21
V/NI	2.65	----	2.62	5.92	49.25	9.14	56.50	40.67	14.00

* ANALYSES PERFORMED BY N. R. SUHR. ALL OTHERS PERFORMED BY E. M. TAYLOR (NA ANALYSES PROVIDED BY OREG. DEPT. GEOL. MIN. IND.).

** NA ANALYSES NOT AVAILABLE.

SAMPLE:

77. Dacite from the Middle Sister. Collected east of Skyline Trail above Sunshine Shelter.
78. Dacite from Broken Top collected east of southeast lobe of the Newberry rhyodacite flow.
79. Same flow as Sample 77. Dacite collected northeast of Linton Lake; from the Middle Sister.
80. Collier Cone dacite. Collected in the crater of the cone.
81. Dacite from Kokostick Butte.
82. Dacite from high bluff along Skyline Trail above Sunshine Shelter; from the Middle Sister.
83. Dacite from large black hump on the northwest side of the Middle Sister.
84. Dacite collected 4 1/2 miles southeast of Linton Lake; from the Middle Sister.
85. Glassy dacite from the Middle Sister. Collected on Lane Mesa.

TABLE 11 (CONT.)

PARTIAL CHEMICAL ANALYSES AND TRACE ELEMENT RESULTS
FOR PYROXENE ANDESITES, DACITES, AND RHYODACITES: TOTAL IRON GIVEN AS FEO
(MAJOR ELEMENTS GIVEN AS OXIDE WEIGHT PERCENTAGES--TRACE ELEMENTS GIVEN IN PPM)

SAMPLE	86	87	88	89	90	91	92	93*
SiO ₂	71.50	71.80	71.90	72.30	73.10	75.50	75.60	76.20
Al ₂ O ₃	15.30	15.30	14.70	14.70	14.80	13.40	13.10	13.00
FEO	2.40	2.90	2.40	2.60	1.90	1.60	1.60	1.10
MGO	0.60	0.70	0.70	0.40	0.40	0.30	0.20	0.22
CAO	2.10	2.10	2.10	1.70	1.70	0.90	1.10	0.83
Na ₂ O	**	**	**	4.75	**	**	**	4.46
K ₂ O	2.88	2.92	3.09	3.02	3.35	3.35	3.40	3.51
TiO ₂	0.32	0.32	0.32	0.27	0.28	0.05	0.05	0.09
FEO/MGO	4.00	4.14	3.43	6.50	4.75	5.33	8.00	5.00
BA	950	835	915	598	835	1030	1010	1480
SR	204	237	237	405	188	90	99	123
MN	435	395	428	815	325	198	217	229
NI	--	1	1	1	1	--	5	9
CR	1	2	2	2	2	1	15	22
CO	2	3	2	9	2	--	--	--
SC	5	4	5	15	4	3	2	--
V	18	29	27	120	23	--	--	--
ZR	174	207	193	337	156	117	123	112
CU	7	7	7	10	6	4	6	4
ZN	--	21	--	60	--	--	--	--
BA/SR	4.66	3.52	3.86	1.48	4.44	11.44	10.20	12.03
NI/CO	----	0.33	0.50	0.11	0.50	----	----	----
CR/V	0.06	0.07	0.07	0.02	0.09	----	----	----
V/NI	----	29.00	27.00	120.00	23.00	----	----	----

* ANALYSES PERFORMED BY N. R. SUHR. ALL OTHERS PERFORMED BY E. M. TAYLOR (NA ANALYSES PROVIDED BY OREG. DEPT. GEOL. MIN. IND.).

** NA ANALYSES NOT AVAILABLE.

SAMPLE:

86. Rhyodacite from east base of the South Sister just west of Green Lakes. Very old siliceous flow.
87. Devils Lake rhyodacite; recent flow.
88. Newberry rhyodacite flow; collected on the southwest side of Green Lakes.
89. Rhyodacite from Kathleen Butte.
90. Rock Mesa rhyodacite flow.
91. Obsidian Cliffs rhyodacite flow from the Middle Sister.
92. Same flow as 91. Collected at mid-point of flow.
93. Same flow as Samples 91 and 92. Collected near vent at the western foot of the Middle Sister.

BIBLIOGRAPHY

- Ahrens, L. H., and Taylor, S. R., 1961, Spectrochemical analysis: Addison-Wesley Publishing Co., Reading, Mass., 454 p.
- Al'mukhamedov, A. I., 1967, Behavior of Ti during differentiation of basaltic magma: *Geochem. Int.*, v. 4, p. 47-56.
- Berlin, R., and Henderson, M. B., 1968, A reinterpretation of Sr and Ca fractionation trends in plagioclases from basic rocks: *Earth Planet. Sci. Lett.*, 4, p. 79-83.
- , 1969, The distribution of Sr and Ba between alkali feldspar, plagioclase, and groundmass phases of porphyritic trachytes and phonolites: *Geochim. Cosmochim. Acta*, v. 33, p. 247-256.
- Best, M. G., 1969, Differentiation of calc-alkaline magmas: *Oreg. Dept. Geol. Min. Ind. Bull.* 65, p. 65-75.
- Borodin, L. S., and Gladkikh, V. S., 1967, Geochemistry of Zr in differentiated alkali basalt series: *Geochem Int.*, v. 4, p. 925-935.
- Brooks, C. K., 1968, On the interpretation of trends in element ratios in differentiated igneous rocks, with particular reference to strontium and calcium: *Chem. Geol.*, v. 3., p. 15-20.
- Brown, R. E., 1941, The geology and petrography of the Mount Washington area, Oregon: Master's thesis, Yale University.
- Callaghan, E., 1933, Some features of the volcanic sequence in the Cascade Range in Oregon: *Am. Geophys. Union Trans.*, 14th Ann. Meeting, p. 243-249.
- Chao, E. C. T., and Fleischer, M., 1960, Abundance of zirconium in igneous rocks: 21st Internat. Geol. Cong. Rept., pt. 1, p. 106-131.
- Cornwall, H. R., and Rose, H. J., 1957, Minor elements in Keweenawan lavas, Michigan: *Geochim. Cosmochim. Acta*, v. 12, p. 209-224.
- Darling, R., 1968, The distribution of fluorine and other elements in quartz monzonite near ore, Pine Creek contact-metasomatic tungsten deposits, Inyo County, California: Ph.D. thesis, Stanford University, 134 p.
- Deer, W. A., Howie, R. A., and Zussman, J., 1962, Rock forming minerals: ortho- and ring silicates, vol. 1: Longmans, London, 333 p.

- , 1963, Rock forming minerals: chain silicates, vol. 2: Longmans, London, 379 p.
- Dickinson, W. R., 1968, Circum-Pacific andesite types: *J. Geophys. Res.*, v. 73, p. 2261-2269.
- , 1970, Relations of andesites, granites, and derivative sandstones to arc-trench tectonics: *Rev. Geophys.*, v. 8, no. 4, p. 813-860.
- , 1971, Plate tectonic models of geosynclines: *Earth Planet. Sci. Lett.*, 10, p. 165-174.
- Dickinson, W. R., and Hatherton, T., 1967, Andesitic volcanism and seismicity around the Pacific: *Science*, v. 157, p. 801-803.
- Duncan, A. R., and Taylor, S. R., 1968, Trace element analysis of magnetites from andesitic and dacitic lavas from Bay of Plenty, New Zealand: *Contrib. Mineral. Petrol.*, v. 20, p. 30-33.
- Emmons, R. C., 1943, The universal stage (with five axes of rotation): *Geol. Soc. Am. Mem.* 8, 205 p.
- Ewart, A., Taylor, S. R., and Capp, A. C., 1968, Trace and minor element geochemistry of the rhyolitic volcanic rocks, central North Island, New Zealand: total rock and residual liquid data: *Contrib. Mineral. Petrol.*, v. 18, p. 76-104.
- Flanagan, F. J., 1967, U. S. Geological Survey silicate rock standards: *Geochim. Cosmochim. Acta*, v. 31, p. 289-308.
- , 1969, U. S. Geological Survey standards-II: first compilation of data for the new U. S. G. S. rocks: *Geochim. Cosmochim. Acta*, v. 33, p. 81-120.
- Gast, P. W., 1968, Trace element fractionation and the origin of tholeiitic and alkaline magma types: *Geochim. Cosmochim. Acta*, v. 32, p. 1057-1086.
- Goldschmidt, V. M., 1954, *Geochemistry*: Oxford Press, London, 730 p.
- Gorshkov, G. S., 1962, Petrochemical features of volcanism in relation to the types of the Earth's crust: *Am. Geophys. Union Mono.* 6, p. 110-115.
- , 1969, Geophysics and petrochemistry of andesite volcanism of

- the circum-Pacific belt: Oreg. Dept. Geol. Min. Ind. Bull. 65, p. 91-98.
- Green, T. H., in press, Crystallization of an island arc andesite: Contrib. Mineral. Petrol.
- Green, T. H., and Ringwood, A. E., 1966, Origin of the calc-alkaline igneous rock suite: Earth Planet. Sci. Lett., 1, p. 307-316.
- , 1968, Genesis of the calc-alkaline igneous rock suite: Contrib. Mineral. Petrol., v. 18, p. 105-162.
- , 1969, High pressure experimental studies on the origin of andesites: Oreg. Dept. Geol. Min. Ind. Bull. 65, p. 21-32.
- Greene, R. C., 1968, Petrography and petrology of volcanic rocks in the Mount Jefferson area, High Cascade Range, Oregon: U. S. Geol. Surv. Bull. 1251-G, 48 p.
- Gunn, B. M., and Mooser, F., 1971, Geochemistry of the volcanics of Central Mexico: Bull. Volcan., v. 34, no. 2, p. 557-616.
- Hamilton, W., 1964, Origin of high-alumina basalt, andesite, and dacite magmas: Science, 146, p. 635-637.
- Harrison, G. R., ed., 1963, M. I. T. wavelength table: M. I. T. Press, Cambridge, 429 p.
- Hedge, C. E., 1966, Variations in radiogenic strontium found in volcanic rocks: Jour. Geophys. Res., v. 71, p. 6119-6126.
- , 1971, Nickel in high-alumina basalts: Geochim. Cosmochim. Acta, v. 35, p. 522-524.
- Hedge, C. E., Hildreth, R. A., and Henderson, W. T., 1970, Strontium isotopes in some Cenozoic lavas from Oregon and Washington: Earth Planet. Sci. Lett., 8, p. 434-438.
- Hess, H. H., 1949, Chemical composition and optical properties of common clinopyroxenes, Pt. 1: Am. Mineral., v. 34, p. 621-666.
- , 1962, History of the ocean basins, in Petrological Studies (Buddington Volume), edited by A. E. J. Engel et al: Geol. Soc. Am., New York, p. 599-620.
- Higgins, M. W., and Waters, A. C., 1967, Newberry Volcano, a preliminary report: Ore Bin, v. 29, p. 37-60.

- , 1968, Newberry Caldera field trip: Oreg. Dept. Geol. Min. Ind. Bull. 62, p. 59-77.
- Hodge, E. T., 1925, Mount Multnomah, ancient ancestor of the Three Sisters: Univ. of Oreg. Pub., v. 2, no. 10, 160 p.
- Isacks, B., Oliver, J., and Sykes, L. R., 1968, Seismology and the new global tectonics: Jour. Geophys. Res., v. 73, p. 5855-5899.
- Korringa, M. K., and Noble, D. C., 1971, Distribution of Sr and Ba between natural feldspar and igneous melt: Earth Planet. Sci. Lett., 11, p. 147-151.
- Kuno, H., 1960, High-alumina basalt: J. Petrol., v. 1, p. 121-145.
- , 1966, Lateral variation of basalt magma across continental margins and island arcs: Can. Geol. Surv. Paper 66-15, p. 317-336.
- , 1967, Volcanological and petrological evidences regarding the nature of the upper mantle: The Earth's Mantle, edited by T. F. Gaskell, Academic Press, London, p. 89-110.
- , 1968a, Differentiation of basaltic magmas, in Basalts, vol. 2, edited by H. H. Hess and A. Poldervaart: Interscience, New York, p. 623-688.
- , 1968b, Origin of andesite and its bearing on the island arc structure: Bull. Volcan., v. 32, p. 141-176.
- , 1969a, Andesite in time and space: Oreg. Dept. Geol. Min. Ind. Bull. 65, p. 13-20.
- , 1969b, Plateau basalts, in the Earth's Crust and Upper Mantle: Am. Geophys. Union Geophys. Mon. 13, p. 495-501.
- McBirney, A. R., 1968, Petrochemistry of Cascade andesite volcanoes: Oreg. Dept. Geol. Min. Ind. Bull. 62, p. 101-107.
- , 1969, Andesitic and rhyolitic volcanism of orogenic belts, in the Earth's Crust and Upper Mantle: Am. Geophys. Union Geophys. Mon. 13, p. 501-507.
- Markhinin, E. K., and Sapozhnikova, A. M., 1962a, Content of Ni, Co, Cr, V, and Cu in volcanic rocks of Kamchatka and the Kurile Islands: Geochem., p. 427-432.
- , 1962b, Zirconium content in volcanic rocks of Kamchatka and

- the Kurile Islands: *Geochem.*, p. 965-966.
- Meggers, W. F., Corliss, C. H., and Scribner, B. F., 1961, Tables of spectral-line intensities--arranged by elements: N. B. S. Mono. 32, 473 p.
- Norman, J. C., and Haskin, L. A., 1968, The geochemistry of Sc, a comparison to the rare earths and Fe: *Geochim. Cosmochim. Acta*, v. 32, p. 93-108.
- Osborn, E. F., 1959, Role of oxygen pressure in the crystallization and differentiation of basaltic magma: *Am. Jour. Sci.*, v. 257, p. 609-647.
- , 1962, Reaction series for subalkaline igneous rocks based on different oxygen pressure conditions: *Am. Mineral.*, v. 47, p. 211-226.
- , 1969a, Experimental aspects of calc-alkaline differentiation: *Oreg. Dept. Geol. Min. Ind. Bull.* 65, p. 33-42.
- , 1969b, The complementariness of orogenic andesite and alpine peridotite: *Geochim. Cosmochim. Acta*, v. 33, p. 307-324.
- Oxburgh, E. R., and Turcotte, D. L., 1970, Thermal structure of island arcs: *Geol. Soc. Am. Bull.*, v. 81, p. 1665-1688.
- Peacock, M. A., 1931, Classification of igneous rock series: *J. Geol.*, v. 39, p. 54-67.
- Peck, D. L., Griggs, A. B., Schlicker, H. G., Wells, F. G., and Dole, H. M., 1964, Geology of the central and northern parts of the Western Cascade Range in Oregon: U. S. Geol. Surv. Prof. Paper 449, 56 p.
- Peterman, Z. E., Hedge, C. E., Coleman, R. G., and Snavely, Jr., P. D., 1967, $\text{Sr}^{87}/\text{Sr}^{86}$ ratios in some eugeosynclinal sedimentary rocks and their bearing on the origin of granitic magma in orogenic belts: *Earth Planet. Sci. Lett.*, 2, p. 443-439.
- Peterman, Z. E., Carmichael, I. S. E., and Smith, A. L., 1970, $\text{Sr}^{87}/\text{Sr}^{86}$ ratios of Quaternary lavas of the Cascade Range, northern California: *Geol. Soc. Am. Bull.*, v. 81, p. 311-318.
- Poldervaart, A., and Hess, H. H., 1951, Pyroxenes in the crystallization of basaltic magma: *J. Geol.*, v. 59, p. 472-489.

- Powell, J. L., and DeLong, S. E., 1966, Isotopic composition of strontium in volcanic rocks from Oahu: *Science*, v. 153, p. 1239-1242.
- Presnall, D. C., 1966, The join forsterite-diopside-iron oxide and its bearing on the crystallization of basaltic and ultramafic magmas: *Am. Jour. Sci.*, v. 264, p. 753-809.
- Prinz, M., 1967, Geochemistry of basaltic rocks: trace elements, in Basalts, vol. 1, edited by H. H. Hess and A. Poldervaart: Interscience, New York, p. 271-323.
- Pushkar, P., 1968, Strontium isotopic ratios in volcanic rocks of three island arc areas: *Jour. Geophys. Res.*, v. 73, p. 2701-2714.
- Ringwood, A. E., 1969, Composition of the crust and upper mantle: *Am. Geophys. Union Geophys. Mon.* 13, p. 1-17.
- Rittmann, A., 1929, Die zonenmethode: ein beitrag zur methodik der plagioklas bestimmung mit hilfe des theodolithisches: *Schweizer. Mineralog. Petrograph. Mitt.*, v. 9, p. 1-46.
- Roeder, P. L., and Osborn, E. F., 1966, Experimental data for the system $MgO-FeO-Fe_2O_3-CaAl_2Si_2O_8-SiO_2$ and their petrologic implications: *Am. Jour. Sci.*, v. 264, p. 428-480.
- Sheppard, R. A., 1962, Iddingsitization and recurrent crystallization of olivine in basalts from the Simcoe Mountains, Washington: *Am. Jour. Sci.*, v. 260, p. 67-74.
- Shimizu, T., and Kuroda, R., 1969, Abundance of scandium in igneous rocks of Japan: *Geochim. Cosmochim. Acta*, v. 33, p. 290-292.
- Smith, A. L., and Carmichael, I. S. E., 1968, Quaternary lavas from the southern Cascades, western U.S.A.: *Contrib. Mineral. Petrol.*, v. 19, p. 212-238.
- Taylor, E. M., 1965, Recent volcanism between Three Fingered Jack and North Sister, Oregon Cascade Range: *Ore Bin*, v. 27, p. 121-147.
- , 1968, Roadside geology, Santiam and McKenzie Pass Highways, Oregon: *Oreg. Dept. Geol. Min. Ind. Bull.* 62, p. 3-33.
- Taylor, S. R., 1967, Origin and growth of continents: *Tectonophysics*, v. 4, p. 17-34.
- , 1968, Geochemistry of andesites: *Proc. Intern. Symposium*,

- Origin and Distribution of Elements V, Intern. Assoc. Geochem. Cosmochem., p. 559-583.
- , 1969, Trace element chemistry of andesites and associated calc-alkaline rocks: *Oreg. Dept. Geol. Min. Ind. Bull.* 65, p. 43-63.
- Taylor, S. R., Kaye, M., White, A. J. R., Duncan, A. R., and Ewart, A., 1969, Genetic significance of Co, Cr, Ni, Sc, and V content of andesites: *Geochim Cosmochim. Acta*, v. 33, p. 275-286.
- Taylor, S. R., and White, A. J. R., 1965, Geochemistry of andesites and the growth of continents: *Nature*, v. 208, p. 271-273.
- , 1966, Trace element abundances in andesites: *Bull. Volcan.*, v. 29, p. 177-194.
- Thayer, T. P., 1936, Structure of the North Santiam River section of the Cascade Mountains in Oregon: *J. Geol.*, v. 44, p. 701-716.
- , 1937, Petrology of later Tertiary and Quaternary rocks of the north-central Cascade Mountains in Oregon, with notes on similar rocks in western Nevada: *Geol. Soc. Am. Bull.*, v. 48, p. 1611-1651.
- , 1939, Geology of the Salem Hills and the North Santiam River basin, Oregon: *Oreg. Dept. Geol. Min. Ind. Bull.* 15, 40 p.
- Trüger, W. E., 1959, Optische bestimmung der gesteinsbildenden minerale, teil 1, bestimmungstabellen: E. Schweizerbartische Verlagsbuchhandlung, Stuttgart, 147 p.
- Turekian, K. K., 1963, The chromium and nickel distribution in basaltic rocks and eclogites: *Geochim. Cosmochim. Acta*, v. 27, p. 835-846.
- Turner, F. S., and Verhoogen, J., 1960, *Igneous and metamorphic petrology*: McGraw-Hill, New York, 694 p.
- Vine, F. J., 1966, Spreading of the ocean floor, new evidence: *Science*, v. 154, p. 1405-1414.
- Vine, F. J., and Matthews, P. M., 1963, Magnetic anomalies over ocean ridges: *Nature*, v. 199, p. 947-949.
- Wager, L. R., and Mitchell, R. L., 1951, The distribution of trace elements during strong fractionation of basic magma—a further study of the Skaergaard intrusion, East Greenland: *Geochim. Cosmochim. Acta*, v. 1, p. 129-208.

- Wells, F. G., and Peck, D. L., 1961, Geologic map of Oregon west of the 121st meridian: U. S. Geol. Surv. Misc. Inv. Map I-325, scale 1:500,000.
- Wilcox, R. E., 1954, Petrology of Parícutin volcano, Mexico: U. S. Geol. Surv. Bull. 965-C, p. 281-353.
- Wilkinson, J. F. G., 1959, The geochemistry of a differentiated teschenite sill near Gunnedah, New South Wales: *Geochim. Cosmochim. Acta*, v. 16, p. 123-150.
- Williams, H., 1932a, Geology of the Lassen Volcanic National Park, California: *Calif. Univ. Dept. Geol. Sci. Bull.*, v. 21, no. 8, p. 195-385.
- , 1932b, Mount Shasta, a Cascade volcano: *J. Geol.*, v. 40, p. 417-429.
- , 1933, Mount Thielsen, a dissected Cascade volcano: *Calif. Univ. Dept. Geol. Sci. Bull.*, v. 23, no. 6, p. 195-213.
- , 1942, The geology of Crater Lake National Park, Oregon, with a reconnaissance of the Cascade Range southward to Mount Shasta: *Carnegie Inst. Wash. Pub.* 540, 162 p.
- , 1944, Volcanoes of the Three Sisters region, Oregon Cascades: *Calif. Univ. Dept. Geol. Sci. Bull.*, v. 27, no. 3, p. 37-83.
- , 1957, A geologic map of the Bend quadrangle, Oregon, and a reconnaissance geologic map of the central portion of the High Cascade Mountains: *Oreg. Dept. Geol. Min. Ind.*, in coop. with U. S. Geol. Surv., scale 1:125,000.
- Williams, H., Turner, F. J., and Gilbert, C. M., 1954, Petrography--an introduction to the study of rocks in thin sections: San. Fran., W. H. Freeman and Co., 406 p.
- Wise, W. S., 1969, Geology and petrology of the Mt. Hood area, a study of High Cascade volcanism: *Geol. Soc. Am. Bull.*, v. 80, p. 969-1006.
- Zantop, H. A., 1969, Trace element distribution in manganese oxides from the San Francisco manganese deposit, Jalisco, Mexico: Ph.D. thesis, Stanford University, 161 p.